

The Pennsylvania State University

The Graduate School

**TWO BACTERIAL ENHANCER BINDING PROTEINS LUXO AND SYPG
ACTIVATE EXPRESSION OF A SMALL RNA QRR1 IN THE BENEFICIAL MICROBE
*VIBRIO FISCHERI***

A Dissertation in

Biochemistry, Microbiology, and Molecular Biology

by

Ericka D. Surret

© 2022 Ericka D. Surret

Submitted in Partial Fulfillment
of the Requirements
for the Degree of

Doctor of Philosophy

August 2022

The dissertation of Ericka D. Surret was reviewed and approved by the following:

Timothy Miyashiro
Associate Professor of Biochemistry and Molecular Biology
Dissertation Advisor
Chair of Committee

Sarah Ades
Associate Dean, The Graduate School
Professor of Biochemistry and Molecular Biology

Shaun Mahony
Associate Professor of Biochemistry and Molecular Biology

Tim Meredith
Associate Professor of Biochemistry and Molecular Biology

Charles Fisher
Emeritus Professor and Distinguished Senior Scholar of Biology

J. Gregory Ferry
Stanley R. Person Professor of Biochemistry and Molecular Biology

Ken Keiler
Associate Department Head for Graduate Education
Professor of Biochemistry and Molecular Biology

ABSTRACT

Many bacteria and eukaryotes can establish long-term, intimate associations, which are referred to as symbioses. The process by which symbiotic bacteria colonize, grow, and express specific symbiotic traits within a host is called symbiosis establishment. In many cases, the bacterial symbionts are also called beneficial bacteria because they express traits that confer fitness advantages to their eukaryotic hosts. Beneficial bacteria perform many functions from synthesizing essential vitamins within the human gut to inhibiting colonization by pathogenic microbes on epithelial surfaces. Because beneficial bacteria improve host physiology, it is important to increase understanding of how these microbes establish symbiosis with a host. The outcomes of such studies have the potential to facilitate the development of therapeutics and prebiotics that promote colonization by beneficial bacteria.

The symbiotic relationship between the Hawaiian bobtail squid, *Euprymna scolopes*, and the bioluminescent bacterium *Vibrio fischeri* offers a platform to study the molecular mechanisms that enable host-colonization by a beneficial microbe. *V. fischeri* inhabits the squid light organ and produces light via bioluminescence, which aids the squid in avoiding detection by prey. *V. fischeri* is horizontally transmitted, which means that the squid acquires the bacteria from an environmental reservoir. To successfully establish symbiosis with its host, *V. fischeri* must express specific traits that permit light organ colonization. The expression of these traits is regulated at the level of transcription by a special class of proteins called transcription factors. The alternative sigma factor σ^{54} is a transcription factor that allows bacteria to rapidly respond to changes in the environment by activating transcription of specific genes. A specialized type of transcription factor called a bacterial enhancer binding protein, or bEBP, is required for σ^{54} -dependent transcriptional activation. In *V. fischeri*, σ^{54} is absolutely required for cells to establish light organ symbiosis, suggesting there are also bEBPs that are implicated in this process. Currently, there exists a gap in

knowledge regarding the ways in which bEBPs function in *V. fischeri* to permit symbiosis establishment. The work presented in this dissertation addresses this knowledge gap by increasing understanding how two bEBPs regulate expression of a small RNA Qrr1 which promotes symbiosis establishment.

The experimental results provided here demonstrate that Qrr1 promotes symbiosis establishment by facilitating entry into the light organ. This work provides insight into how Qrr1 expression is regulated during the initial stages of light organ colonization. LuxO is a bEBP that activates expression of Qrr1, which is a small, regulatory RNA that post-transcriptionally inhibits the master regulator, LitR. LuxO activity is inhibited by quorum sensing, which is the process that describes how bacteria synthesize and detect of small, signaling molecules called autoinducers. As the number of cells within a population increases, so does the ambient concentration of autoinducer such that quorum sensing is a way for cells to gauge cell density. Autoinducers alter the activity of signaling networks in ways that effect changes in gene expression, which leads to the coordinated expression of specific traits, such as bioluminescence and motility, within a bacterial population. Because autoinducer concentrations increase with cell density, Qrr1 is typically not expressed in populations of *V. fischeri* that have reached a quorum. However, this work revealed that an additional bEBP, SypG, leads to increased *qrr1* transcriptional activity in a LuxO-independent manner. LuxO and SypG are homologs that share similar structures that suggest they depend on the same regulatory mechanisms. LuxO is active when *V. fischeri* are free-living in seawater, whereas SypG is active during the initial stages of host-colonization under conditions that are predicted to inhibit LuxO activity. *V. fischeri* has adapted to maintain these two homologous bEBPs as their overlapping functions are compartmentalized to different stages of the symbiont's lifecycle. These findings have expanded the model regarding how Qrr1 is transcriptionally regulated in *V. fischeri*.

V. fischeri is a member of the *Fischeri* clade within the *Vibrionaceae* family. The *Vibrionaceae* family consists of a diverse group of bacteria that include free-living, beneficial, and pathogenic microbes. This work also demonstrated that approximately half of the taxa within the *Vibrionaceae* encode homologs of LuxO and SypG and a least one *qrr* gene, which highlights the possibility that Qrr1 transcription is also activated by both bEBPs in other microbes. In addition, this work revealed that the fish pathogen *Aliivibrio salmonicida*, which is another member of the *Fischeri* clade, encodes a SypG homolog that can also induce P_{qrr1} activity from the promoter of its own *qrr1* gene. As Qrrs regulate symbiotic traits in other *Vibrios*, these finding suggests SypG and LuxO activation of *qrr* among the *Vibrionaceae* and warrants further investigation. Altogether, these studies have increased understanding of ways in which host-associated microbes utilize bEBPs to establish symbiosis.

TABLE OF CONTENTS

LIST OF FIGURES	viii
LIST OF TABLES	x
ACKNOWLEDGEMENTS	xi
Chapter 1: Introduction	1
Beneficial microbes confer fitness advantages to their host	1
The Squid- <i>Vibrio</i> symbiosis	2
The steps of light organ colonization by <i>V. fischeri</i>	3
σ^{54} is required for <i>V. fischeri</i> to colonize the light organ	7
The structure and function of bEBPs	8
The bEBP LuxO promotes symbiosis establishment	12
The bEBP SypG is required for symbiosis establishment	15
Investigating how LuxO and SypG promote symbiosis establishment through Qrr1	16
 Chapter 2: Investigating transcriptional activation of Qrr1 in quorum sensing populations of <i>V. fischeri</i>	 18
Introduction	18
Results	22
Qrr1 promotes access to crypt spaces	22
BinK inhibits Qrr1 transcriptional activity under quorum sensing conditions	25
The cellular aggregation pathway functions independently of Qrr1	30
The impact of BinK on Qrr1-regulated traits	32
BinK inhibits P_{qrr1} in <i>V. fischeri</i> cells within the light organ crypts	35
Factors that promote P_{qrr1} activation in the $\Delta binK$ mutant	36
Discussion	39
Methods	45
 Chapter 3: The bacterial enhancer binding proteins LuxO and SypG activate transcription of P_{qrr1}	 49
Introduction	49
Results	53
LuxO activation of P_{qrr1} depends on two UASs	53
SypG as a candidate bEBP of Qrr1 transcription	57
Overexpression of SypG is sufficient to activate P_{qrr1}	59
Signaling through the cellular-aggregation pathway impacts Qrr1 expression	61
Genetic elements that promote SypG activation of P_{qrr1}	64
Assessing cross-activation by LuxO and SypG	66
LuxO, SypG, and Qrr1 are conserved among the <i>Fischeri</i> clade	69
SypG activation of P_{qrr1} in <i>Aliivibrio salmonicida</i>	74
Conservation between LuxO and SypG in the <i>Vibrionaceae</i>	75
Discussion	78

Chapter 3: (continued)

Methods

81

Chapter 4: Perspectives and Future Direction

85

Appendix

97

References

112

LIST OF FIGURES

Figure 1.1: The squid light organ	3
Figure 1.2: The steps of light organ colonization	6
Figure 1.3: The LuxIR signaling network regulates bioluminescence in <i>V. fischeri</i>	7
Figure 1.4: Transcription initiation by σ^{54} and bEBPs	9
Figure 1.5: LuxO activates expression of Qrr1 at low cell densities	14
Figure 1.6: The cellular aggregation signaling network	16
Figure 2.1: The impact of Qrr1 on crypt colonization	24
Figure 2.2: Transposon mutagenesis screen identifies BinK as a negative regulator of Qrr1 transcription	27
Figure 2.3: BinK inhibits P_{qrr1} under quorum sensing condition	29
Figure 2.4: The impact of Qrr1 on cellular aggregation	31
Figure 2.5: BinK inhibits the ability of cells to access crypt spaces	33
Figure 2.6: The impact of BinK on Qrr1-regulated traits	34
Figure 2.7: BinK inhibits P_{qrr1} activity <i>in vivo</i>	36
Figure 2.8: Factors that promote $P_{qrr1-gfp}$ activity in the $\Delta binK$ mutant	38
Figure 2.9: Model of $qrr1$ transcription in <i>V. fischeri</i>	41
Figure 3.1: LuxO is a Group I bEBP of the <i>Vibrionaceae</i>	51
Figure 3.2: Genetic elements that promote LuxO activation of P_{qrr1}	54
Figure 3.3: LuxO activation of P_{qrr1} depends on two UASs	56
Figure 3.4: Amino acid alignment of LuxO and SypG	58
Figure 3.5: SypG is sufficient to activate P_{qrr1}	60
Figure 3.6: RscS promotes P_{qrr1} activation	62
Figure 3.7: RscS inhibits luminescence	63
Figure 3.8: Genetic elements that promote SypG activation of P_{qrr1}	65

Figure 3.9: Assessing cross-activation by LuxO and SypG	68
Figure 3.10: <i>luxO-uvrB</i> intergenic region in the <i>Fischeri</i> clade	70
Figure 3.11: SypG in the <i>Fischeri</i> clade	72
Figure 3.12: The potential for SypG activation of <i>qrr1</i> in the <i>Fischeri</i> clade	73
Figure 3.13: The potential for SypG activation of <i>P_{qrr1}</i> in <i>A. salmonicida</i>	74
Figure 3.14: LuxO, SypG, and <i>qrr</i> in the <i>Vibrionaceae</i>	76
Figure 3.15: Conservation of SypG-LuxO structural features in the <i>Vibrionaceae</i> family	77

LIST OF TABLES

Table 1: Strains	93
Table 2: Plasmids	94
Table 3: Primers	95

ACKNOWLEDGEMENTS

I am so grateful to everyone who encouraged and supported me on this journey. I could not have made it this far on my own. I would, first, like to thank my amazing husband, Steven Surret, who has supported me in every way imaginable during the last four years of my graduate studies. He motivates me to be the best version of myself and encourages me to accomplish whatever I set out to do. There were so many times I wanted to quit, but he pushed me to keep going so I could look back on this time and have no regrets. I could not have asked for a better person to “do life” with. To my two love-bugs, Zion and Zoey, whose hugs and cuddles remind me what really matters in life. I hope that my contributions to science will improve the world they inherit.

I thank my mom, Cheryl Reed, who encouraged me to take this opportunity in hopes it would provide a better life. She taught me that the world owes me nothing, and that whatever I want, I would have to work for. I’m still indebted to her for the many “counseling sessions” she gave during my time in graduate school. I thank my dad, Everett Reed, for his prayers and words of wisdom. He once said, “Don’t let someone else’s vision become my own”, which to me meant I must follow my own path and not one predetermined for me by someone else. I would also like to thank my aunts, uncles, cousins, and family friends who donated time and money to help me move from Mississippi to Pennsylvania. Knowing I had so many people supporting me helped get me through the difficult times. I also thank the members of Unity Church of Jesus Christ, who provided a home away from home my first few years in Pennsylvania.

I’m also grateful for the friends I’ve made at Penn State throughout my time in State College. I appreciated having people around to encourage me to persist through the challenges of graduate school. I would also like to thank many of the BMB department faculty for their advice, encouragement, and support. I extend a special thanks to Dr. Heather Giebink, Dr. Kristin Finch, and Dr. Stephanie Preston. They helped solve every issue I encountered in graduate school, and I

am immensely grateful for their help. I would also like to thank my graduate committee for their patience and for believing in my potential even when I struggled to believe in it myself. I'm fortunate to have had this team of accomplished scientists supporting me on this journey.

Lastly, I would like to thank the Miyashiro Lab. First, I thank Tim, who has served as both an advisor and mentor. Because of his training, I am confident I can excel in whatever discipline I pursue. I'm grateful to have had an advisor who was so invested in my success and who sacrificed time and effort to help me develop as a scientist. I also thank the members of the lab. Thanks to the lab manager, Andrew Cecere, who keeps the lab running smoothly so we can focus on our research. Thanks to the post-doctoral scholar Kirsten Guckes, who was always there to answer my questions and offer advice on everything ranging from the bench to the babies. A very special thanks to the undergraduate researcher turned post-baccalaureate scholar, Shyan Cousins, who was always available to help run assays, including those that required late nights. I could always count on Shyan's assistance, and for that, I am forever thankful to her. Her support and encouragement also helped me complete this degree, especially towards the end. It has been such an honor watching her grow into the researcher she is today. Thanks to all the undergraduates, graduate students, and post-docs who made working in the lab a pleasant experience.

Funding acknowledgements:

Bunton-Waller Fellowship

Alfred P. Sloan Scholarship

NIH R01 GM129133

Howard Hughes Medical Institute Gilliam Fellowship

Daniel R. Tershak Memorial Scholarship (Donor: Richard Nichol)

*The findings and conclusions do not necessarily reflect the view of the funding agency.

Chapter 1

Introduction

Beneficial microbes confer fitness advantages to their hosts

Bacteria are single-celled organisms that replicate and maintain homeostasis. They are ubiquitous in nature, and consequently, it is impossible for higher organisms to avoid encountering microbes. Many organisms, from plants to animals, establish long-term and intimate associations, *i.e.*, symbioses, with bacteria. These microbes can be transmitted either vertically, *i.e.*, from parent to offspring, or horizontally, which is when the host acquires bacteria from an external reservoir. Symbiotic bacteria can impact the physiology of their host in both positive and negative ways. Bacteria that cause disease are commonly referred to as pathogens, while those that confer some physiological advantage to their host are called beneficial microbes. Traditionally, efforts have been aimed at understanding how pathogens negatively impact host health [1-4]. However, an increasing amount of attention is being given to understanding the ways in which beneficial microbes improve the health of their host [5-8]. While many studies have elucidated mechanisms that enable pathogenic microbes to infect host tissues [9-11], more work is needed to better understand what factors allow beneficial microbes to colonize within or on a host organism. As beneficial microbes improve host physiology, it is advantageous to identify ways to promote their ability to colonize their hosts. This could potentially lead to the development of therapeutics designed to facilitate host-colonization by beneficial microbes, thereby improving host fitness. This work has revealed that a beneficial microbe employs a non-canonical method of gene regulation to express traits necessary for colonizing host tissues.

The Squid-*Vibrio* symbiosis

The complexity of the human anatomy coupled with the immense diversity of symbiotic microbes has led researchers to turn to simple model systems to better understand how beneficial microbes colonize hosts [12-14]. One such system is the mutualistic relationship that exists between the Hawaiian bobtail squid *Euprymna scolopes* and its horizontally-transmitted symbiont, the marine microbe *Vibrio fischeri*. *E. scolopes* is a tiny, bobtail squid found in coastal Hawaiian waters. Adults measure approximately 25 centimeters (cm) in length. *V. fischeri* is a gammaproteobacterial marine microbe that exists as free-living, planktonic cells or in symbiosis with fish and other squid species [15, 16]. *V. fischeri* colonizes a specific structure called the squid light organ, which is located beneath the squid's mantle cavity. The symbiotic function of *V. fischeri* is to produce light via bioluminescence from within the squid light organ (reviewed in [17, 18]). The squid light organ is attached to an ink sac, which can control the amount of light emitted based on the intensity of downwelling moonlight. This reduces the squid's silhouette and functions as a form of camouflage referred to as counterillumination, which is predicted to help the nocturnal squid evade detection by predators during their foraging hours [19]. Each dawn, the squid expel their light organ contents, which releases approximately 95% of *V. fischeri* from the light organ into the seawater. This daily event is commonly referred to as venting. The remaining bacteria replicate, and by the next evening, light-emitting populations of *V. fischeri* have been reestablished in the light organ. This vent-regrowth cycle continues such that the squid harbor clonal populations of the original *V. fischeri* symbionts throughout their life [20, 21].

The squid-*Vibrio* symbiosis serves as a model system for the study of factors that promote host-colonization by a beneficial microbe for several reasons. First, the initial steps of light organ colonization have been well characterized, including the spatial-temporal location of the bacteria during this process [22]. In addition, the symbiosis can be initiated in a lab, simply by adding squid

to an inoculum of bacteria [23]. Lastly, *V. fischeri* is genetically tractable, such that individual factors can be isolated and assessed for their role in light organ colonization [24, 25].

The steps of light organ colonization by *V. fischeri*

The symbiosis between the squid and *V. fischeri* is established early in the animal's lifecycle. Female squid lay eggs clutches that typically produce 50-250 offspring. Freshly hatched, or juvenile, squid emerge from egg clutches with uncolonized and immature light organs and acquire *V. fischeri* from the surrounding seawater [26, 27]. The light organ is a host structure with bilateral symmetry and features with two sets of ciliated appendages on either side. Located at the base of the appendages are three pores which open into an antechamber followed by narrow ducts, each leading to one of three epithelial-lined crypts. The crypts vary in size and development, with Crypt I being the largest and most developed crypt and Crypt III being the smallest and least mature (**Fig. 1.1**). These crypt spaces serve as the colonization sites for populations of *V. fischeri* [22]. The process of symbiosis establishment is a complex series of events and is divided into three stages: cellular aggregation, migration, and bioluminescence.

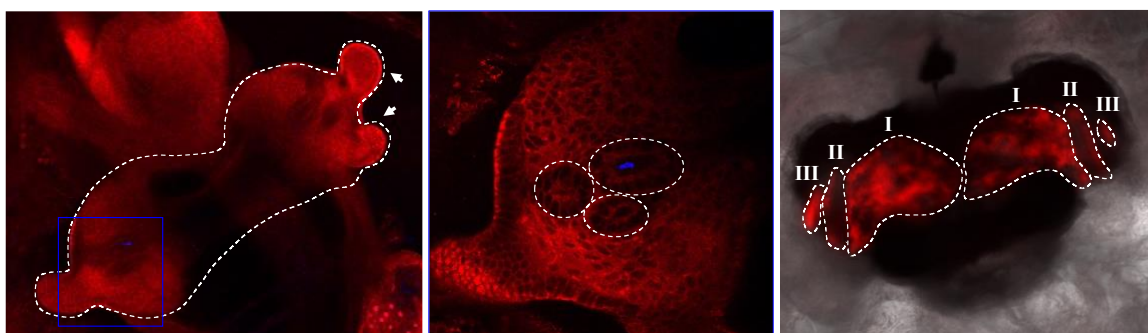


Figure 1.1: The squid light organ

Left, microscopy image of a juvenile squid light organ stained with Cell Tracker Orange. The arrows point to the two right appendages. The blue box highlights the location of the three pores. *Middle*, magnification of the left side of the light organ shows the three pores. The pores are outlined in white dashed ovals. An aggregate of *V. fischeri* cells harboring a cyan-fluorescent reporter, or CFP, (blue) can be seen within one of the pores. *Right*, a juvenile squid light organ harboring populations of *V. fischeri* expression the red fluorescent protein mCherry within each crypt (labeled I-III).

Cellular aggregation

The host anatomy enables coordinated recruitment of *V. fischeri*. Water is drawn into the squid mantle cavity via a siphon. Bacterioplankton and other cell-sized particles are captured within host-secreted mucus covering the light organ appendages and shuttled to a “shelter zone” located near the pores via the metachronal movement of long cilia [28]. Within 3.5 hours, *V. fischeri* secrete exopolysaccharide and become encased in a biofilm-like matrix to form densely packed cellular aggregates near the light organ pores (**Fig. 1.2**). Cells that lack the ability to form cellular aggregates are unable to colonize the light organ, suggesting this process is essential in establishing symbiosis [29]. Although several species of aquatic bacteria can be found within aggregates at the light organ exterior, *V. fischeri* cells outcompete these other microbes over time to become the dominant species [30].

Migration

Following aggregation, *V. fischeri* cells must swim through narrow ducts, traverse the light organ antechamber, and cross a physical bottleneck before entering the crypt spaces. Non-motile *V. fischeri* mutants are less efficient than wild-type (WT) cells at colonizing the light organ crypts, suggesting flagellar-mediated motility is necessary for cells to enter the light organ [31]. The migration of *V. fischeri* cells to the symbiotic site depends on chemotaxis towards host-derived chitin. Chemotaxis is the migration of bacterial cells towards specific chemoattractants, which are typically nutritional compounds. Chitin is a polymer of the monosaccharide *N*-acetylglucosamine (GlcNAc) and serves as a nutrient source for *V. fischeri*. The chemoattractant is produced by the host within the light organ interior and helps guide *V. fischeri* to the crypt spaces [32]. *V. fischeri* mutants unable to chemotax towards GlcNAc₂ have reduced colonization efficiency compared to WT cells, highlighting the significance of a functional chemotactic system during symbiosis initiation [32].

Only 1-2 *V. fischeri* cells are predicted to enter each crypt space [33]. These initial colonizers are referred to as “founder cells” and proliferate to establish clonal populations of the symbiont. The presence of *V. fischeri* within the crypts causes constriction of the physical bottleneck, restricting the number of additional cells that can pass through [22]. Microorganism-associated molecular patterns (or MAMPs), specifically the cell surface components lipopolysaccharide (LPS) and tracheal cytotoxin (TCT) shed by *V. fischeri* within the crypts, triggers morphological changes that result in regression of the ciliated appendages [34]. Thus, symbiotic populations of *V. fischeri* promote maturation of the squid light organ.

Bioluminescence

As the concentration of *V. fischeri* cells within the crypts increases, the bacteria begin to produce light via bioluminescence [15]. Bioluminescence production depends on quorum sensing, a process in which bacterial cells sense the presence of kin via the detection of small, signaling molecules called autoinducers (AIs). AIs freely diffuse across the cell membrane such that bacteria can sense AI produced by self and neighboring microbes, *i.e.*, the “sensing” of the quorum. The binding of AIs to their cognate receptors typically leads to changes in gene expression either directly by complexing with transcription factors to modulate their activity or indirectly, via signaling cascades. The accumulation and proliferation of AI-producing cells leads to elevated concentrations of autoinducer within a bacterial population, thus increasing the opportunity for AI to interact with their cognate receptors within all members of the populations [35]. As a result, the quorum of cells can coordinate gene expression to collectively express specific traits [36-39].

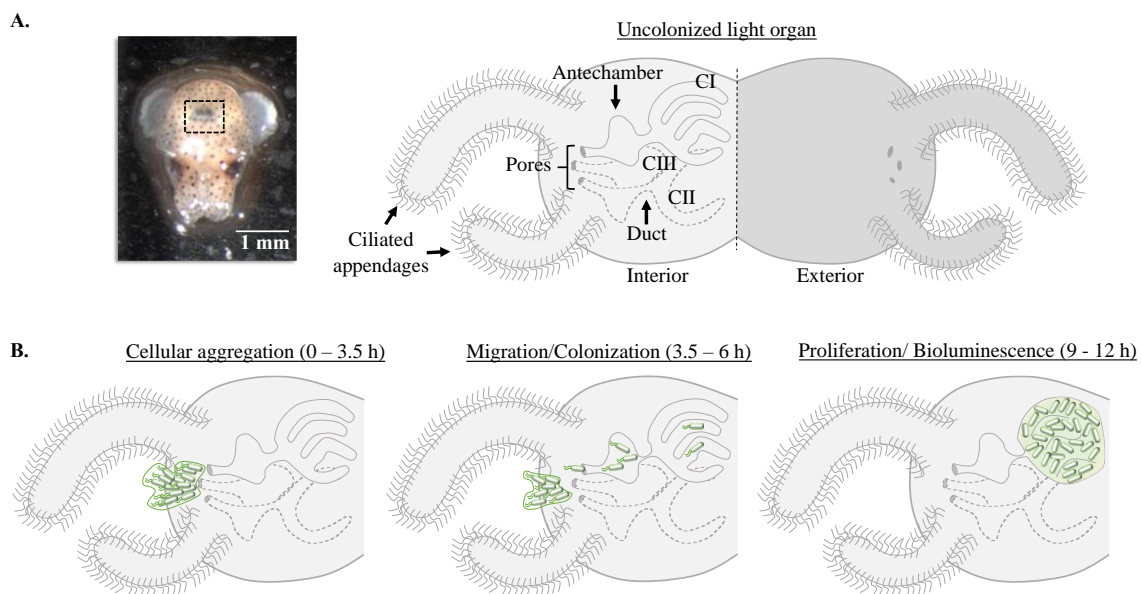


Figure 1.2: The steps of light organ colonization

- A. *Left*, Image of a juvenile squid. The light organ is outlined in a black dashed box. *Right*, A cartoon image showing the interior and exterior features of the squid light organ. CI, CII, and CIII represent Crypt I, Crypt II, and Crypt III, respectively.
- B. The stages of light organ colonization. **Cellular aggregation:** Within 3.5 hours of *V. fischeri* cells encountering the squid light organ, the cells aggregate within the shelter zone and produce an extracellular exopolysaccharide matrix at the light organ pores. **Migration/Colonization:** Between 3.5 – 6 hours, the cells escape the aggregate and, using flagella-mediated motility, swim into the light organ crypts. Only 1-2 cells are predicted to enter the light organ crypts. The presence of these “founder cells” within the crypt spaces triggers morphological changes in which the light organ ducts constrict, leading to a physical bottleneck that prohibits subsequent colonization by additional *V. fischeri* cells. **Proliferation/Bioluminescence:** Between 9 -12 hours, the founder cells proliferate to establish bioluminescence-emitting populations of *V. fischeri* within the light organ crypts.

In *V. fischeri*, bioluminescence is regulated via the LuxIR quorum sensing system (**Fig. 1.3**). LuxI synthesizes the AI *N*-(3-oxo-hexanoyl)-L-homoserine lactone (3OC6), which binds the transcription factor LuxR. When bound by 3OC6, LuxR activates expression of the *luxICDEBAG* (*lux*) operon, which encodes enzymes necessary for the light-producing reaction [40-42]. *V. fischeri* cells within the light organ crypts produce 3OC6, and the concentration of AI increases with proliferation of the symbiont. As a result, LuxR activation of the *lux* operon increases within quorum sensing populations of *V. fischeri*. Transcriptional activation of the *lux* operon results in

increased *luxI* expression, and consequently, more 3OC6 is synthesized and available to bind LuxR. This creates a positive feedback loop generating high levels of bioluminescence per cell [43]. Cells that lack the ability to produce light are eliminated from the light organ over time, suggesting that bioluminescence production is required for *V. fischeri* to maintain symbiosis with its host [44, 45]. The LuxIR quorum sensing signaling network ensures *V. fischeri* cells only produce light when advantageous, such as when inhabiting the squid light organ, thereby preserving cellular energy.

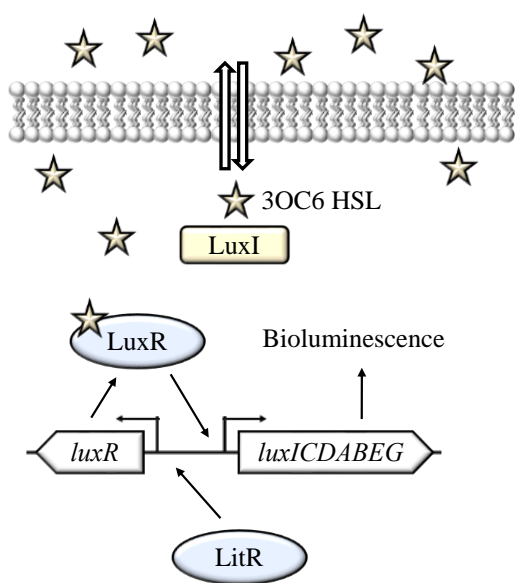


Figure 1.3 The LuxIR signaling network regulates bioluminescence in *V. fischeri*

In *V. fischeri*, LuxI synthesizes the autoinducer 3OC6, which freely diffuses across the cell membrane. 3OC6 binds LuxR within the cytoplasm. LuxR transcription is enhanced by the transcription factor LitR. The LuxR-3OC6 complex promotes transcription of the *lux* operon, which encodes factors required to produce light via bioluminescence. The *lux* operon also encodes LuxI, and therefore, expression of the *lux* operon results in a positive feedback loop that leads to increased production of 3OC6.

σ^{54} is required for *V. fischeri* to colonize the light organ

V. fischeri cells must express specific traits at each stage of light organ colonization to successfully establish symbiosis. The expression of traits is governed by changes in gene expression, which is mediated by transcription factors. In bacteria, transcription of genes depends on the RNA polymerase (RNAP) and an additional protein called a sigma factor. Sigma factors bind RNAP, forming a holoenzyme, and function to direct RNAP to specific sequences called promoters located upstream the transcriptional start site (designated as +1) of target genes [46, 47]. While the σ^{70} family of sigma factors regulates the expression of genes involved in growth and metabolism, the alternative sigma factor σ^{54} , which is encoded by *rpoN*, promotes transcription of

genes in response to external stimuli such as environmental signals and stressors [48, 49]. In *V. fischeri*, σ^{54} is absolutely required for *V. fischeri* for cells to colonize the host light organ [50, 51]. Currently, there is a gap in knowledge regarding how σ^{54} -dependent transcription regulates the expression of genes governing traits that facilitate the early stages of light organ colonization.

The σ^{54} factor recognizes and binds the consensus sequence GG and TGC located at the -24 and -12 positions, respectively [52]. When bound to the promoter, a portion of σ^{54} blocks DNA from entering the activate site of RNAP. To initiate transcription requires an activator protein, which contacts σ^{54} via DNA bending and induces a conformational change that displaces the sigma factor from the RNAP active site. Additionally, the activator is predicted to facilitate DNA melting at the -12 position by rearranging σ^{54} such that the DNA is appropriately positioned for transcription initiation to proceed [53]. Therefore, activator proteins are absolutely required for σ^{54} -dependent transcription activation to occur.

The structure and function of bEBPs

The activator proteins in bacteria that are necessary for σ^{54} -dependent transcription are called bacterial enhancer binding proteins (bEBPs). bEBPs are members of the AAA+ family of proteins, which hydrolyze ATP, which can hydrolyze ATP for various cellular process such as protein modifications and DNA synthesis and repair [54]. These bEBPs typically have an N-terminal signal sensing receiver (R) domain, a central catalytic ATPase (C) domain, and a C-terminal DNA-binding (D) domain. bEBPs are classified into one of five groups based on the organization of these three domains (reviewed in [55]). While the signaling mechanisms of the R domain and the presence of the D domain vary among groups, the C domain is highly conserved and is absolutely required to mediate transcriptional activation by σ^{54} . This work focuses on the regulatory mechanism by which two group I bEBPs promote *V. fischeri* colonization of the squid light organ (**Fig. 1.4**).

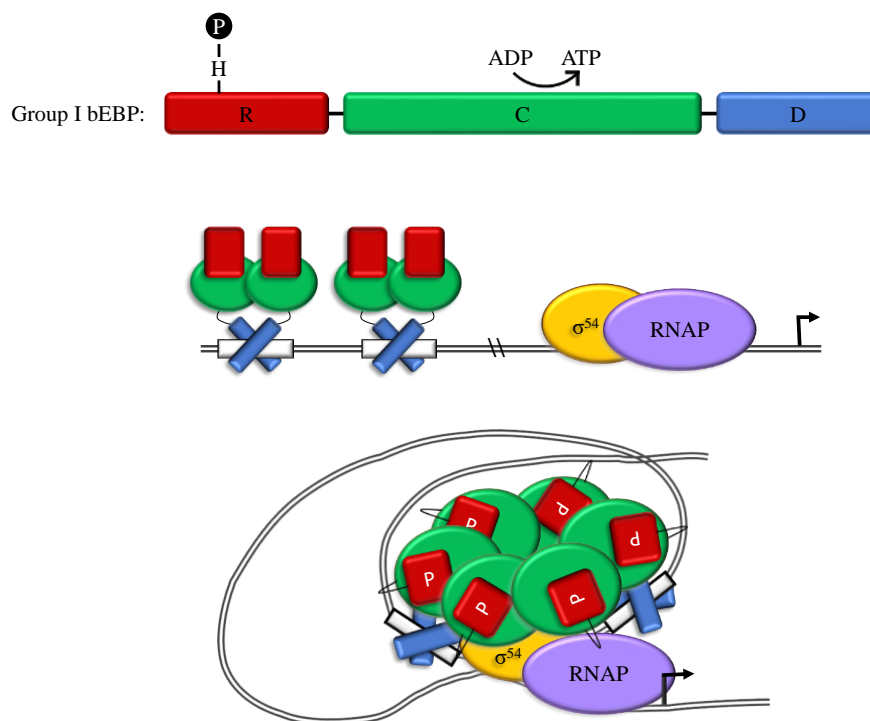


Figure 1.4: Transcription initiation by σ^{54} and bEBPs

Top: Group I bEBPs contain a N-terminal receiver (R) domain which contains a conserved histidine residues which is the site of phosphorylation, a central catalytic ATPase (C) domain which hydrolyzes ATP into ADP, and a C-terminal DNA-binding (D) domain. *Middle:* bEBPs recognizes upstream activating sequences (UASs) within the promoter of target genes. bEBP bind as dimers at UASs (white rectangles). *Bottom:* bEBP hexamers interact with σ^{54} . Phosphorylation of the receiver domain drives conformational changes that permit ATP binding. ATP hydrolysis provides the energy necessary for remodeling σ^{54} , which allows for open complex formation.

The receiver domain (R) of group I bEBPs contains a phosphorylation site and are typically part of two component signaling (TCS) systems. TCSs consist of a histidine kinase (HK) and a response regulator (RR). In the archetypical HK-RR system, the detection of a specific environmental signal causes the HK to autophosphorylate on a conserved histidine (H) residue. This phosphoryl group is then transferred to an aspartate (D) residue within the RR. The signaling cascade can continue if the RR donates a phosphate to the histidine of another RR or end in alterations in gene expression if the RR is a transcription factor. For example, the bEBP NtrC is

phosphorylated within the R domain by the HK, NtrB, under nitrogen-limiting conditions and activates the expression of genes involved in nitrogen assimilation [56, 57]. As the flow of phosphates can be reversed depending on the presence or absence of environmental signals, phosphorylation within the R domain of group I bEBPs enables cells to rapidly adapt to changing conditions in a way that promotes cellular fitness.

The primary molecular function of bEBPs is to relocate σ^{54} , such that the inhibitory interaction of σ^{54} at the promoter is abolished [58]. This occurs through ATP binding and hydrolysis, which is carried out within the central ATPase (C) domain [59, 60]. Residues within this domain also facilitate oligomerization [61]. The C domain of a bEBP typically multimerizes as a hexamer with the ATP active site located at the interface of bEBP protomers. Therefore, oligomerization is required for ATPase activity [62, 63]. DNA-bending allows the bEBP hexamer to contact σ^{54} (**Fig. 1.4**). This interaction with σ^{54} depends on the GAFTGA motif, which is conserved within the C domains of all bEBPs. ATP hydrolysis relocates the GAFTGA motif, effecting a conformational change that alleviates the inhibitory interactions of σ^{54} at the promoter [64-66]. Therefore, the GAFTGA motif couples ATP hydrolysis with open complex formation and is essential to drive σ^{54} -dependent transcription [53, 55].

The activity of the C domain can be regulated by the R domain. BEBPs exhibit either positive or negative modes of regulation. In negative regulation, the R domain forms inhibitory interactions with the C domain that inhibits oligomerization such that ATP binding and hydrolysis cannot occur, and phosphorylation alleviates this repression. For example, in *Aquifex aeolicus*, the R and C domains of the bEBP NtrC1 form repressive interactions in which the C domain protomers are locked in an inhibitory front-to-front conformation [67]. Phosphorylation disrupts this interaction, and the protomers are rearranged to a productive back-to-front conformation that permits ATP binding and hydrolysis. Deletion of the R domain results in a constitutively active protein. The bEBP DctD of *Sinorhizobium meliloti* employs a similar regulatory mechanism [63,

67-70]. In positive regulation, signal sensing by the R domain promotes oligomerization. NtrC of *Salmonella typhimurium* binds the promoter as a dimer. Phosphorylation of the R domain results in hexamerization, which permits ATP binding and hydrolysis. Mutants lacking the R domain are trapped in an inactive conformation and fail to initiate transcription [55, 71, 72]. Residues within the R domain can also interfere with ATPase activity and disrupt interactions with σ^{54} [60, 73, 74].

The DNA-binding (D) domain of group I bEBPs is connected to the C domain by a variable linker. This domain also contains a helix-turn-helix (HTH) motif, which is predicted to bind DNA [75]. In most cases, such as in NifA of *Klebsiella pneumoniae*, the second helix harbors residues that interact directly with DNA, and is thus referred to as the recognition helix [76]. BEBPs recognize specific sites, called upstream activating sequences (UASs) that are located 80-150 base pairs upstream the +1 start site of target genes (**Fig. 1.4**). These usually consist of inverted palindromic repeats where each half-site serves as a dock for a single recognition helix. Therefore, the bEBPs bind as dimers at each UAS, and these dimerization determinants are also located in the D domain. Some σ^{54} -dependent genes possess two or more UASs. The presence of multiple UASs is predicted to increase the concentration of bEBP dimers at promoters of their target genes to facilitate oligomerization. Furthermore, UASs confer specificity for their cognate bEBPs [53, 55, 77-79].

bEBPs and σ^{54} regulate genes involved in processes such as motility, biofilm formation, stress response, and nutrient utilization in a variety of bacterial species, including *V. fischeri* [48, 80-82]. As *V. fischeri* cells transition from the seawater to the host, specific traits must be expressed to permit light organ colonization. Because *V. fischeri* depends on σ^{54} to establish symbiosis, this suggests there are one or more bEBPs regulating the expression of symbiotic traits in response to changing environmental conditions. This work addresses how two bEBPs function in *V. fischeri* to promote host colonization.

The bEBP LuxO promotes symbiosis establishment

The activity of bEBPs is modulated by signaling networks activated by environmental signals. Consequently, bEBPs enable cells to respond to these signals by effecting changes in gene expression through σ^{54} -dependent transcriptional regulation [55]. In *V. fischeri*, the bEBP LuxO integrates information regarding cellular density to regulate the expression of specific traits [83]. LuxO is a 476-amino acid Group I bEBP. Under conditions of low AI concentrations, LuxO is phosphorylated on an aspartate residue (D55) within the receiver domain [84, 85]. Based on studies of the LuxO homolog in *Vibrio angustum*, LuxO employs a unique method of regulation in which a 20-aa linker connecting the R and C domains occupies the ATP active site [62]. Phosphorylation of LuxO results in a conformational change that displaces the linker and allows for ATP binding and hydrolysis [62].

V. fischeri produces two autoinducers known to affect LuxO activity (**Fig. 1.5**) [85, 86]. The first, *N*-(3-oxo-octanoyl)-L-homoserine lactone (C8) is synthesized by AinS and binds the membrane-bound hybrid HK AinR. The second is the furanosyl-borate diester Autoinducer-2 (AI-2), which is synthesized by LuxS and binds the periplasmic protein LuxP. LuxP contacts the membrane-bound hybrid HK LuxQ. Binding of AI-2 to LuxP results in a conformational change that stimulates the phosphatase activity of LuxQ [87, 88]. Similarly, AinR also functions as a phosphatase when bound by its respective ligand. Conversely, the two HK exhibit kinase activity at low concentrations of AI. In the absence of AI, both AinR and LuxQ autophosphorylate on a conserved histidine residue within the histidine phosphotransfer (Hpt) domain, and this phosphoryl group is transferred to an aspartate within the RR domain [86, 88, 89]. Both HKs, then, shuttle phosphates to a histidine residue in the N-terminal region of LuxU, which then phosphorylates LuxO [90]. Therefore, the phosphorylation state, and thus activity, of LuxO is regulated by the AIs AI-2 and C8 through LuxPQ and AinR, respectively.

LuxO activates expression of a small, regulatory RNA, Qrr1. In *V. fischeri*, Qrr1 is 106 nucleotides in length [83]. LuxO is predicted to recognize two UASs upstream of the *qrr1* gene with the consensus sequence TTGCA-N₃-TGCAA [91]. When expressed, Qrr1 post-transcriptionally inhibits expression of the master regulator LitR, which activates expression of LuxR [92]. Qrr1 forms base pairs with the 5' untranslated region (UTR) of LitR mRNA, and this interaction is stabilized by the chaperone protein Hfq. Binding of Qrr1 to LitR mRNA is predicted to block the ribosome binding site (RBS). As a result of this binding, the mRNA is not transcribed but is instead targeted for degradation by RNAses, thus lowering expression of LitR protein in the cell [91, 93]. Consequently, *luxR* expression decreases which reduces the capacity of cells to respond to 3OC6 and produce light. Consistent with this model, *V. fischeri* cells lacking *luxO* or *qrr1* have increased bioluminescence in the presence of 3OC6, suggesting the LuxO-Qrr1 regulatory module inhibits light production [83].

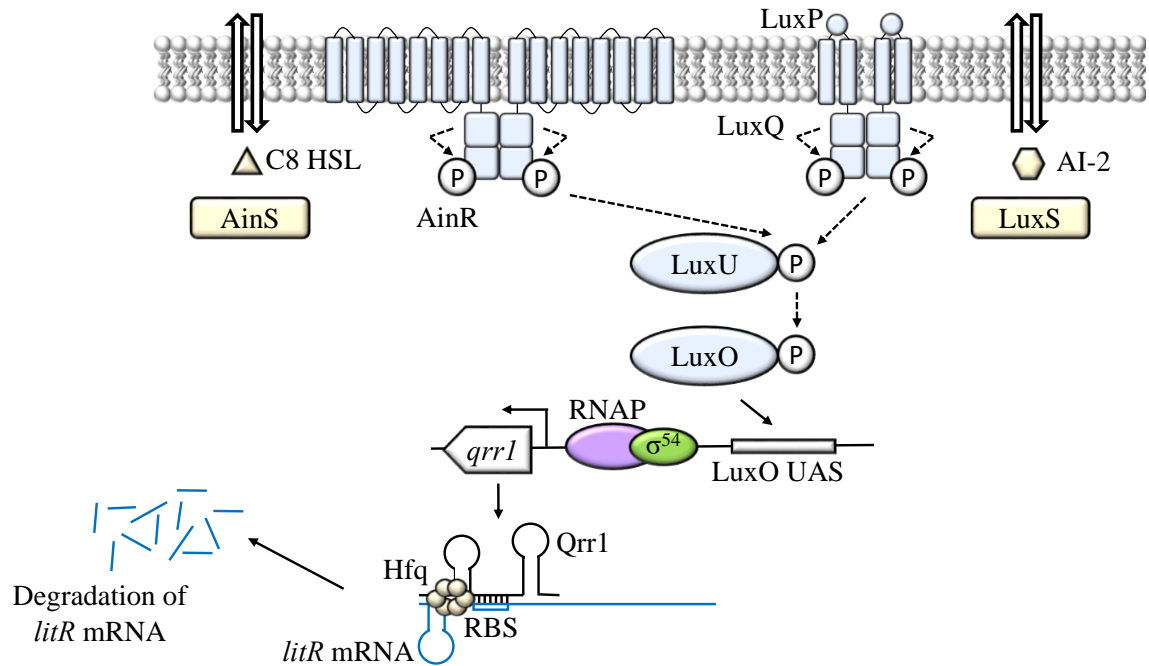


Figure 1.5: LuxO activates expression of Qrr1 at low cell densities

AinS and LuxS synthesize the autoinducers C8 HSL and AI-2, respectively. AinR is the receptor for C8 HSL, and LuxP senses AI-2, which transduces the signal to LuxQ. In the absence of their cognate autoinducers, AinR and LuxQ function as kinases and shuttle phosphates to LuxU, which phosphorylates LuxO. LuxO binds an upstream activating sequence (UAS) and facilitates σ^{54} -dependent activation of *qrr1*, which encodes a small regulatory RNA. When expressed, Qrr1 makes base pair interactions with the ribosome binding site (RBS) of *litR* mRNA. This interaction is stabilized by the chaperone protein Hfq. Qrr1 binding to *litR* destabilizes the mRNA, leading to its degradation. Therefore, LitR is not translated into a functional protein under conditions of low cell density.

LuxO also impacts symbiosis establishment. When juvenile squid were exposed to a mixed inoculum containing wild-type (WT) *V. fischeri* and $\Delta luxO$ mutants, fewer $\Delta luxO$ cells were recovered from the light organs of homogenized squid, suggesting LuxO confers an advantage to cells when colonizing the light organ. *V. fischeri* cells that lack the gene encoding Qrr1 also exhibit reduced colonization efficiency when competed against WT cells, suggesting LuxO functions through Qrr1 to promote symbiosis establishment [83]. Furthermore, these results suggest Qrr1 must be expressed during the initial stages of light organ colonization.

The bEBP SypG is required for symbiosis establishment

SypG is another Group I bEBP in *V. fischeri* required for successful light organ colonization. *V. fischeri* Δ *sypG* mutants are unable to establish symbiosis [94]. SypG activates σ^{54} -dependent transcription of the 18-gene symbiotic polysaccharide (*syp*) locus (**Fig. 1.6**), which encodes factors required for the cellular aggregation stage [29]. SypG binds UASs within the *syp* locus, which are located upstream of *sypA*, *sypI*, *sypM*, and *sypP* [80, 95]. SypG is regulated by several factors. First, the HK RscS autophosphorylates on a histidine (H) residue in response to some unknown host signal. The phosphate is transferred to an intramolecular aspartic acid (D) residue, then donated to a histidine with the Hpt domain of the HK SypF [96]. SypF phosphorylates SypG on an aspartic acid within the receiver domain, which enables SypG to activate σ^{54} -dependent activation of the *syp* locus [96-98]. In addition, the HK BinK inhibits calcium-dependent biofilm formation through an unknown mechanism that involves SypG [99, 100]. Altogether, these studies highlight that SypG activity is altered by signaling networks that respond to both host-produced and environmental signals.

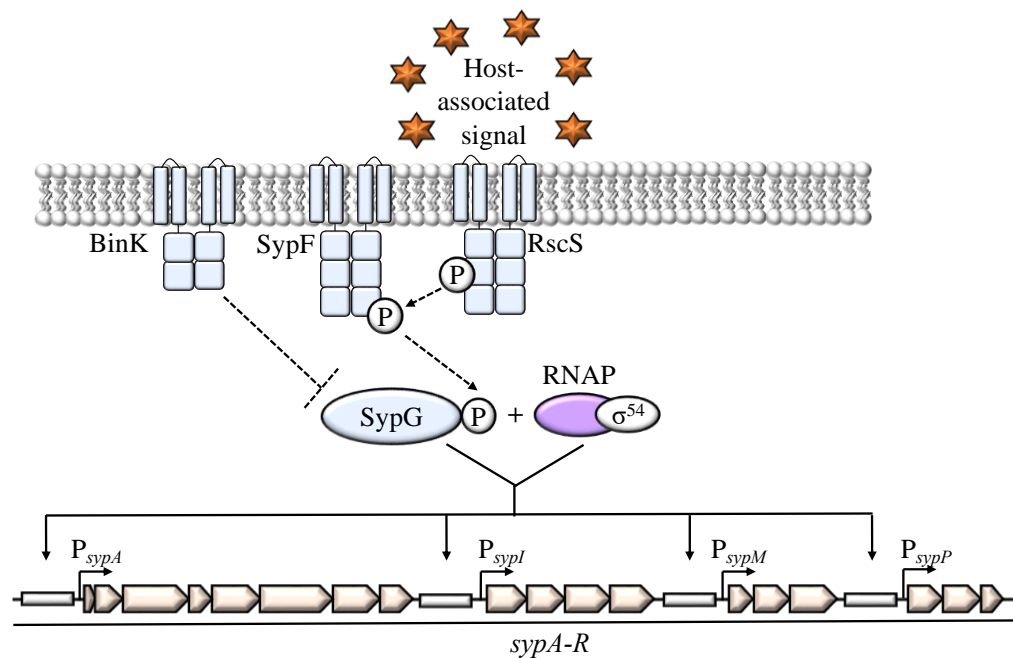


Figure 1.6 The cellular aggregation signaling network

Detection of a host-associated signal results in autophosphorylation of RscS, which donates a phosphate to SypF. SypF phosphorylates SypG. SypG recognizes UASs (white boxes) upstream of four separate operons to activate σ^{54} -dependent transcription of the *syp* locus.

Investigating how LuxO and SypG promote symbiosis establishment through Qrr1

Transcriptional regulation by σ^{54} and bEBPs enables cells to express specific traits under select conditions, such as when cells are initiating symbiosis with a host. Because the expression of these traits facilitates the establishment and maintenance of host-microbe interactions, it is important to increase understanding of how σ^{54} and bEBPs are integrated into the signaling networks that regulate these behaviors. Both LuxO and SypG promote σ^{54} -dependent transcription of genes encoding factors that promote symbiosis establishment, suggesting the two bEBPs are active during the initial stages of light organ colonization. SypG is absolutely required for cells to produce the polysaccharide matrix that encapsulates aggregates of *V. fischeri* at the light organ pores [97]. Short cilia near the pores are predicted to facilitate mixing of biochemical signals

produced by aggregating cells, suggesting quorum sensing might occur within the aggregates [26, 28]. While LuxO also promotes symbiosis establishment, it is unclear how LuxO can activate σ^{54} -dependent transcription of Qrr1 when the cells are potentially exposed to AI within the aggregate. Therefore, the studies described in this dissertation were designed to determine how Qrr1 is expressed during early symbiosis establishment. The activity of LuxO and SypG is regulated by two distinct signaling networks. However, this work revealed that these two signaling networks intertwine at Qrr1 as SypG can activate expression of the small, regulatory RNA independently of LuxO. These findings highlight that in *V. fischeri*, activation of the biofilm formation pathway enables cells to bypass quorum-sensing mediated repression of Qrr1 expression. Furthermore, there is evidence this two bEBP activation model is widely conserved across the *Vibrionaceae*. Overall, these studies increased understanding of how bEBPs and σ^{54} function to facilitate light organ colonization. This knowledge could potentially lead to the development of therapeutics aimed to enhance the ability of clinically relevant microbes to establish symbiosis with a host.

Chapter 2

Investigating transcriptional activation of Qrr1 in quorum sensing populations of *V. fischeri*

Introduction

Beneficial bacteria are microbes that associate with an organism and express traits that confer some physiological advantage to its host [101]. Many beneficial microbes are horizontally transmitted, which means the hosts acquires them from an external reservoir. Once acquired, these bacteria typically migrate to a specific location within the host anatomy, such as the gut, where they perform their symbiotic functions. As beneficial microbes migrate from an external reservoir to the symbiotic site of their host, they encounter a range of biochemical compounds produced by the host and, often, other microbes in the vicinity. The detection of these compounds activate complex signaling networks, leading to changes in gene expression. These changes in gene expression alter bacterial physiology, which promotes their acclimation to the specific environment. As a result, the bacteria can colonize the symbiotic site and be maintained within the host. However, there currently exist gaps in knowledge regarding how signaling networks function during the initial stages of host-colonization by symbiotic bacteria. Understanding the molecular mechanisms by which beneficial microbes establish symbiosis could lead to the development of therapeutics that promote this process, resulting in improved host physiology.

The mutually beneficial symbiosis between the Hawaiian bobtail squid and the marine microbe *Vibrio fischeri* offers a platform to study how signaling networks function during the initial stages of symbiosis establishment. *V. fischeri* cells emit light via bioluminescence from the squid light organ [27]. This light is predicted to aid the squid in avoiding detection by prey during its nocturnal activities [19]. *V. fischeri* is the only bacteria capable of colonizing the squid light organ [102]. Therefore, the process of symbiosis establishment can be observed without concern for competition from non-symbiotic microbes.

The initial steps of symbiosis have been extensively studied (reviewed in [17], **Fig. 1.2B**). Juvenile squid, or squid that have freshly hatched, acquire *V. fischeri* cells from the seawater. Within three hours of the two partners meeting, *V. fischeri* cells aggregate and form a biofilm-like matrix near the light organ pores. This site of cellular aggregation is referred to as the shelter zone where it is predicted host cilia facilitate the mixing of host-derived and bacterial biochemicals [28]. Cellular aggregation depends on expression of the *syp* locus, which contains 18 genes necessary for polysaccharide biosynthesis (**Fig. 1.6**) [29]. Next, *V. fischeri* cells escape the aggregate and, using flagellar-mediated motility, migrate towards a chitin gradient within the light organ crypts [32]. Only 1-2 cells are predicted to enter the crypt spaces, and these founder cells trigger morphological changes in the host light organ that inhibit subsequent colonization by additional cells [22, 33]. As these cells proliferate within the light organ crypts, they produce increasing amounts of signaling molecules called autoinducers (AIs). Binding of AIs to their cognate receptors alters the activity of signaling networks and allows for the coordinated expression of genes within a population, such as those required for bioluminescence. This process is called quorum sensing, and when cells sense when a quorum of cells has been established, they collectively emit light from within the light organ crypts [85, 103].

Three signaling networks that respond to separate autoinducers influence the expression of genes required for bioluminescence in *V. fischeri*. Direct regulation occurs via the LuxIR signaling network [42] (**Fig. 1.3**). LuxR is the receptor for the AI *N*-3-oxohexanoyl homoserine lactone (3OC6), which is synthesized by LuxI. In complex with 3OC6, LuxR binds upstream of the *luxICDABEG*, or *lux*, operon which encodes the luciferase enzymes that drive light production. As LuxI is also encoded within the *lux* operon, the detection of 3OC6 results in a positive feedback loop, resulting in increased bioluminescence levels per cell. LuxR expression is activated by the TetR-like transcription factor LitR [85, 92, 104]. The two other AI-regulated signaling networks, AinSR and LuxS/PQ, promote bioluminescence by controlling transcription of a small RNA, *Qrr1*,

which negatively regulates expression of light genes via post-transcriptional inhibition of LitR [83] (**Fig. 1.5**). AinS and LuxS synthesize the autoinducers *N*-3-octanoyl homoserine lactone (C8) and Autoinducer-2 (AI-2), respectively. When unbound by their respective ligands, AinS and LuxPQ functions as kinases, and a phosphorelay cascade is activated, which results in phosphorylation of LuxO [86, 89]. Phosphorylated LuxO activates σ^{54} -dependent transcription of the *qrr1* gene. Qrr1, assisted by Hfq, binds the untranslated region (UTR) of LitR mRNA, which destabilizes the transcript and targets it for degradation. Consequently, LitR-dependent activation of *luxR* decreases, which impedes the ability of the cells to sense 3OC6, resulting in lower levels of bioluminescence per cell. Increasing concentrations of C8 and AI-2 reverses phosphate flow, reducing LuxO~P levels, and thus, expression of Qrr1 sRNA [83, 91]. These AI-regulated signaling promote the conservation of cellular energy by ensuring light is only produced during the symbiotic stage of the *V. fischeri* life cycle when cells are within the nutrient-rich light organ.

The AinSR and LuxS/PQ signaling networks also modulate expression of genes required for light organ colonization through the Qrr1-LitR regulatory connection (**Fig 1.5**). When juvenile squid were exposed to a mixed inoculum of wild-type (WT) *V. fischeri* cells and a $\Delta litR$ mutant, more $\Delta litR$ colony-forming units (CFU) were recovered from the light organ of homogenized squid, suggesting that LitR inhibits factors that promote symbiosis establishment [83]. However, when a $\Delta qrr1$ mutant served as the competitor strain, more WT CFU were recovered. Light organ cellular abundance of a $\Delta litR \Delta qrr1$ mutant was comparable to that of a WT strain, suggesting LitR-inhibited colonization factors are expressed [83]. Together, these data provide evidence that Qrr1 promotes symbiosis establishment through its post-transcriptional inhibition of LitR. Furthermore, this suggests Qrr1 expression is integral to the symbiotic stage of *V. fischeri*.

Because of its central location within the AinSR and LuxS/PQ signaling networks and its influence on LitR levels, Qrr1 enables cells to quickly alter gene expression in response to changing AI concentrations in the environment. Exogenously added C8 in concentrations as low as 50

picomolar is sufficient to decrease the activity of a Qrr1 transcriptional reporter in cultures of *V. fischeri* [105]. These data suggest activation of *qrr1* transcription is easily influenced by C8 concentrations. During symbiosis establishment, *V. fischeri* cells are exposed to varying, and sometimes unpredictable, concentrations of AI produced from other cells within the aggregate. Because Qrr1 must be expressed to prevent LitR-inhibition of colonization factors, exposure to AI could jeopardize the ability of *V. fischeri* cells to establish symbiosis. This study was designed to determine when during symbiosis establishment is Qrr1 expressed and to yield insight regarding how *qrr1* transcription is regulated during this process.

Results

Qrr1 promotes access to crypt spaces

The finding that more $\Delta qrr1$ than WT CFU were recovered from the light organ of homogenized squid suggests Qrr1 expression facilitates colonization of the crypt spaces. However, what remained unclear was precisely how expression of Qrr1 influences the biogeography of *V. fischeri* crypt populations. Homogenizing whole animals results in a loss of information regarding the composition of *V. fischeri* populations within the light organ crypts. However, juvenile squid can be dissected to reveal the light organ crypt, which can then be imaged by fluorescence microscopy [44, 106-108]. Because only 1-2 cells are predicted to enter the crypts [33], the identity of these founder cells can be inferred by observing established populations of *V. fischeri* within the light organ. To determine whether expression of Qrr1 impacts the location of *V. fischeri* populations within the light organ, a co-colonization assay was conducted in which juvenile squid were exposed to an equal inoculum of WT *V. fischeri* cells and $\Delta qrr1$ mutants labeled with a cyan fluorescent protein (CFP-WT) and a yellow fluorescent protein (YFP- $\Delta qrr1$). After light organ colonization had occurred, each animal was dissected to reveal the light organ and imaged to determine the location of each strain type (**Fig. 2.1A**). Each colonized crypt was scored as CFP+ (WT only), YFP+ ($\Delta qrr1$ only), or CFP+/YFP+ (both strain types). When animals were exposed to a mixed inoculum of CFP-WT cells and YFP- $\Delta qrr1$ mutants, the majority of crypts (99/104) combined within the group were singly colonized by one strain type, suggesting each crypt was primarily founded by one strain type. When assessing each individual animal, fewer crypts per squid contained the YFP- $\Delta qrr1$ mutant relative to CFP-WT cells, suggesting fewer $\Delta qrr1$ mutants founded the populations relative to WT cells. (**Fig. 2.1B,C**). More specifically, only 21/104 crypts contained YFP- $\Delta qrr1$, whereas 88/104 crypts harbored CFP-WT. These results reveal the light organ crypts contained fewer crypt colonized by the YFP- $\Delta qrr1$ mutants, which suggests fewer founder cells were of this strain type. Furthermore, this data suggest expression of Qrr1 enhances

a cell's ability to access the light organ crypts. In the control group where animals were exposed to an equal inoculum of differentially labeled wild-type cells, the number of crypts per animal colonized by each strain type was roughly equal (**Fig. 2.1C**), suggesting the presence of the fluorophore did not have an impact on the ability of *V. fischeri* cells to access the light organ. Together, these results indicate Qrr1 enables cells to access more crypts than a competitor strain, which leads to a competitive advantage. Qrr1 promotes motility [109], which is necessary for *V. fischeri* to initiate light organ colonization [31]. Therefore, cells expressing Qrr1 likely have an advantage in accessing the light organ crypts compared to those that do not express Qrr1, possibly by enhancing motility. Altogether, these data also imply must be Qrr1 expressed prior to cells entering the crypt spaces.

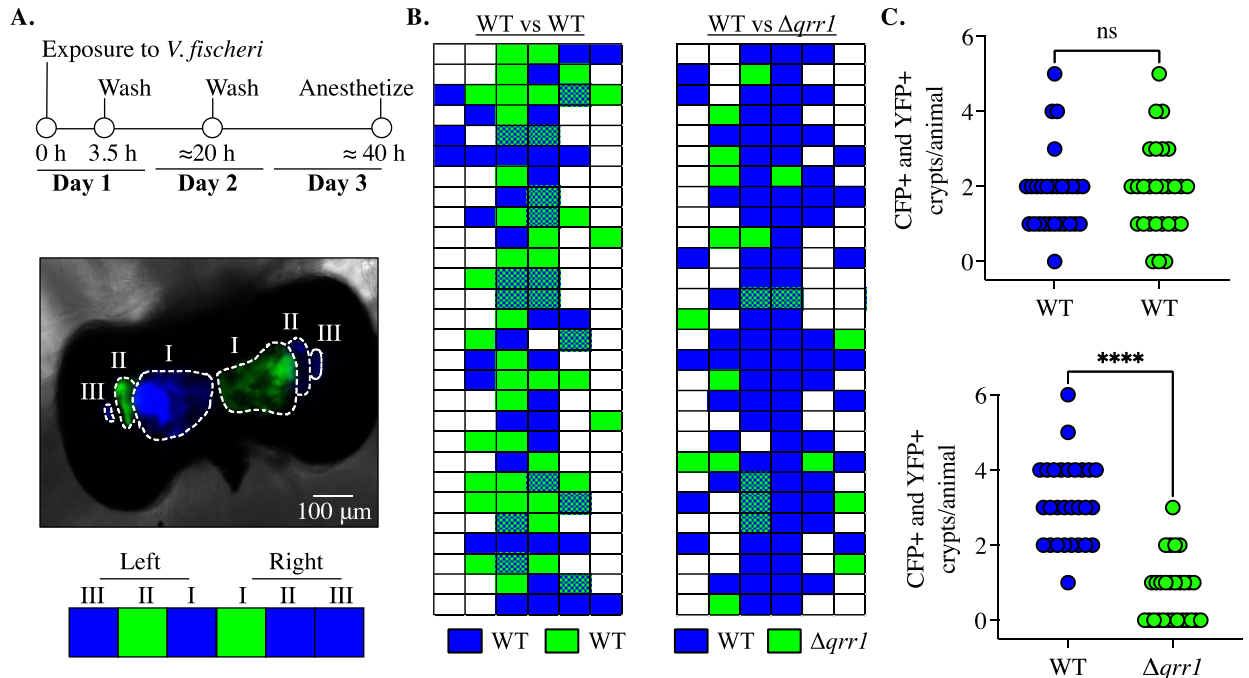


Figure 2.1: The impact of Qrr1 on crypt colonization

Juvenile squid were exposed to an inoculum of seawater containing 160 μ L of each competitor strain as indicated below. (Bacterial cultures were normalized to a defined OD₆₀₀ and washed as described in the Methods prior to introducing to squid).

- A.** *Top*, Timeline of squid co-colonization experiment; *Middle*, Microscopy image of the squid light organ with fluorescently labeled populations of *V. fischeri* within the crypts (outlined in white and labeled I-III); *Below*, The scoring metric used to visualize the identity and location of *V. fischeri* populations. Blue = CFP+; Green = YFP+; Blue and green checkered pattern = CFP+ and YFP+ (not shown).
- B.** The colonization profiles for *left*, the control competition with pYS112/ES114 (CFP-labeled wild-type) versus pSCV38/ES114 (YFP-labeled wild-type) and *right*, the test competition with pYS112/ES114 (CFP-labeled wild-type) and pSCV38/TIM305 (YFP-labeled $\Delta qrr1$). Inoculum conditions for the control competition: 89,667 CFU/ml; 1.02 (YFP/CFP ratio). Inoculum conditions for the test competition: 134,000 CFU/ml; 1.38 (YFP/CFP ratio).
- C.** Crypts colonized by each strain type per animal for *top*, the control competition and *bottom*, the test competition.

A Wilcoxon paired *t*-test was used to compare the mean ranks between the total number of crypts colonized per animal for each competition (**C**) and a Mann-Whitney test to compare the number of crypts colonized by CFP+ and YFP+ strains per animal within each group (**D**); (**** = $p < 0.0001$; n.s. = not significant).

BinK inhibits Qrr1 transcriptional activity under quorum-sensing conditions

The findings above suggest Qrr1 expression promotes entry into the light organ crypts. Prior to entering the crypts, *V. fischeri* cells are located within the shelter zone, where they are exposed to unpredictable concentrations of autoinducer due to the accumulation of AI-producing cells [28]. The detection of the autoinducers C8 and AI-2 leads to dephosphorylation of LuxO, thus impacting the extent to which Qrr1 is expressed (**Fig. 1.5**). Therefore, it was hypothesized *V. fischeri* cells possess a mechanism for bypassing AI-regulated inhibition of Qrr1 expression. A genetics screen was conducted under quorum sensing conditions to identify factors that could activate Qrr1 transcriptional activity in the presence of autoinducer. This screen was conducted using a *qrr1* transcriptional reporter plasmid (P_{qrr1} -*gfp*) harboring the *luxO-qrr1* intergenic region cloned upstream of the gene encoding green fluorescent protein, or GFP [83] (**Appendix A.1**). Therefore, green fluorescence serves as a proxy for *qrr1* transcriptional activity (P_{qrr1}). The plasmid also encodes the red fluorescent protein mCherry downstream of the *tetA* promoter. *V. fischeri* lacks TetR, which represses *tetA* expression, such that in *V. fischeri*, the *tetA* promoter is constitutively active, which enables red fluorescence to be as a measure of cellular abundance [110]. An *E. coli* donor strain harboring this plasmid was mixed with a library of *V. fischeri* transposon mutants, and the conjugates were plated onto rich medium. Colonies of transposon mutants were screened for elevated levels of GFP, which suggests an increase in P_{qrr1} (**Fig. 2.2A**). Due to the number of AI-producing cells within these colonies, these populations of *V. fischeri* are predicted to be engaged in quorum sensing and exhibit low *qrr1* transcriptional activity (**Appendix A.1**). Indeed, green fluorescence was low in colonies of WT cells (**Fig. 2.2B**). The colonies with elevated GFP suggests that in those cases, the transposon had inserted in a genetic element that inhibits Qrr1 transcription. One of the mutants with elevated GFP contained an insertion in the gene *VF_A0360*, which has not been reported to be linked to the any AI-regulated signaling networks in *V. fischeri*. *VF_A0360* encodes BinK, a hybrid histidine kinase which contains both a

histidine phosphotransferase domain and a receiver domain [99] (**Fig. 2.2C**). BinK negatively regulates expression of the genes required for cellular aggregation such that cells lacking BinK form larger aggregates at the light organ pores [99]. Strikingly, colonies of the *binK* mutants had elevated levels of green fluorescence in the center of the colonies. However, the mechanism underlying this “bullseye” phenotype is unknown. Altogether, these findings suggest BinK inhibits Qrr1 transcription under quorum-sensing conditions. Furthermore, it appears BinK regulation of Qrr1 transcription is spatially constrained to sub-populations of *V. fischeri*.

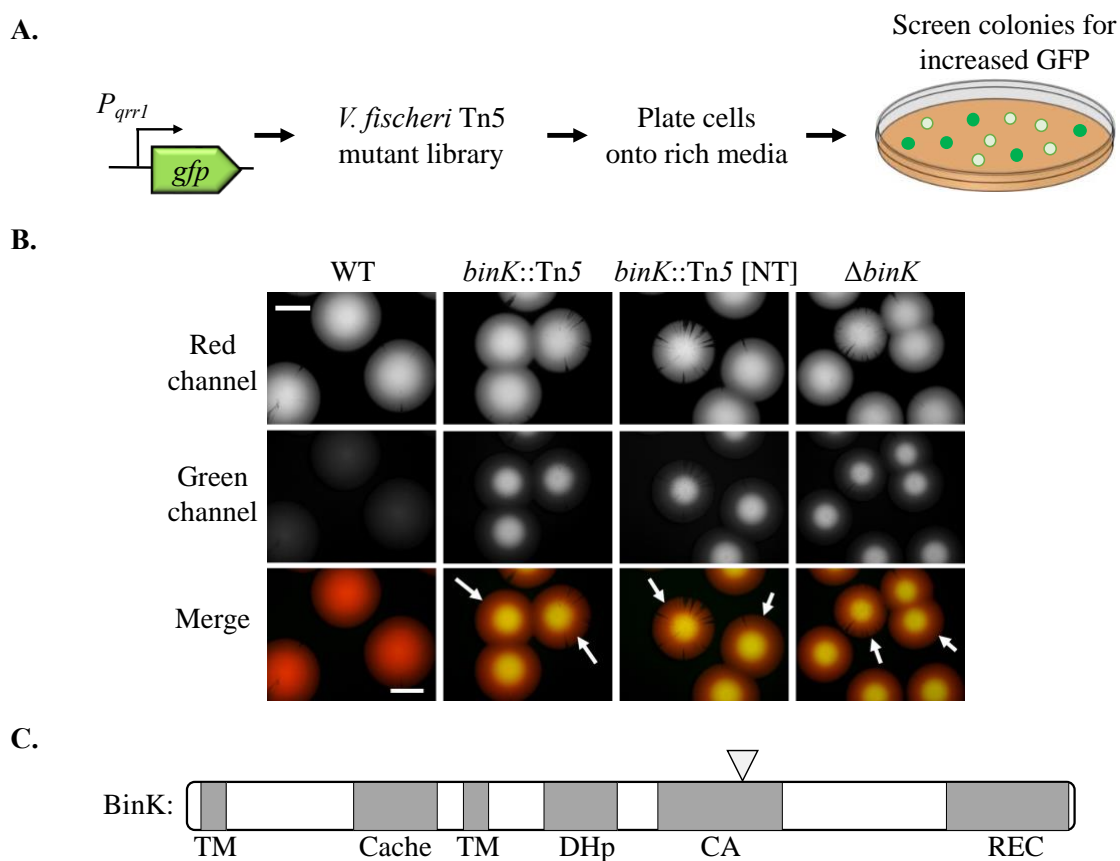


Figure 2.2: Transposon mutagenesis screen identifies BinK as a negative regulator of Qrr1 transcription

- A.** Transposon mutagenesis screen experimental set-up. A *qrr1* transcriptional reporter plasmid (P_{qrr1} -*gfp*) was conjugated into a library of *V. fischeri* transposon mutants. The conjugate cells were plated onto rich media, and the resulting colonies that grew were screened by fluorescence microscopy for elevated levels of green fluorescence.
- B.** Red, green, and red + green merged channel images of *V. fischeri* colonies harboring the P_{qrr1} -*gfp* reporter pTM268. Strains are ES114 (WT), DRO22 (*binK*::Tn5), DRO204 (*binK*::Tn5 [NT]), and MJM2251 ($\Delta binK$). The arrows point to colonies with elevated green fluorescence in the center. The scale bar = 1 mm.
- C.** Domain map of the hybrid histidine kinase BinK. The triangle indicates the site of the transposon insertion that resulted in increased P_{qrr1} -*gfp* activity. The predicted domains of BinK are labeled as follows: transmembrane domain (TM), cache (signal sensing) domain, dimerization and histidine phosphotransferase domain (DHp), catalytic domain (CA), and the receiver domain (REC)

To elucidate how Qrr1 transcription is activated in the absence of BinK, a spotting assay was developed to systematically measure factors that contribute to increased P_{qrr1} in a *binK* mutant under conditions of quorum sensing (**Fig. 2.3A**). In the spotting assay, cultures of *V. fischeri* harboring the P_{qrr1} -*gfp* reporter were grown overnight, and a defined amount was spotted onto rich media. After a 24-hour incubation, green fluorescence images were captured for each spot of growth. First, to determine the extent to which quorum-sensing was inhibiting P_{qrr1} , green fluorescence was measured in spots of WT cells and a $\Delta ainS \Delta luxIR$ sensor strain, which lacks the ability to produce the AIs C8 and 3OC6 but can detect C8. In spots of WT cells, green fluorescence was low, indicating low levels of Qrr1 transcription. Spots of the AI- sensor strain exhibited a 6.3-fold increase in green fluorescence relative to WT (**Fig 2.3B**), suggesting an increase in Qrr1 transcription, presumably due to the absence of C8. Adding C8 to spots of the AI- sensor strain resulted in decreased levels of green fluorescence, consistent with C8 inhibiting Qrr1 transcription. (**Fig 2.3B**). These results, which are consistent with the current model of AI-regulated signaling in *V. fischeri*, validate the spotting assay for use to further investigate how Qrr1 transcription is regulated under QS conditions in the $\Delta binK$ mutant. Indeed, in spots of the $\Delta binK$ mutant, green fluorescence was elevated 3.7-fold relative to WT and complementing *binK* in *trans* reduced green fluorescence to WT levels (**Fig. 2.3C**), suggesting the presence of BinK inhibits Qrr1 transcription under QS conditions.

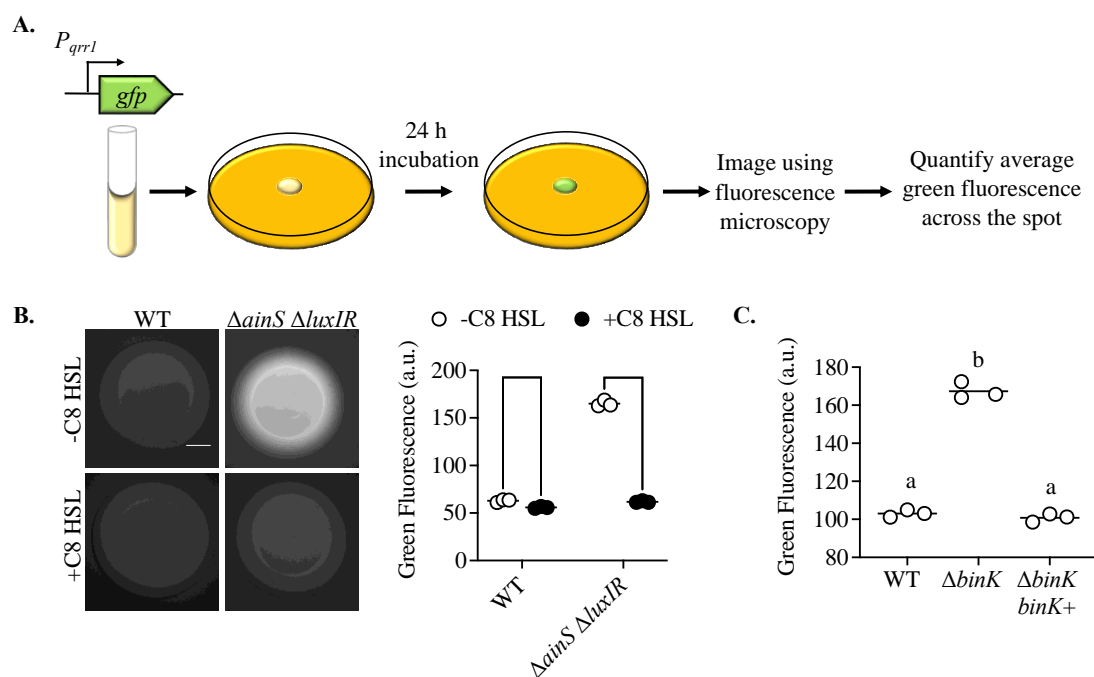


Figure 2.3: BinK inhibits P_{qrr1} under quorum sensing condition

A. Schematic of the spotting assay set-up.

B. *Left*, Overnight cultures of ES114 (WT) and JHK007 ($\Delta ainS \Delta luxIR P_{luxI-luxICDABEG}$) harboring the transcriptional reporter ($P_{qrr1-gfp}$) pTM268 were spotted onto rich media agar with 0 nM (open circles) and 100 nM C8 HSL (closed circles) and grown at 28°C. Shown are the green channel images for each spot of growth. *Right*, Average green fluorescence for each spot of growth shown in B. Each point represents an independent sample, with bars indicating group average (N = 3). Statistical significance among group means was determined using an unpaired t-test to compare the control and treatment group (* = $p \leq 0.01$; **** = $p \leq 0.0001$).

C. Overnight cultures of TIM313 (WT Tn7::erm), MJM2481 ($\Delta binK$ Tn7::erm), and TIM412 ($\Delta binK$ Tn7::binK) harboring the $P_{qrr1-gfp}$ reporter pTM268 were spotted onto rich media and grown overnight. Each point represents an independent sample, with bars indicating group average (N = 3). The dotted line indicates auto-fluorescence of a non-fluorescent sample (pVSV105/TIM313). Statistical significance among group means was determined by One-way ANOVA ($F_{2,6} = 466.9$, $d.f. = 8$). A Tukey's *post-hoc* test was used to determine statistical significances among groups, with p -values adjusted for multiple comparisons. Comparisons between groups marked by different letters indicate significant differences ($p < 0.0001$), whereas comparisons between groups with same letter indicating no significant difference ($\alpha = 0.05$).

The cellular aggregation pathway functions independently of Qrr1

The results of the squid co-colonization assay described above suggest Qrr1 expression promotes access to the light organ crypts (**Fig 2.1**). Thus, it can be deduced that symbiont cells express Qrr1 prior to entering the light organ crypts. Before migrating into the crypt spaces, *V. fischeri* cells form dense aggregates near the light organ pores [26] (**Fig. 1.2B**). BinK reduces the ability of *V. fischeri* cells to aggregate at the light organ pores [99], which suggests BinK and Qrr1 both influence the physiology of *V. fischeri* cells during the initial stages of light organ colonization.

Due to the discovered connection between BinK and Qrr1 expression, it was pertinent to also assess the extent to which Qrr1 impacts the cellular aggregation pathway. In *V. fischeri*, the pathway governing cellular aggregation *in vivo* also regulates biofilm formation [97]. Therefore, the factors that influence cellular aggregation can be studied *in vitro* using a wrinkled colony assay, in which cells spotted onto solid media form rugose colonies [111]. The rugose colony morphology results from cells secreting exopolysaccharides, which occurs when the *syp* locus is expressed [97, 111]. One way to induce wrinkled colony formation in WT cells is through the overexpression of the histidine kinase RscS [111, 112]. Furthermore, RscS-dependent induction of wrinkled colony formation is enhanced with incubation at 25°C rather than the standard 28°C that is used for propagating *V. fischeri* [99]. Therefore, the assay was conducted at both 25°C and 28°C, the former being closer to the temperature of Hawaiian seawater and the latter being the optimal growth temperature for the *V. fischeri* type strain. Consistent with previously published results [99], RscS overexpression in WT cells that were spotted and grown on rich media formed wrinkled colonies by 24 hours, and further progression of the wrinkled colony morphology was observed by 48 hours (**Fig 2.4**). The wrinkled colony phenotype was less pronounced at 25°C than at 28°C. The $\Delta binK$ mutant expressing *rscS* formed wrinkled colonies at both 25°C and 28°C, indicating the absence of BinK allows cells to overcome temperature-related inhibition of wrinkled colony formation. However, colonies of a $\Delta qrr1$ mutant expressing *rscS* exhibited a wrinkled colony pattern similar

to WT cells, whereas colonies of a $\Delta binK \Delta qrr1$ double mutant expressing *rscS* displayed a pattern similar to the $\Delta binK$ mutant (**Fig. 2.4**). Together, these results suggest that wrinkled colony formation is independent of Qrr1.

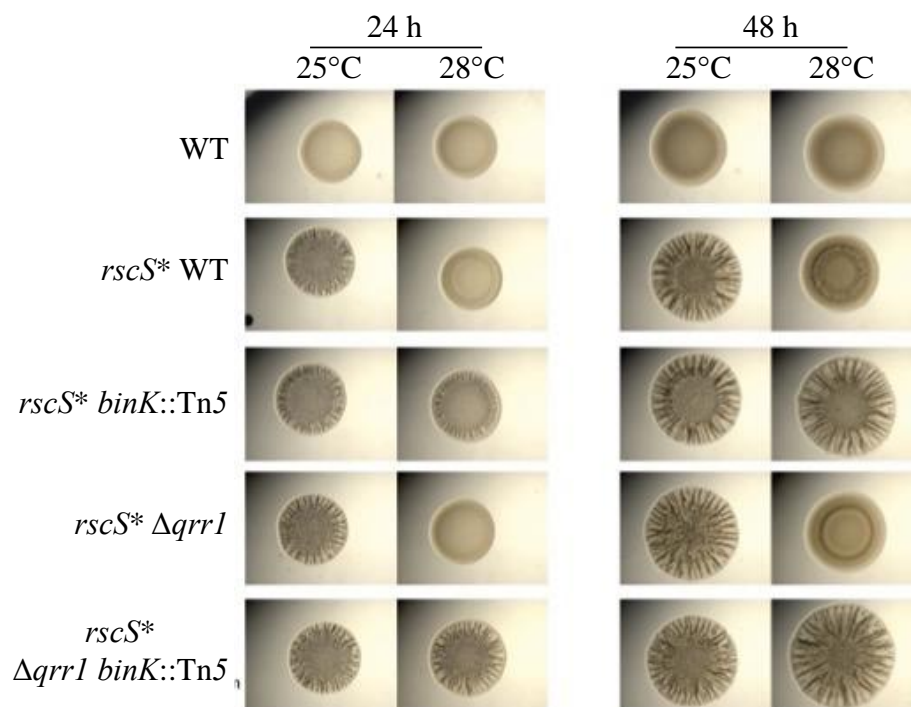


Figure 2.4: The impact of Qrr1 on cellular aggregation

Cultures of *V. fischeri* strains MJM1100 (WT), MJM1198 (*rscS** WT), MJM2839 (*rscS** $\Delta qrr1$), MJM2012 (*rscS** *binK*::Tn5), and MJM2834 (*rscS** $\Delta qrr1$ *binK*::Tn5) were spotted onto rich media and incubated for at 25°C and 28°C. Bright field images were captured at 24 h and 48 h post inoculation. The *rscS** allele contains a point mutation resulting in increased translation of the *rscS* mRNA transcript. This experiment was performed by Denise Ludvik in the lab of Mark Mandel at the University of Wisconsin-Madison, who granted permission to use this data in this dissertation.

The impact of BinK on Qrr1-regulated traits

In a previous study where juvenile squid were exposed to an equal inoculum of WT cells and $\Delta binK$ mutants, more $\Delta binK$ CFU were recovered from the light organs of homogenized squid compared to the WT competitor, suggesting that BinK negatively impacts symbiosis establishment [99]. Cells lacking *binK* have increased $P_{qrr1-gfp}$ activity, and Qrr1 provides cells with a competitive advantage in accessing the light organ crypts. Therefore, one hypothesis is BinK- cells are also more efficient at colonizing the crypt spaces relative to a BinK+ competitor strain. To test this hypothesis, a co-colonization competition was performed by exposing juvenile squid to an equal inoculum of CFP-WT cells and YFP- $\Delta binK$ mutant. In the test group of animals, 78% (78/112) of all crypts colonized contained populations of the YFP- $\Delta binK$ mutant whereas 46% (52/112) of the crypts were colonized by CFP-WT cells (**Fig. 2.5**). No difference in colonized crypts per strain type was observed in the control group. This finding suggests that BinK inhibits the ability of *V. fischeri* to successfully compete for crypt spaces.

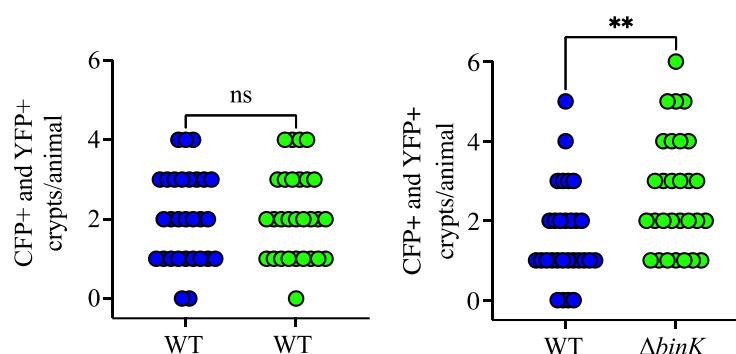


Figure 2.5: BinK inhibits the ability of cells to access crypt spaces

Juvenile squid were exposed to an inoculum of seawater containing 150 μ L of each competitor strain as indicated below. (Bacterial cultures were normalized to a defined OD₆₀₀ and washed as described in the Methods prior to introducing to squid). *Left*, control competition. Strains are pYS112/ES114 (CFP-labeled wild-type) and pSCV38/ES114 (YFP-labeled wild-type). *Right*, test competition. Strains are pYS112/ES114 (CFP-labeled wild-type) and pSCV38/MJM2251 (YFP-labeled $\Delta binK$). Shown are the total crypts colonized per animal for each competition. Inoculum conditions for the control competition: 636,667 CFU/ml; 0.91 (YFP/CFP ratio). Inoculum conditions for the test competition: 696,667 CFU/ml; 1.08 (YFP/CFP ratio). A Mann-Whitney test was conducted to compare the number of crypts colonized by CFP+ and YFP+ strains per animal within each group (C); (** = $p < 0.01$; n.s. = not significant).

To determine whether the $\Delta binK$ mutant depends on Qrr1 to outcompete WT cells, another co-colonization competition was conducted in which juvenile squid were exposed to an equal inoculum of CFP-WT cells and YFP- $\Delta binK \Delta qrr1$ mutants. The $\Delta binK \Delta qrr1$ mutant colonized fewer crypts per animal than the WT competitor (**Fig. 2.6A**). While the $\Delta binK$ mutant in the control competition occupied 70% of the colonized crypts per animal, the $\Delta binK \Delta qrr1$ mutant only occupied 35% of the colonized crypts. These results suggest the competitive advantage of BinK- cells depends on Qrr1.

Cells overexpressing *qrr1* have enhanced motility (**Appendix A.2**). Therefore, it is possible BinK- cells have an advantage over BinK+ cells in accessing the crypt spaces due increased Qrr1 expression, which would permit these cells to outswim a competitor. To test this hypothesis, *V. fischeri* cells were injected into soft agar motility plates, and the rate of motility was

determined by measuring the diameter of the motility ring that formed over time. Under the conditions tested, WT cells swam at a rate of about 3 mm per hour (**Fig. 2.6B**). The $\Delta binK$ mutant swam at a rate comparable to WT cells, which suggests that BinK- cells do not have enhanced motility. The $\Delta qrr1$ mutant had a reduced motility rate relative to WT cells, consistent with results of a previous study [109]. The motility rate of cells lacking both $binK$ and $qrr1$ was similar to that of the $\Delta qrr1$ mutant. These data suggest BinK does not inhibit Qrr1 expression under the conditions in which the motility assay was performed.

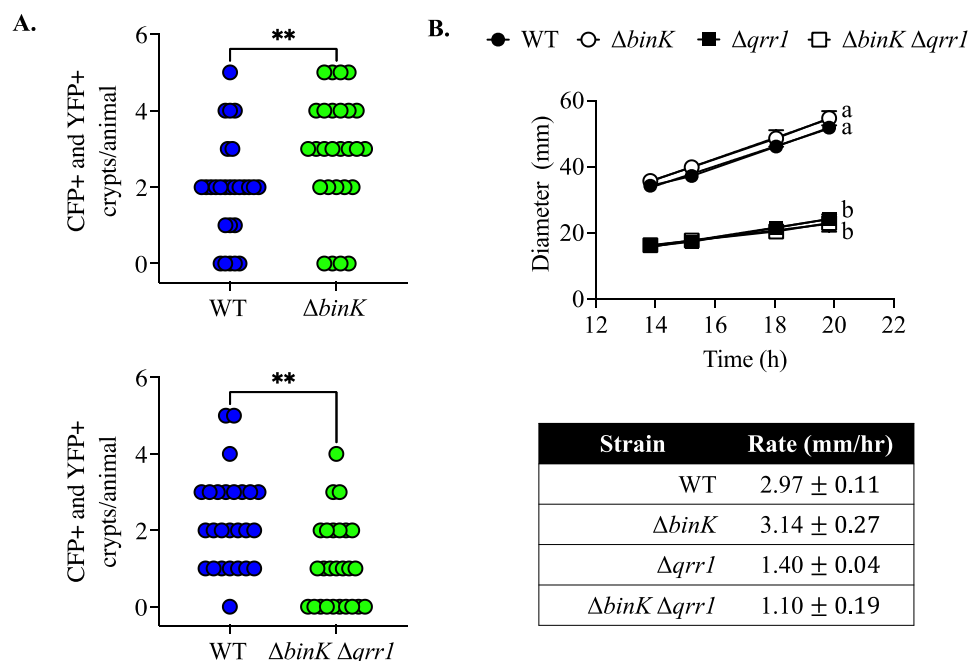


Figure 2.6: The impact of BinK on Qrr1-regulated traits

- A.** Juvenile squid were exposed to an inoculum of seawater containing 60 μ l of pYS112/ES114 (CFP-labeled wild-type) and *top*, 40 μ L of pSCV38/ES114 (YFP-labeled WT) or *bottom*, 40 μ l of pSCV38/EDR010 (YFP-labeled $\Delta binK \Delta qrr1$). Shown are the total crypts colonized per animal for each competition. Inoculum conditions for the control competition (*top*): 2670 CFU/ml; 0.88 (YFP/CFP ratio). Inoculum conditions for the test competition (*bottom*): 3560 CFU/ml; 0.98 (YFP/CFP ratio). A Mann-Whitney test was performed to compare the number of crypts colonized by CFP+ and YFP+ strains per animal within each group; (** = $p < 0.01$).
- B.** *Top*, The *V. fischeri* strains ES114 (WT), TIM305 ($\Delta qrr1$), MJM2251 ($\Delta binK$), and EDR010 ($\Delta binK \Delta qrr1$) were injected into minimal media soft agar motility plates and incubated at 28°C. The diameter of the motility ring was measured over time starting at 14 hours post incubation. *Bottom*, The slope of each line was calculated.

BinK inhibits P_{qrr1} in *V. fischeri* cells within the light organ crypts

The production of bioluminescence within the host suggests *V. fischeri* populations actively engage in quorum sensing *in vivo*. The absence of BinK allows for increased P_{qrr1} activity under quorum-sensing conditions, *i.e.*, in the presence of AI (**Fig. 2.3**). In addition, BinK also inhibits transcriptional activity of *syp* genes within the light organ crypts [113], suggesting BinK is active in symbiotic populations of WT cells. Therefore, it was also worthwhile to determine the extent to which BinK inhibits Qrr1 transcription *in vivo*. To begin this inquiry, juvenile squid were exposed to an inoculum of either *V. fischeri* WT cells or $\Delta binK$ mutants, both engineered with a P_{qrr1} -*gfp* reporter plasmid. The plasmid also encoded *mCherry* under the control of a constitutively active promoter so that red fluorescence could be used to determine the location of *V. fischeri* populations within the crypt spaces. On Day 3 post-inoculation, animals were anesthetized and prepared for imaging (**Fig. 2.7**). In the group of animals exposed to WT cells, green fluorescence was low in all colonized crypts for each animal (**Fig. 2.7**), suggesting P_{qrr1} was low within these populations. This finding is consistent with the model of low Qrr1 expression in cells exposed to AI. In the group of animals exposed to the $\Delta binK$ mutant, 17/20 of the animals contained at least one crypt in which green fluorescence was elevated within a subset of the crypt population (**Fig. 2.7**). This increase in green fluorescence was not uniform throughout the crypts, nor did it consistently localize to one specific area within the crypt spaces. Qrr1 reduces the ability of cells to respond to 3OC6 [83] such that cells overexpressing Qrr1 have reduced levels of bioluminescence in culture (**Appendix A.3**). Yet, there was no difference in luminescence levels measured on Days 2 and 3 post-inoculation between the two groups (**Appendix A.4**), suggesting the increase in Qrr1 expression in the $\Delta binK$ mutant was insufficient to affect bioluminescence output in the animals. Altogether, these data indicate while AI-regulated signaling inhibits Qrr1 expression in the majority of cells within the crypts, there are subpopulations in which only BinK

inhibits Qrr1 expression. However, the reason underlying this pattern is unclear and warrants further investigation.

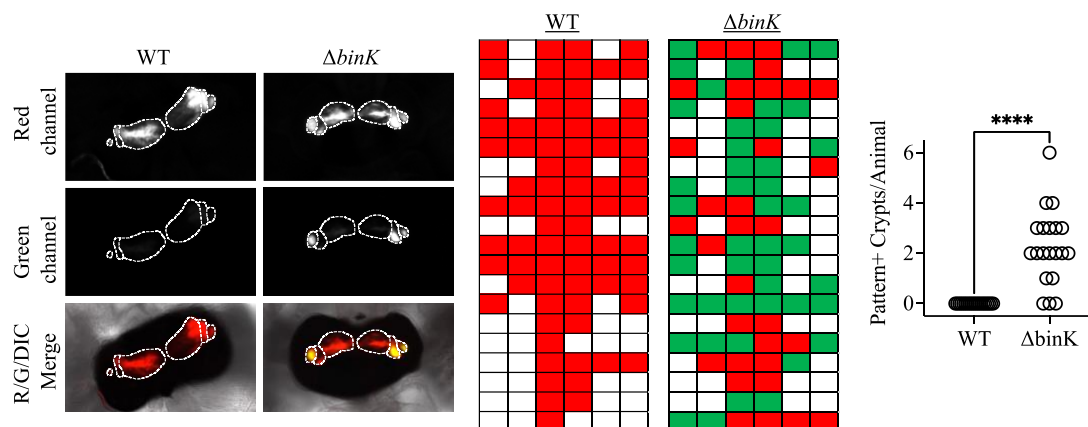


Figure 2.7: BinK inhibits P_{qrr1} activity *in vivo*

Juvenile squid were exposed to an inoculum of ES114 (WT) or MJM2251 ($\Delta binK$) cells harboring the P_{qrr1} - gfp transcriptional reporter pTM268. *Left*, Microscopy images of a sample light organ from each group of animals. *Middle*, Crypt scores for each animal within the groups. Red = colonized crypt; Green = crypt with elevated green fluorescence. *Right*, Number of crypts displaying pattern of elevated green fluorescence within a subset of the population. A Mann-Whitney test was conducted to compare the mean ranks between the two groups (**** = $p < 0.0001$).

Factors that promote P_{qrr1} activity in the $\Delta binK$ mutant

Next, we investigated factors that promote increased P_{qrr1} in the $binK$ mutant. In other members of the *Vibrionaceae*, transcription of the Qrr1 homolog is regulated by the alternative sigma factor σ^{54} , which binds the -12 and -24 positions upstream from the transcriptional start site of target genes [91, 93]. Transcription from σ^{54} -dependent promoters requires the activity of specific factors called bacterial enhancer binding proteins, or bEBPs, which interact with σ^{54} . BEBPs hydrolyze ATP, when enables bEBPs to remodel σ^{54} in a way that permits transcription [53]. A putative σ^{54} -binding site with the consensus sequence TGGCA-N7-TGC is located upstream the $qrr1$ gene in *V. fischeri* (**Appendix A.1**). Therefore, a spotting assay was performed to measure P_{qrr1} in a $\Delta binK$ mutant lacking $rpoN$, the gene encoding σ^{54} . Green fluorescence in spots of the $\Delta binK \Delta rpoN$ mutant was lower than that of the $\Delta binK$ parent strain and comparable

to levels observed in the $\Delta rpoN$ mutant (**Fig. 2.8A**). This data suggests Qrr1 expression in the BinK mutant is regulated by σ^{54} .

As σ^{54} fails to initiate transcription initiation without a cognate bEBP, these findings also indicate P_{qrr1} activation in the BinK- cells absolutely requires a bEBP. LuxO is a bEBP predicted to activate σ^{54} -dependent activation of *qrr1* in WT cells under conditions of low AI [83]. To determine whether LuxO contributes to increased P_{qrr1} in the $\Delta binK$ mutant, P_{qrr1} activity was assessed in spots of a $\Delta binK \Delta luxO$ strain. The level of green fluorescence in spots of the $\Delta binK \Delta luxO$ mutant was decreased relative to the $\Delta binK$ parent strain, suggesting LuxO contributes to P_{qrr1} activation in the absence of BinK. However, the level of green fluorescence in the double mutant was higher than the $\Delta luxO$ control strain, suggesting another factor is capable of activating P_{qrr1} in the $\Delta binK$ mutant (**Fig. 2.8B**). Because P_{qrr1} activation in BinK- cells completely depends on σ^{54} (**Fig. 2.8A**), it appears an additional bEBP also promotes expression of Qrr1. Altogether, this study reveals BinK can inhibit LuxO and an unknown bEBP from activating Qrr1 transcription in the presence of AI. **Chapter 3** discusses how a second bEBP was identified that can activate Qrr1 transcription independently of LuxO.

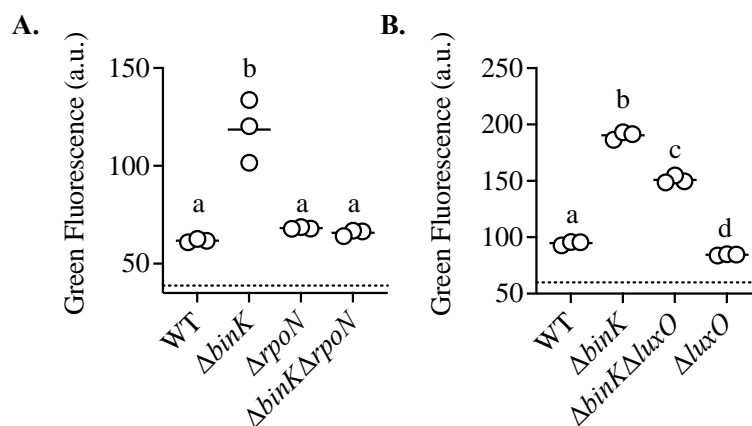


Figure 2.8: Factors that promote $P_{qrr1-gfp}$ activity in the $\Delta binK$ mutant

Overnight cultures of *V. fischeri* strains **A:** ES114 (WT), MJM2251 ($\Delta binK$), KRG003 ($\Delta rpoN$), and KRG011 ($\Delta binK \Delta rpoN$) harboring the $P_{qrr1-gfp}$ reporter pEDR003 and **B:** ES114 (WT), MJM2251 ($\Delta binK$), EDR009 ($\Delta binK \Delta luxO$), and TIM306 ($\Delta luxO$) harboring the $P_{qrr1-gfp}$ reporter pTM268 were spotted onto rich media and grown overnight. Each point represents an independent sample, with bars indicating group average ($N = 3$). The dotted line indicates auto-fluorescence of a non-fluorescent sample (pVSV105/ES114). Statistical significance among group means was determined by one-way ANOVA (**A:** $F_{3,8} = 32.66$, $d.f. = 11$; **B:** $F_{3,8} = 1127$, $d.f. = 11$). A Tukey's *post-hoc* test was used to determine statistical significances among groups, with p -values adjusted for multiple comparisons. Comparisons between groups marked by different letters indicate significant differences ($p < 0.0001$), whereas comparisons between groups with same letter indicating no significant difference ($\alpha = 0.05$).

Discussion

The goal of this study was to increase understanding of when during symbiosis establishment Qrr1 is expressed and how its transcription is regulated during this process. While the steps of light organ colonization have been well described, there are gaps in knowledge regarding how AI-mediated signaling networks function in *V. fischeri* cells colonizing the light organ crypts. Qrr1 was worthwhile to study as it integrates signals from two QS-systems (AinSR and LuxPQ) to control the activity of the master regulator LitR, which regulates the expression of traits require for *V. fischeri* to establish and maintain symbiosis. The results of the squid co-colonization assay revealed fewer $\Delta qrr1$ cells founded crypt populations when challenged against a Qrr1+ competitor strain (WT), suggesting Qrr1 provides *V. fischeri* cells with a competitive advantage in accessing the light organ crypts (**Fig. 2.1**). The genetic background of a $\Delta binK$ mutant led to the discovery that *qrr1* transcription can be activated in the presence of AI, which indicates *V. fischeri* cells possess mechanisms to bypass QS-regulated inhibition of Qrr1 transcription (**Fig. 2.2B** and **2.3B**). Qrr1 transcription in the $\Delta binK$ mutant depends on the alternative sigma factor, σ^{54} , and LuxO (**Fig. 2.8**). In addition, a second, yet unidentified bEBP also contributes to P_{qrr1} activation in the $\Delta binK$ mutant. Together, the results of this study yielded greater insight into the role of Qrr1 during light organ colonization and led to the development of an updated model of transcriptional activation of *qrr1* in *V. fischeri* (**Fig. 2.9A**).

Previous studies revealed cells expressing Qrr1 have increased cellular abundance within the light organ relative to a Qrr1- competitor strain [83]. However, it was unclear when and how during the initial stages of light organ colonization Qrr1 was having an impact. This study highlights the dynamics of Qrr1 transcriptional activation over the symbiotic lifecycle of *V. fischeri* cells (**Fig. 2.9B**). When detection of the autoinducers C8 and AI-2 are low, expression of Qrr1 is predicted to be high, which leads to low LitR levels and bioluminescence [83, 92, 105]. When *V. fischeri* cells encounter the host, they aggregate with other bacteria within the shelter zone and,

consequently, may be exposed to increased concentrations of AI [28, 30]. Because Qrr1 facilitates access to the light organ crypts, (**Fig. 2.1**), it is advantageous for cells within the aggregate to express Qrr1. However, if cells within the aggregate are exposed to AI, this might jeopardize Qrr1 transcription and inhibit its expression. It appears *V. fischeri* cells have evolved to express Qrr1 under QS-conditions, most likely to prime cells for motility (**Fig 2.6B, Appendix A.2**), which is required for entering the crypt spaces. Once cells have proliferated within the crypts, the increasing concentrations of C8 HSL and AI-2 produced attenuate Qrr1 expression within the population, presumably to allow for the expression of genes involved in light production. Qrr1 expression is low during this stage as factors that enable the QS-bypass mechanism in the aggregate may be inactive in the crypts.

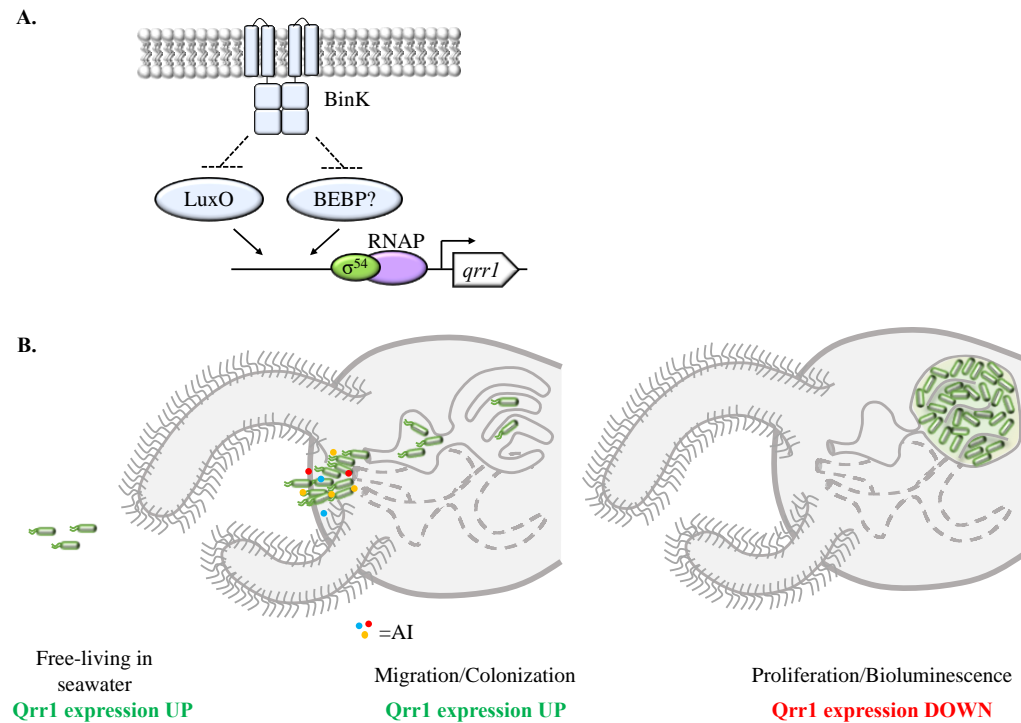


Figure 2.9: Model of *qrr1* transcription in *V. fischeri*

- A.** In WT cells, BinK inhibits the ability of LuxO and another bEBP to activate σ^{54} transcription of *qrr1*. The absence of BinK allows both bEBPs to activate P_{qrr1} under QS-conditions.
- B.** In free-living *V. fischeri* cells, Qrr1 expression is high due to the decreased detection of AI. Cells within the aggregate are potentially exposed to AI, but cells have a mechanism to bypass quorum-sensing and express Qrr1 under these conditions. No quorum-sensing bypass mechanism is active to activate *qrr1* transcription in the crypts; thus, Qrr1 expression remains low.

The physiology of the *binK* mutant permits increased Qrr1 transcriptional activity under quorum-sensing conditions (**Figs. 2.2B** and **2.3B**). However, BinK inhibition of *qrr1* appears to be spatially regulated. Colonies and crypt populations of the *binK* mutants show non-uniform elevations in P_{qrr1} (**Figs. 2.2B** and **2.7**). This suggests the initial colony forming unit in colonies or founder cell in the crypts exhibited increased P_{qrr1} that decreased as cells proliferated. This “bullseye” pattern is not observed in colonies of *V. fischeri* cells with a constitutively active variant of LuxO that also harbors the *qrr1* transcriptional reporter (**Appendix A.1**). This observation refutes the idea that the P_{qrr1} construct is responsible for this phenotype. Elevated green fluorescence in sub-populations of *binK* mutants was not observed *in vivo* when other BinK-regulated genes are assessed [113]. Thus, this phenotype appears to be specific to BinK regulation of P_{qrr1} .

Transcription of *qrr1* in the $\Delta binK$ mutant depends on σ^{54} , LuxO, and an unknown bEBP. Furthermore, this suggests that the activity of LuxO and the unknown bEBP is typically inhibited by BinK in WT cells under quorum-sensing conditions. BinK is encoded as an orphan hybrid histidine kinase [99], and its cognate partner has yet to be determined, which impedes a straightforward approach to understanding exactly how BinK inhibits *qrr1* transcription. Deleting *luxO* in the $\Delta binK$ mutant attenuated $P_{qrr1-gfp}$ activity, suggesting LuxO contributes to P_{qrr1} activation in this strain (**Fig. 2.8B**). Typically, LuxO must be phosphorylated by LuxU or be in a conformation that mimics its phosphorylated state to activate *qrr1* transcription, which occurs at low AI concentrations or via an aspartic acid-to-glutamate substitution in the receiver domain, respectively [83, 90, 109, 114]. Therefore, the finding that LuxO activates P_{qrr1} in the $\Delta binK$ mutant under QS-conditions challenges the current model of AI-regulated signaling in *V. fischeri* (**Fig. 1.5**). As LuxU contains a histidine phosphotransferase (Hpt) domain, one possibility is BinK functions as a phosphatase towards LuxU. Other studies suggests BinK could exhibit phosphatase activity towards SypF, which also contains an Hpt domain [113]. SypF phosphorylates SypG,

which is a bEBP that activates σ^{54} -dependent transcription of the *syp* locus that encodes factors necessary for cellular aggregation [96, 98]. Indeed, transcriptional activity of SypG-regulated genes is increased in the absence of BinK [99]. The possibility SypG is the unknown bEBP capable of activating *qrr1* transcription will be explored further in Chapter 3. In addition to expanding the current model of Qrr1 transcription in *V. fischeri*, this study hints towards an integration of the AI-regulated signaling and cellular aggregation pathways during symbiosis establishment.

In *Vibrionaceae*, including *V. fischeri*, several QS-independent factors have been reported to regulate the expression of Qrrs. For example, in *V. fischeri*, overexpression of the sugar translocase SypK leads to increased P_{qrr1} activation through LuxO, presumably by activating the LuxQ kinase activity [109]. However, how this regulatory connection impacts symbiosis remains unknown. The canonical mechanism of activating transcription of the *qrr* genes is through LuxO and σ^{54} [114, 115]. However, in *Vibrio parahaemolyticus*, transcription of one of the *qrr* homologs, *qrr2*, can be activated by σ^{70} in an *rpoN* mutant [116]. This may indicate, under specific conditions, transcription of this *qrr1* homolog can be activated in the presence of AI. Additionally, increasing AI concentrations are not the only inhibitors of *qrr* transcription. In the foodborne pathogen *Vibrio vulnificus*, which encodes five *qrrs*, expression of these sRNAs is repressed under iron-rich conditions [117]. One of the ways this occurs is through competitive exclusion of LuxO from its binding site by the iron-responsive protein Fur. The Qrrs in *V. vulnificus* indirectly inhibit the expression of virulence factors through the LitR homolog SmcR [10, 117]. Thus, the detection of iron could signal to cells they are within a host-environment where the expression of virulence factors is energetically favorable.

These studies highlight the need to consider how multiple signaling networks might influence the expression of specific traits required to establish symbiosis. Doing so could possibly uncover additional mechanisms by which symbiotic microbes have evolved to adapt to unpredictable conditions when colonizing a host. Symbiotic microbes impact host physiology, and

this information could be useful in the development of more effective therapeutics that enhance or inhibit the ability of bacteria to engage in symbiosis.

Methods

Media and growth conditions: *V. fischeri* strains were grown at 28°C under aerobic conditions shaking at 200 rpm in LBS (Luria-Broth Salt) media [1% (wt/vol) tryptone, 0.5% (wt/vol) yeast extract, 2% (wt/vol) NaCl, 50mM Tris-HCl (pH 7.5)].

Strains and Plasmids: Strains and plasmids used in this study are listed in **Table 1** and **Table 2**, respectively.

Integration of Tn7::*binK*: The *binK* gene was cloned from ES114 genomic DNA using PFU Ultra AD Polymerase into pEVS107 using the primers listed in **Table 3**. The pEVS107-derived plasmid was integrated into the Tn7 site of the $\Delta binK$ mutant MJM2251 via quadra-parental mating using the helper plasmids pEVS104 and pUX-BF13.

Construction of deletion alleles: The $\Delta binK \Delta luxO$ and $\Delta binK \Delta qrr1$ double mutants were generated by introducing the $\Delta luxO$ allele or the $\Delta qrr1$ allele into $\Delta binK$ by allelic exchange via the plasmid pTM235 or pTM238, respectively [83]. The $\Delta rpoN$ deletion allele was generated via SOE PCR and recombineering mutagenesis [25, 50] using the primers listed in **Table 3**.

Construction of pEDR003: pEDR003: A 377-bp region containing the *luxO-qrr1* intergenic region was amplified from *V. fischeri* ES114 genomic DNA using the primers listed in **Table 3** and subcloned into pTM267 [83].

Squid co-colonization assays: *V. fischeri* cells harboring a fluorescent reporter plasmid were inoculated into 3 ml LBS media supplemented with chloramphenicol (Cm) at 2.5 $\mu\text{g}/\text{mL}$ and incubated at 28°C shaking at 200 rpm. Cultures grown overnight were normalized to an $\text{OD}_{600} = 1.0$ in 1 mL LBS. A 30- μL volume of normalized culture was diluted into 3 ml LBS with Cm 2.5 $\mu\text{g}/\text{mL}$ and grown until cultures reached an OD_{600} close to 1.0 (~3.5 hours). The amount of cells that corresponded to 1 ml of cells at $\text{OD}_{600} = 1.0$ were pelleted at 9000 x g for 2 minutes. Most of the supernatant was removed leaving ~100 μL . The cells were washed by adding ~900 μL FSSW bringing the final volume to 1 ml. The spin and wash were repeated. The washed cells were

diluted 1:10 into FSSW. For each competition, 160 μ l of each strain type that had been washed and diluted were further diluted into 50 ml FSSW. The bacterial suspensions were added to animals in 50 ml FSSW. Each inoculum was sampled by plating 100 μ l of a 10^{-2} dilution in triplicate onto LBS solid agar plates. Plates were incubated at 28°C and the resultant CFU were enumerated to determine the inoculum ratio and total inoculum size. 3.5 hours after animals were exposed to the competition inoculum, the animals were washed by transferring to 100 ml FSSW for 5 minutes. The wash was repeated, and each animal was transferred to an individual fly vial containing 4 ml FSSW. The next day, the animals were washed again by transferring to 4 ml fresh FSSW. On the third day, animals were anesthetized on ice then placed in a 4% paraformaldehyde solution and rotated at 4°C overnight. The following day, the animals were washed in 1x mPBS (modified phosphate-buffered saline). Animals were dissected to reveal the light organ, and fluorescently-labeled bacteria within the light organ were imaged using a Zeiss 780 confocal microscope.

Gene-expression in light organ crypts: *V. fischeri* cells harboring the *P_{qrr1}-gfp* promoter reporter pTM268 inoculated into 3 ml LBS media supplemented with Cm 2.5 μ g/ml and incubated at 28°C shaking at 200 rpm. 30 μ l of cultures grown overnight were diluted into 3 ml LBS with Cm 2.5 μ g/ml and grown until cultures reached an OD₆₀₀ close to 1.0. Intermediate cultures were diluted 1:100 into FSSW (20 μ l culture into 980 μ l FSSW). 200 μ l of the diluted cells were added to 50 ml FSSW, and the bacterial suspension was added to animals in 50 ml FSSW. 25 μ l of the inoculum was plated in duplicate onto LBS solid agar plates. Plates were incubated at 28°C and the resultant CFU were enumerated to determine the inoculum ratio and total inoculum size. 3.5 hours after animals were exposed to the single-strain inoculums, the animals were washed by transferring to 4 ml FSSW. The next day, the animals were washed again by transferring to 4 ml fresh FSSW. On the third day, animals were anesthetized on ice then placed in a 4% paraformaldehyde solution and rotated at 4°C overnight. The following day, the animals were washed in 1x mPBS (modified phosphate-buffered saline). Animals were dissected to reveal the light organ, and fluorescently-

labeled bacteria within the light organ were imaged using a Zeiss 780 confocal microscope. Inoculum conditions for single-strain control group: 1,300 CFU/ml; Inoculum conditions for single-strain test group: 1,620 CFU/ml.

Transposon mutagenesis screen: Published in [109].

Gene-expression on rich media assays: *V. fischeri* strains harboring the P_{qrr1} -*gfp* transcriptional reporters pTM268 or pEDR003, as indicated, were grown aerobically overnight in LBS broth and supplemented with 2.5 µg/ml chloramphenicol. Prior to initiating the assay, each culture was adjusted to an $OD_{600} = 1.0$. To initiate each spot, a 2.5-µl volume of a cell suspension was placed onto the surface of LBS agar supplemented with 2.5 µg/ml chloramphenicol and 100 nM C8 HSL where indicated. Plates were incubated at 28°C. After 24 h, the spots were examined at 4X magnification using an SZX16 fluorescence dissecting microscope (Olympus) equipped with an SDF PLFL 0.3X objective and both GFP and mCherry filter sets. Images of green fluorescence and red fluorescence of the spot were obtained using an EOS Rebel T5 camera (Canon) with the RAW image format setting. Image analysis was performed using ImageJ (NIH) as follows. First, RAW images were converted to RGB TIFF format using the DCRaw macro using the following settings: use_temporary_directory, white_balance = [Camera white balance], do_not_automatically_brighten, output_colorspace = [sRGB], read_as = [8-bit], interpolation = [High-speed, low-quality bilinear], and half_size. For each spot, the green channel of the green fluorescence image was used for quantifying GFP fluorescence, and the red channel of the mCherry fluorescence image was used for quantifying mCherry fluorescence. The region of interest (ROI) corresponding to the spot was identified in the red channel by thresholding, and this ROI was used to determine the mean red and green fluorescence levels for each spot. A non-fluorescent sample (pVSV105/ES114 or pVSV105/TIM313) was used to determine the levels of cellular auto-fluorescence. Fold changes in fluorescence between groups were calculated by subtracting auto-fluorescence levels from sample fluorescence levels.

Wrinkled colony assay: *V. fischeri* cultures were grown overnight at 25°C rotating. The next day, 8 µl of culture were spotted onto LBS plates. Plates were incubated at 25°C and 28°C. At 24- and 48-hours post spotting, each spot of growth was imaged using a Leica M60 stereomicroscope with Leica Firecam software. Strains were constructed by Denise Ludvik and Mark Mandel (University of Wisconsin – Madison; Madison, WI)

Motility Assay: Overnight cultures of *V. fischeri* were diluted 1:100 into LBS. Once cultures reached mid-log, cells were injected into minimal media soft agar motility plates (50 mM MgSO₄, 10 mM CaCl₂, 300 mM NaCl, 10 mM KCl, 0.0058% (wt/vol) K₂HPO₄, 0.1 mM FeSO₄, 84 mM Tris-HCl (pH 7.5) containing 1 mM GlcNAc and 0.25% agar). Plates were incubated at 28°C. After a 14-hour incubation, the diameter of the rings that formed was measured over time.

Chapter 3

The bacterial enhancer binding proteins LuxO and SypG activate transcription of P_{qrr1}

Introduction

Symbiotic bacteria that are horizontally transmitted between hosts must quickly acclimate to different environments as they transition from an external reservoir to the site of colonization within a host. Bacteria can sense specific changes and cues in the environment, such as autoinducers and nutrients [35, 106, 118, 119]. The alternative sigma factor, σ^{54} , facilitates a rapid response to environmental signals by altering transcription of its target genes, which is accomplished with the aid of a specialized type of transcription factor called a bacterial enhancer binding protein, or bEBP [55, 82, 120]. The bEBPs are members of the AAA+ family of proteins, and their primary function is to hydrolyze ATP, which provides σ^{54} with the energy to initiate transcription [53, 55]. BEBPs and σ^{54} regulates the expression of genes involved in the establishment and maintenance of host-microbe interactions, such as motility, biofilm formation, and the production of virulence factors [29, 121-124]. The function of bEBPs is to couple environmental signals with changes in gene expression by facilitating σ^{54} -dependent transcription of genes, such that specific traits are expressed only when needed under the appropriate conditions, such as when colonizing a host. Therefore, it is important to understand how bEBPs respond to such signals and effect changes in gene expression during the initial stages of symbiosis establishment.

LuxO is a bEBP that is conserved in the majority of *Vibrionaceae* [84, 125, 126]. It is a member of the Group I bEBPs, which are characterized by an N-terminal receiver (R) domain, the conserved central AAA+ (C) domain, and a C-terminal DNA-binding (D) domain (**Fig. 3.1A**) [127]. The R domain contains the site of phosphorylation, which in LuxO is an aspartate residue [62, 128]. Within the C domain lies residues involved in ATP binding and hydrolysis along with a GAFTGA motif, which contacts σ^{54} [64-66, 129]. The C domain also facilitates hexamer formation of the bEBP [130, 131]. In LuxO, the R and C domains are connected by a short linker

with residues that occupy the ATP active site (**Fig. 3.1B**). A glycine residue (G143) within the linker region appears to be a key residue stabilizing this inhibitory conformation. Upon phosphorylation of the R domain, this linker region is displaced allowing for nucleotide binding and hydrolysis. To date, LuxO is the only known bEBP that employs this method of regulation [62]. The D domain contains a helix-turn-helix motif, which is involved in DNA binding [76, 79]. LuxO binds as dimers at specific sites called upstream activating sequences (UASs), which are typically 80 to 150 base pairs upstream of σ^{54} -dependent genes [55, 77, 95]. As the concentration of the protein increases, LuxO is predicted to form a hexamer at each UAS [62]. Because the σ^{54} binding site is located at the -12 and -24 regions, DNA-binding proteins are predicted to be required to place the LuxO hexamer in close proximity with σ^{54} . ATP is hydrolyzed and σ^{54} is remodeled to a conformation that permits transcription initiation (**Fig. 3.1C**) [64-66].

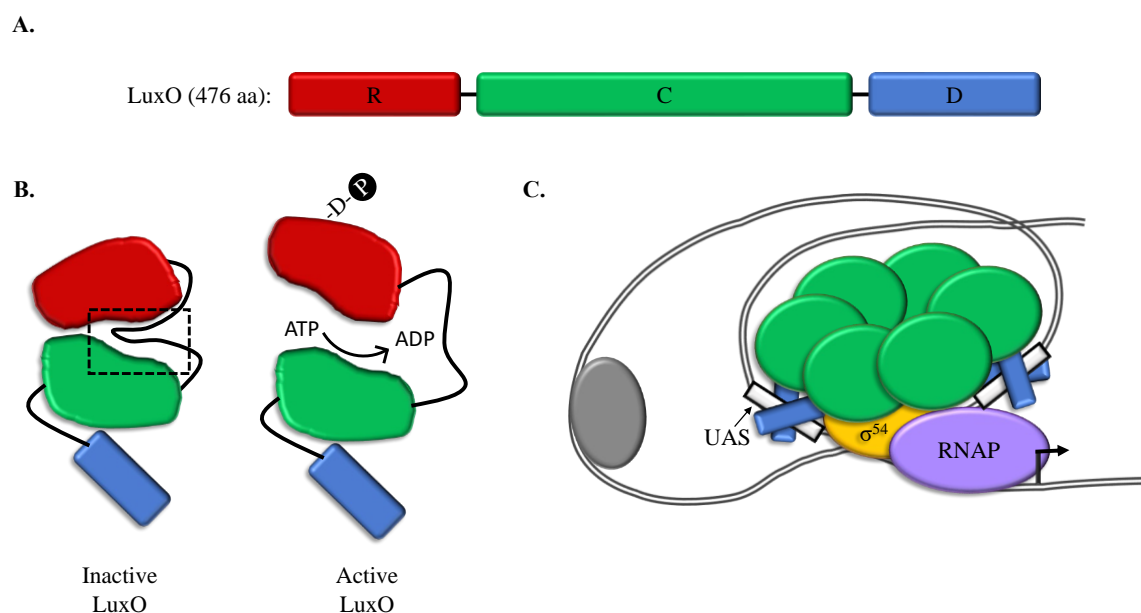


Figure 3.1: LuxO is a Group I bEBP of the *Vibrionaceae*

- A. LuxO is a 476-amino acid (aa) Group I bacterial enhancer binding proteins (bEBPs) have a receiver (R) domain, a AAA+ (C) domain, and a DNA-binding (D) domain.
- B. In the inactive conformation of LuxO, the R-C linker occupies the ATP active site (black outlined box). Phosphorylation of an aspartate (D) residue within the receiver domain (red) displaces the linker, exposing the active site to permit nucleotide binding and hydrolysis. C and D domain are colored green and blue, respectively.
- C. LuxO binds as dimers to upstream activating sequences (UASs) within the promoter of target genes (D domain not shown for the two distal hexamers). Hexamerization is facilitated by residues within the C domain. DNA-binding proteins (gray oval) place the LuxO hexamer near σ^{54} . This interaction is mediated by the GAFTGA motif located within the C domain. ATP hydrolysis energizes σ^{54} to drive open complex formation, allowing for transcription initiation.

The mutualistic symbiosis between the bacterium *Vibrio fischeri* and the Hawaiian bobtail squid, *Euprymna scolopes*, provides a platform to study the role of bEBPs during host-colonization. The life cycle of *V. fischeri* consists of a planktonic state, in which cells are free-living in the seawater, and a host-associated state, in which cells are cooperating within a population to produce bioluminescence [17, 132]. In *V. fischeri*, LuxO integrates information about cellular density through the AinR/LuxPQ phosphorelay cascade. AinR and LuxQ are hybrid histidine kinases whose activity is regulated by quorum sensing, or the detection of small signaling molecules, *i.e.*, autoinducers (AIs) [88, 89, 105, 133]. Under low AI concentrations, such as what occurs at low

cell densities, AinR and LuxQ autophosphorylate and function as kinases towards the phosphorelay protein LuxU [90]. LuxU phosphorylates LuxO on an aspartate residue (D55) within the R domain, which results in σ^{54} -dependent transcription of the small, regulatory RNA Qrr1 [84, 128, 134]. In *V. fischeri*, Qrr1 regulates factors involved in motility, bioluminescence, and host colonization through post-transcriptional inhibition of the master regulator LitR [83, 109]. Therefore, LuxO and σ^{54} enable cells to quickly alter the expression of traits necessary for the free-living or host-associated stages of the *V. fischeri* symbiotic lifecycle by regulating transcription of the *qrr1* gene.

LuxO is the only known bEBP of *qrr1*. However, previous studies provide evidence that an additional, yet unknown bEBP, can also stimulate σ^{54} -dependent activation of the *qrr1* promoter, or P_{qrr1} , even under conditions of high AI. The activity of this unknown bEBP was inhibited by the histidine kinase BinK (**Chapter 2**). BinK is a negative regulator of cellular aggregation, which occurs when *V. fischeri* cells first encounter the squid host [99, 112]. This chapter discusses the identification of the unknown bEBP as SypG, which is sufficient to activate P_{qrr1} . SypG activates transcription of the *syp* locus, which encodes factors necessary for *V. fischeri* to form cellular aggregates at the light organ pore [97]. The finding that LuxO and SypG can both activate P_{qrr1} reveals a connection between the quorum-sensing and cellular aggregation pathways. Altogether, this work increases understanding into the role of bEBPs during the early stages of symbiosis establishment.

Results

LuxO activation of P_{qrr1} depends on two UASs

Results from a previous study revealed that LuxO activates transcription of P_{qrr1} in *V. fischeri* [83]. To determine which region of the $qrr1$ promoter was necessary for LuxO activation of $qrr1$, a series of 5' truncated constructs was generated (**Fig. 3.2A**) using the P_{qrr1} -*gfp* transcriptional reporter (**Appendix A.1**) as a template. These plasmids were conjugated into a *V. fischeri* strain containing an aspartic acid to glutamate substitution in residue 55 of LuxO (D55E), which is the putative site of phosphorylation within the receiver domain. This mutation results in a hyperactive variant of LuxO [84, 85]. The *luxOD55E* mutant harboring the truncated promoter set was spotted onto rich media and green fluorescence was measured in spots resulting from overnight growth. This spotting assay was used to measure gene expression in all experiments described in this study. In spots of the LuxO mutant harboring the construct containing 175 bp upstream the +1 transcriptional start site of $qrr1$, green fluorescence was similar to what was observed with the WT P_{qrr1} plasmid, suggesting this region does not contain genetic elements necessary for LuxO-dependent activation of P_{qrr1} (**Fig. 3.2B**). Using the construct containing only bp upstream the +1 transcriptional start site resulted in decreased green fluorescence with an even further decrease observed in spots of cells with the construct containing only 60 bp upstream the +1 region. These data suggest the 115-bp region between positions -175 and -60 is necessary for LuxO activation of $Qrr1$ transcription.

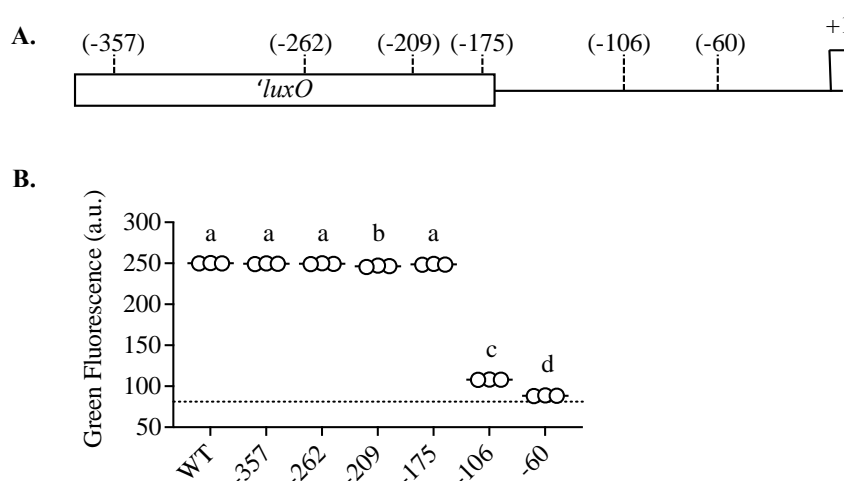


Figure 3.2: Genetic elements that promote LuxO activation of P_{qrr1}

- A.** A cartoon of the 378-bp of the *luxO-qrr1* intergenic region within the P_{qrr1} -*gfp* reporter plasmid. The numbers in parenthesis indicate the site of plasmid truncations relative to the +1 transcriptional start site of *qrr1*. The construct also contains 205 bp of the 3' end of the *luxO* coding region.
- B.** Cultures of the *V. fischeri* CL59 (LuxO D55E) strain harboring WT and truncated P_{qrr1} reporter plasmids were spotted onto rich media and incubated overnight. Plasmids are pEDR003 (WT), pEDR008 (-60), pEDR009 (-106), pEDR006 (-175), pEDR012 (-209), pEDR010 (-262), and pEDR011 (-357). Shown are the average green fluorescence values for each spot of growth. The dotted line indicates the level of background fluorescence determined from *V. fischeri* ES114 (WT) harboring a non-fluorescent plasmid (pVSV105/ES114). One-way ANOVA ($F_{6,14} = 62,658, p < 0.0001$); Tukey's *post-hoc* test with *p*-values corrected for multiple comparisons (same letter = not significant, different letters = $p < 0.001$).

Further inspection of the 115-bp region required for LuxO activation of P_{qrr1} revealed two putative UASs of LuxO were located upstream the $qrr1$ gene. These UASs were labeled UAS-1_(LuxO) and UAS-2_(LuxO) based on their proximity to the transcriptional start site of $qrr1$. (**Fig. 3.3A**). Each matched the consensus sequence (TTGCA-W₃TGCAA, where W represents A or T) for the LuxO UAS identified in other *Vibrio* species [91, 93]. To determine the extent to which each UAS contributed to LuxO activation of P_{qrr1} in *V. fischeri*, single nucleotide substitutions were individually introduced into the P_{qrr1} transcriptional reporter and cloned into the *luxOD55E* mutant. All three mutations generated within the 5' half-site of UAS-1_(LuxO) led to a decrease in P_{qrr1} activation (**Fig. 3.3B**). Substitutions of the last two nucleotides within the half-site had the largest impact on LuxO activation of P_{qrr1} . Similar results were observed when these same nucleotides were mutated within UAS-2_(LuxO). These data suggest that LuxO depends on two UASs within the $qrr1$ promoter region to activate expression of Qrr1.

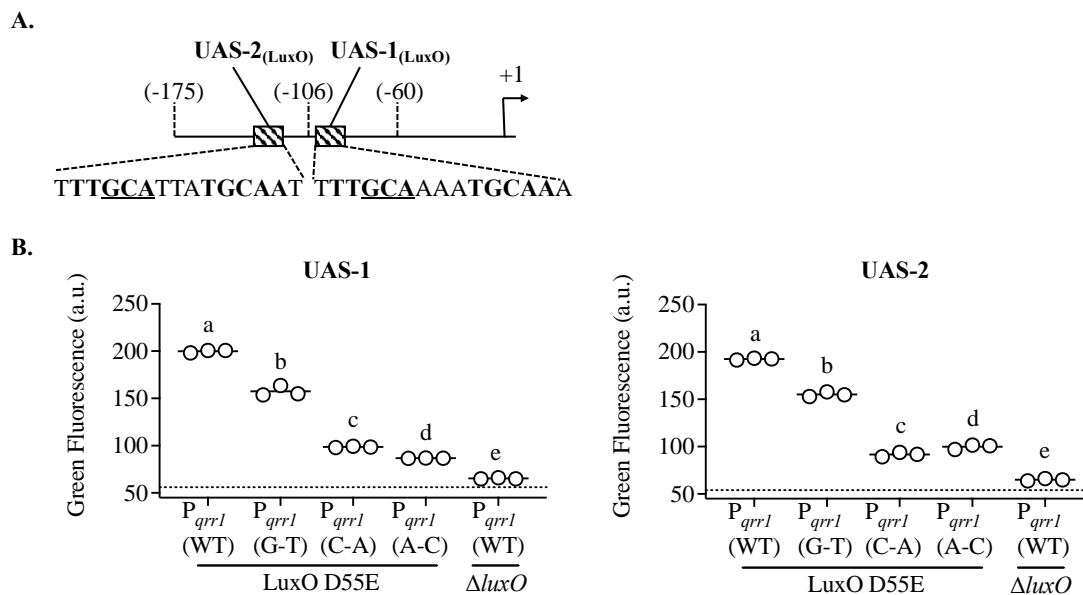


Figure 3.3: LuxO activation of P_{qrr1} depends on two UASs

- A.** Diagram of the 115-bp region required for LuxO activation of P_{qrr1} . The two UAS of LuxO are labeled, and the sequence for each is shown below. Nucleotides targeted for mutagenesis in each UAS are underlined.
- B.** Green fluorescence levels of EDS008 ($\Delta luxO \Delta sypG$) and EDS010 ($\Delta luxO \Delta sypG$ Tn7:: $P_{trc-sypG}$) harboring the P_{qrr1} reporter plasmids pEDR003 and *left* (UAS-1), pEDS007 (G₉₇T), pEDS008 (C₉₆A), and pEDS009 (A₉₅C) and *right* (UAS-2), pEDS004 (G₁₃₁T), pEDS005 (C₁₃₀A), and pEDS006 (A₁₂₉C). Subscripts indicate nucleotide position relative to the +1 transcriptional start site of $qrr1$. One-way ANOVA (*left*: $F_{4,10} = 1425$, $p < 0.0001$; *right*: $F_{4,10} = 2030$, $p < 0.0001$); Tukey's *post-hoc* test with p -values corrected for multiple comparisons (same letter = not significant, different letters = $p < 0.001$).

SypG as a candidate bEBP of *Qrr1* transcription

The results of the previous chapter suggest in addition to LuxO, another bEBP can activate expression of *qrr1*, even under conditions of quorum sensing when P_{qrr1} activation is typically repressed. To identify bEBPs in *V. fischeri*, a BLAST search was performed against the genome of *V. fischeri* ES114 using the AAA+ domain of LuxO as a query. Of the 12 hits, 8 contained a perfect GAFTGA motif. PspF contained a GSFTGA motif, but this substitution still permits σ^{54} -dependent transcription [55]. Therefore, these 9 proteins were classified as bEBPs of *V. fischeri* (**Appendix A.5**). Of these 9, SypG was chosen as a candidate bEBP of *qrr1* for several reasons. BinK, which is a negative regulator of P_{qrr1} activation, also inhibits transcription of genes activated by SypG ([99], **Chapter 2**). LuxO and SypG are homologs that share 65% sequence similarity (49% identity) overall (**Fig. 3.4**). Residues within the linker region, including the residues predicted to occupy the ATP active site, are also conserved in SypG, suggesting LuxO and SypG function using similar mechanisms. Lastly, 14 out of 22 residues (64% identity; 77% similarity) within the putative helix-turn-helix (HTH) domain, which binds DNA, are identical between the two bEBPs, suggesting LuxO and SypG may recognize similar DNA sequences within the promoters of their target genes.

Overexpression of SypG is sufficient to activate P_{qrr1}

To, first, determine the extent to which SypG activates P_{qrr1} in the absence of BinK, green fluorescence was measured in a $\Delta binK \Delta luxO \Delta sypG$ mutant harboring the $P_{qrr1-gfp}$ reporter. The level of green fluorescence in the triple mutant was approximately 3-fold lower than what was observed in the $\Delta binK \Delta luxO$ mutant, suggesting SypG also contributes to P_{qrr1} in the $\Delta binK$ mutant (**Fig. 3.5A**). Green fluorescence levels in the $\Delta binK \Delta sypG$ double mutant were comparable to what was observed in the $binK$ mutant. This potentially indicates that LuxO is a more efficient activator of P_{qrr1} . To assess whether SypG can activate P_{qrr1} when BinK is present, P_{qrr1} activation was measured in a $\Delta luxO \Delta sypG$ mutant with $sypG$ ectopically expressed from the IPTG-inducible P_{irc} promoter ($\Delta luxO \Delta sypG sypG+$). Relative to the parent strain, green fluorescence was elevated 4-fold when $sypG$ was overexpressed (**Fig. 3.5B**). These data suggest that SypG alone is sufficient to activate Qrr1 transcription in *V. fischeri*.

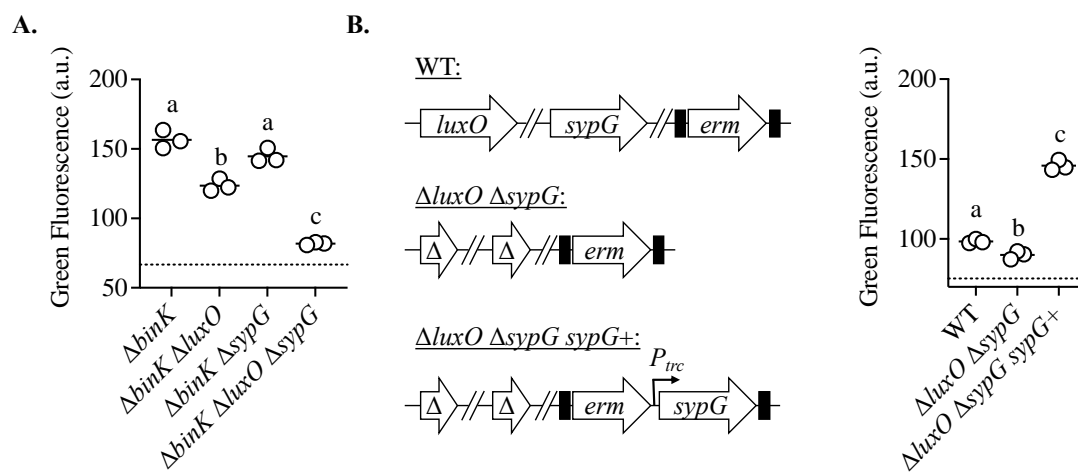


Figure 3.5: SypG is sufficient to activate P_{qrr1}

Green fluorescence levels of **A.** MJM2251 ($\Delta binK$), EDR009 ($\Delta binK \Delta luxO$), EDR014 ($\Delta binK \Delta sypG$), and EDR013 ($\Delta binK \Delta luxO \Delta sypG$) harboring the P_{qrr1} reporter plasmid pTM268 and **B.** TIM313 (WT Tn7::*erm*) EDS008 ($\Delta luxO \Delta sypG$ Tn7::*erm*) and EDS010 ($\Delta luxO \Delta sypG$ Tn7:: $P_{trc}::sypG$) with the P_{qrr1} reporter plasmid pEDR003. The dotted lines indicate the level of background fluorescence determined from *V. fischeri* ES114 (WT) harboring a non-fluorescent plasmid (**A:** pVSV105/ES114; **B:** pVSV105/EDS008). One-way ANOVA (**A:** $F_{3,8} = 1425$, $p < 0.0001$; **B:** $F_{2,6} = 438.8$, $p < 0.0001$); Tukey's *post-hoc* test with p -values corrected for multiple comparisons (same letter = not significant, different letters = $p < 0.001$). **B, left** shows a cartoon diagram of the strain used in **B, right**.

Signaling through the cellular-aggregation pathway impacts Qrr1 expression

The histidine kinase RscS phosphorylates SypG, which results in increased activation of genes within the *syp* locus [97]. Therefore, to investigate whether stimulating SypG through RscS could also increase P_{qrr1} activation, a plasmid encoding a variant of *rscS* (*rscS**) that results in increased translation of RscS was introduced into *V. fischeri* strains with the P_{qrr1} -*gfp* reporter engineered into the chromosome. When RscS is overexpressed, *V. fischeri* cells form colonies with a rugose, or wrinkled, morphology [112]. While WT cells expressing *rscS** formed wrinkled colonies, the Δ *sypG* mutants with the *rscS** allele exhibited a smooth colony morphology **Fig. 3.6**). This result suggests RscS signals through SypG to promote wrinkled colony formation and is consistent with previously published results [97]. Expression of *rscS** in WT cells led to an increase in green fluorescence relative to spots of the parent strain carrying an empty vector, which suggests RscS promotes P_{qrr1} activation. Furthermore, because autoinducer concentrations within the spots are at levels that inhibit P_{qrr1} activity (**Chapter 2**), this result also suggests expression of RscS can activate Qrr1 transcription under quorum-sensing conditions. Next, it was determined the extent to which P_{qrr1} activity in the *rscS** strain depends on *sypG*. The levels of green fluorescence in spots of the Δ *sypG* mutant expressing *rscS** were low, similar to what was observed in WT spots. Together, these data indicate that RscS-dependent stimulation of the signaling network that promotes cellular aggregation also results in SypG activation of Qrr1 transcription.

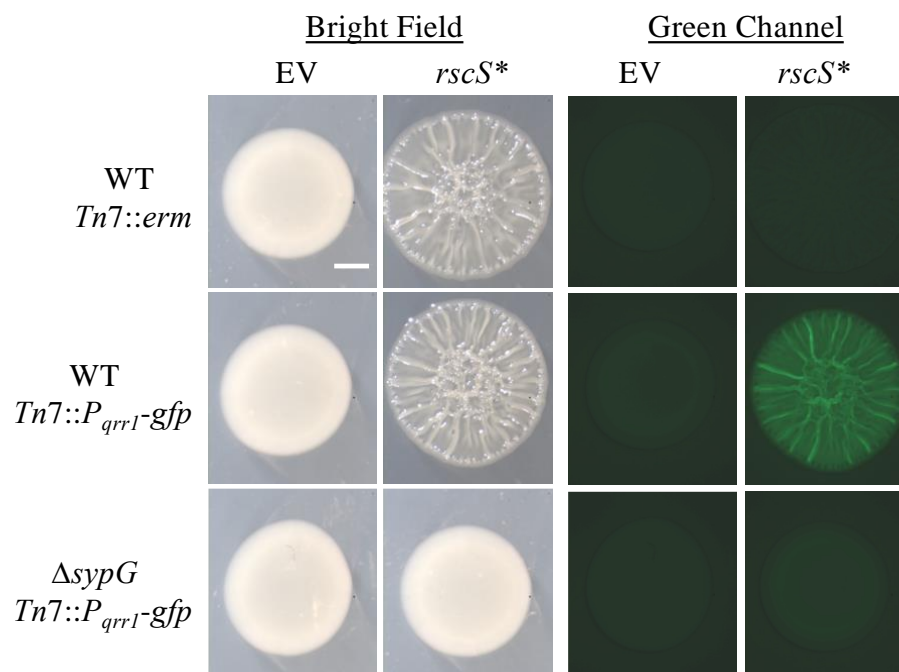


Figure 3.6: RscS promotes P_{qrr1} activation

Bright field and green fluorescence images of spots of growth for TIM313 (WT $Tn7::erm$), TIM303 (WT $Tn7::P_{qrr1}-gfp$), and EDS015 ($\Delta sypG$ $Tn7::P_{qrr1}-gfp$) harboring a plasmid carrying the *rscS** allele, pKG11, or the empty vector (EV) pKV69. Scale bar represents 1 mm. Experiment performed by Shyan Cousins.

The previous finding indicates RscS expression promotes P_{qrr1} activation in a manner that depends on SypG. Because overexpression of Qrr1 results in decreased cellular luminescence (**Appendix A.3**), one hypothesis was that stimulation of the cellular aggregation signaling network by RscS also leads to a reduction in luminescence. To test this hypothesis, luminescence was measured throughout the growth of cultures of *V. fischeri* cells. In cultures of WT cells, specific luminescence values peaked around an OD_{600} of 1.0 (**Fig. 3.7**). However, when *rscS** was expressed in WT cells, luminescence over the growth curve was lower than what was observed in cultures of WT cells. Luminescence values also peaked later around an OD_{600} of 2.0 and were significantly lower than the parent strain. These results suggest expression of RscS inhibits luminescence. Because BinK is a negative regulator of the cellular aggregation pathway [99, 135]

and inhibits P_{qrr1} activation (**Chapter 2**), it was of interest to assess whether the absence of $binK$ would also lead to increased luminescence. Luminescence values for cultures of the $\Delta binK$ mutant followed a similar trend as WT, suggesting BinK has no impact on luminescence. However, previous studies revealed $rscS^*$ expression is necessary to observe some BinK-dependent phenotypes [99]. Indeed, cultures of a $\Delta binK$ mutant expressing $rscS^*$ had lower luminescence levels over the growth curve than the $\Delta binK$ mutant. The $rscS^* \Delta binK$ strain also peaked at a lower OD_{600} , and the average peak luminescence was lower than what was observed in the $\Delta binK$ mutant. Luminescence values were even lower than in cultures of WT cells expressing $rscS^*$. This result suggests that RscS inhibits luminescence through a factor that is inhibited by BinK.

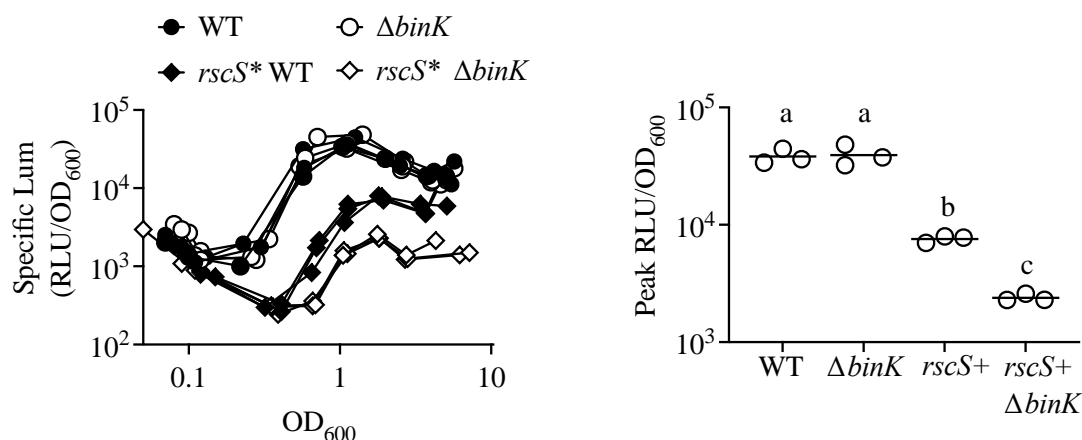


Figure 3.7: RscS inhibits luminescence

Left, Luminescence values of *V. fischeri* strains MJM1100 (WT), MJM1198 ($rscS^*$ WT), MJM2251 ($\Delta binK$), and MJM2255 ($rscS^* \Delta binK$) grown in SWTO were obtained every hour. Plotted is the specific luminescence, or relative light units (RLU) divided by the optical density (OD_{600}), for each culture as a function of growth. *Right*, Peak specific luminescence values for each culture. Each point represents an independent sample with bars indicating the average. Peak specific luminescence (Peak RLU/ OD_{600}) values were log-transformed. One-way ANOVA ($F_{3,8} = 308.6$, $p < 0.0001$); Tukey's post-hoc test with p-values corrected for multiple comparisons (same letter = not significant, different letters = $p < 0.001$). This experiment was performed by Denise Ludvik in the lab of Mark Mandel at the University of Wisconsin-Madison, who granted permission to use this data.

Genetic elements that promote SypG activation of P_{qrr1}

The results described above suggest that SypG is a bEBP that regulates *qrr1* transcription. In this case, SypG activation of P_{qrr1} should depend on elements within the *qrr1* promoter. To test this prediction, the truncated promoter constructs tested in the *luxOD55E* mutant (**Fig. 3.2**) were also introduced into the $\Delta luxO \Delta sypG sypG+$ strain. Deleting up to nucleotide -176 relative to the +1 transcriptional start site of *qrr1* did not attenuate green fluorescence levels, suggesting the region required for SypG activation of P_{qrr1} lies further downstream (**Fig. 3.8B**). Indeed, deleting nucleotides up to position -176 resulted in a 5-fold decrease in green fluorescence relative to the WT P_{qrr1} construct. An even lower level of green fluorescence was observed when nucleotides up to position -61 were deleted. Together, these data suggest the region of DNA between positions -176 and -61 contain genetic elements necessary for SypG activation of *qrr1* transcription.

SypG recognizes one to two UASs within the promoter region of its target genes with the consensus sequence **TTCTCA-N₃-TGMDWN** (where W represents A or T, M is A or C, D is A, T, or G, and N is any nucleotide) [95]. Because LuxO and SypG appear to share the same 115-bp region of *qrr1* promoter DNA to activate P_{qrr1} , it was worthwhile to assess whether SypG activation of P_{qrr1} also depends on the two UASs of LuxO located within this region. P_{qrr1} constructs with single-nucleotide substitutions in each of the putative LuxO UASs were conjugated into the $\Delta luxO \Delta sypG sypG+$ mutant. Each of the three mutations introduced into UAS-1_(LuxO) resulted in decreased green fluorescence (**Fig 3.8B**). Similar results were observed when nucleotides in UAS-2_(LuxO) were substituted. These results suggest SypG activation of *Qrr1* transcription depends on the two putative UASs of LuxO.

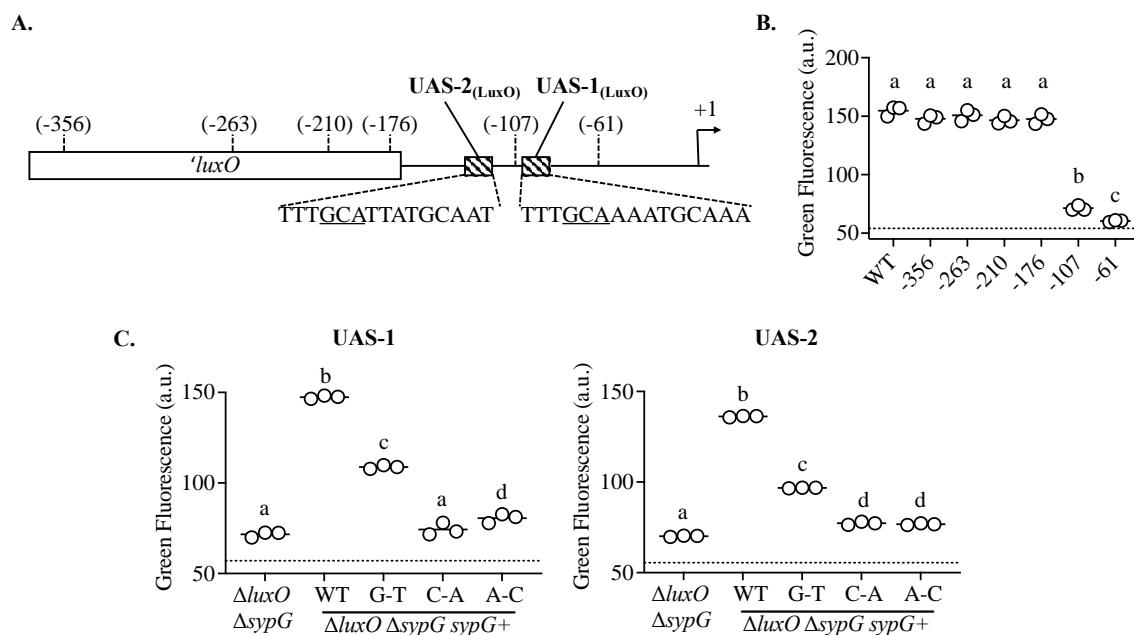


Figure 3.8: Genetic elements that promote SypG activation of P_{qrr1}

Shown in **A** is the truncated promoter diagram with the UASs of LuxO, with the sequences for each UAS shown. Nucleotides targeted for mutagenesis in **C** are underlined. **B**, **C**: Green fluorescence values for cultures of indicated strains. The dotted line indicates the level of background fluorescence determined from a *V. fischeri* ES114-derived strain harboring a non-fluorescent plasmid (pVSV105/EDS008). Tukey's *post-hoc* test with *p*-values corrected for multiple comparisons (same letter = not significant, different letters = $p < 0.001$). (**B**) EDS010 ($\Delta luxO \Delta sypG$ Tn7::*P_{ire-sypG}*) harboring the WT P_{qrr1} reporter plasmid pEDR003 (WT) and truncated plasmids pEDR008 (-60), pEDR009 (-106), pEDR006 (-175), pEDR012 (-209), pEDR010 (-262), and pEDR011 (-357); One-way ANOVA ($F_{6,14} = 411.7$, $p < 0.0001$). (**C**) EDS008 ($\Delta luxO \Delta sypG$ Tn7::*erm*) harboring the WT P_{qrr1} reporter plasmid pEDR003 (WT) and EDS010 ($\Delta luxO \Delta sypG sypG+$) harboring the mutated P_{qrr1} reporter plasmids **left**, pEDS007 (G₉₇T), pEDS008 (C₉₆A) and pEDS009 (A₉₅C) and **right**, pEDS004 (G₁₃₁T), pEDS005 (C₁₃₀A), and pEDS006 (A₁₂₉C). One-way ANOVA (**left**, $F_{4,10} = 712.5$, $p < 0.0001$; **right**, $F_{4,10} = 8232$, $p < 0.0001$).

Assessing cross-activation by LuxO and SypG

The consensus sequences for the putative UASs of LuxO and SypG differ by only two nucleotides within the 5' half-site (**Fig. 3.9A**), suggesting the two bEBPs are able to bind similar sites. Furthermore, similar UAS sites might explain how SypG can activate P_{qrr1} activity. One possibility worth pursuing was to determine whether mutating UAS_{LuxO} to match UAS_{SypG} would increase SypG activation of P_{qrr1} . To test this hypothesis, green fluorescence was measured in the $\Delta luxO \Delta sypG sypG^+$ strain harboring a P_{qrr1} reporter plasmid with a TG to CT mutation within the 5' half-site of $UAS-2_{(LuxO)}$. The levels of green fluorescence in the $\Delta luxO \Delta sypG sypG^+$ strain carrying the mutated P_{qrr1} plasmid were similar to what was observed with the WT P_{qrr1} construct (**Fig. 3.9B**). This result suggests SypG recognizes UAS_{LuxO} as efficiently as it recognizes its own UAS. To assess whether LuxO might recognize UAS_{SypG} , the TG-CT P_{qrr1} construct was moved into the $luxOD55E$ mutant. Green fluorescence in this strain carrying the mutated P_{qrr1} construct was slightly attenuated relative what was observed with the WT P_{qrr1} plasmid, but not completely eliminated, suggesting LuxO can also recognize UAS_{SypG} .

UAS_{SypG} is found upstream of four operons within the *syp* locus. The first UAS is located within the promoter of *sypA* with the sequence **TTCTCATTCTGCAAA** (half-site are bolded) [95]. Because it appears LuxO can recognize UAS_{SypG} , it was considered whether LuxO could also increase the promoter activity of SypG-activated genes. To test this hypothesis, a $P_{sypA-gfp}$ promoter reporter containing UAS_{SypG} was conjugated into the *V. fischeri* strain harboring the hyperactive variant of LuxO. The $P_{sypA-gfp}$ construct was also introduced into various $\Delta binK$ mutants as controls. Green fluorescence levels were elevated in the $\Delta binK$ mutant relative to what was observed in WT, and this increase depended on the presence of *sypG* (**Fig. 3.9C**). These data suggest BinK inhibits SypG-activation of P_{sypA} , which is consistent with previously published results [99]. The levels of green fluorescence in a $\Delta binK \Delta sypG$ mutant was similar to what was observed in spots of WT cells, which suggests no other factors activates P_{sypA} under these

conditions. However, green fluorescence levels in the *luxOD55E* mutant were similar to WT, which suggests LuxO is unable to activate transcription of *sypA*, suggesting LuxO does not recognize the UASs of SypG within the *sypA* promoter. Alternatively, an unknown factor could inhibit the ability of LuxO to activate *sypA*.

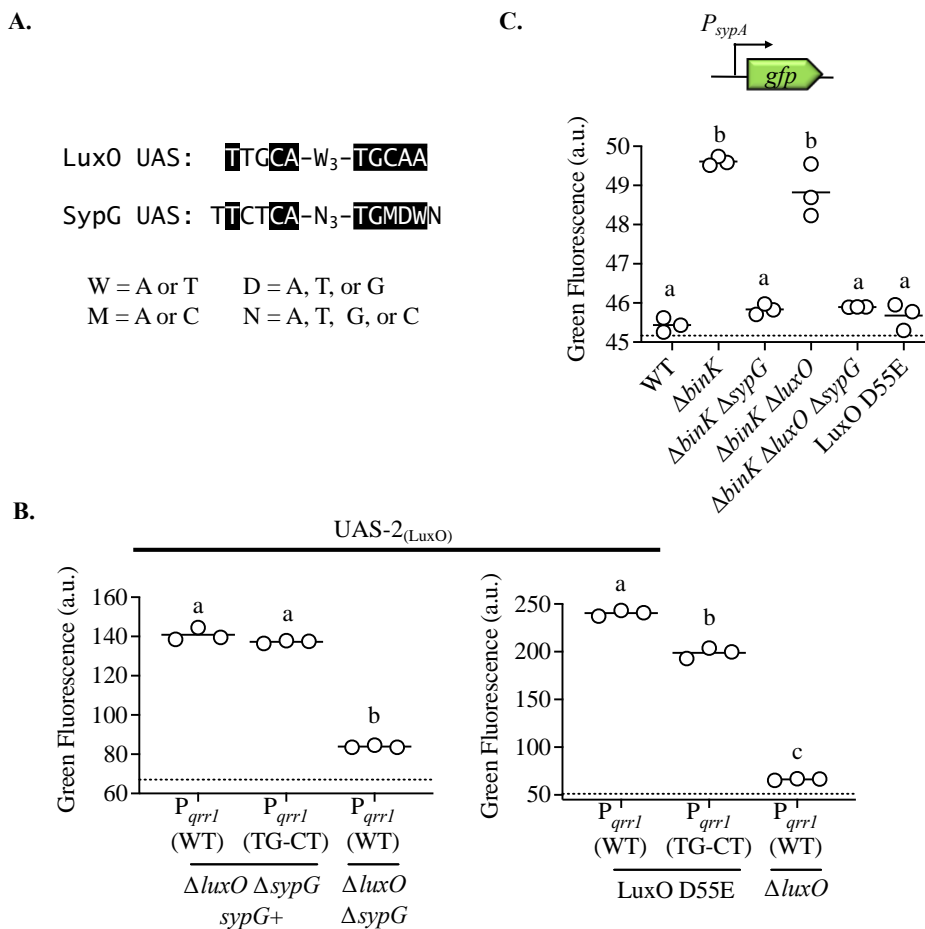


Figure 3.9: Assessing cross-activation by LuxO and SypG

Shown in **A** are the consensus sequences recognized by LuxO and SypG. Identical nucleotides are highlighted in black. (**B**, **C**): Green fluorescence values for cultures of indicated strains. The dotted line indicates the level of background fluorescence determined from a *V. fischeri* ES114-derived strain harboring a non-fluorescent plasmid (**B**, **right** and **C**: pVSV105/ES114 ; **B**, **left**: pVSV105/EDS008). Tukey's *post-hoc* test with *p*-values corrected for multiple comparisons (same letter = not significant, different letters = $p < 0.001$). Experiment performed by Terry Ruskoski. (**B** **left**: EDS008 ($\Delta luxO \Delta sypG$ Tn7::erm) and EDS010 ($\Delta luxO \Delta sypG$ Tn7::P_{trc-sypG}) with pEDR003 and EDS010 with pEDS001. **Right**, CL59 (LuxO D55E) and TIM306 ($\Delta luxO$) harboring the WT P_{qrr1} reporter plasmid pEDR003 and CL59 with plasmid pEDS001 (TG to CT mutation in UAS-2_(LuxO)). One-way ANOVA (**left**, $F_{2,6} = 813.4$, $p < 0.0001$; **right**, $F_{2,6} = 1855$, $p < 0.0001$). (**C**): ES114 (WT), MJM2251 ($\Delta binK$), EDR014 ($\Delta binK \Delta sypG$), EDR009 ($\Delta binK \Delta luxO$), EDR013 ($\Delta binK \Delta luxO \Delta sypG$) and CL59 with the P_{sypA} -*gfp* promoter reporter pVF_A1020P. One-way ANOVA ($F_{5,12} = 96.79$, $p < 0.0001$).

LuxO, SypG, and Qrr1 are conserved among the *Fischeri* Clade

V. fischeri is a member of the *Fischeri* clade within the *Vibrionaceae* family [136]. The five taxa characterized in this clade are *Aliivibrio fischeri* (*V. fischeri*), *Aliivibrio wodanis* (*A. wodanis*), *Aliivibrio sifiae* (*A. sifiae*), *Aliivibrio salmonicida* (*A. salmonicida*), and *Aliivibrio logei* (*A. logei*). All five taxa encode a LuxO homolog (**Appendix A.6**), which is located upstream of a *qrr1* gene. The R-C linker is conserved, including the residues predicted to occupy the ATP active site, suggesting the regulatory role of the linker in LuxO is present throughout the *Fischeri* clade (**Appendix A.6**). Each taxon also contains two potential UASs of LuxO upstream the transcriptional start site of *qrr1* as well as a putative σ^{54} binding site (**Fig. 3.10**). This data suggests that *luxO* and *qrr1* are conserved across the *Fischeri* clade. In addition, there is evidence LuxO depends on two UASs to activate σ^{54} -dependent transcription of *qrr1* in all five taxa.

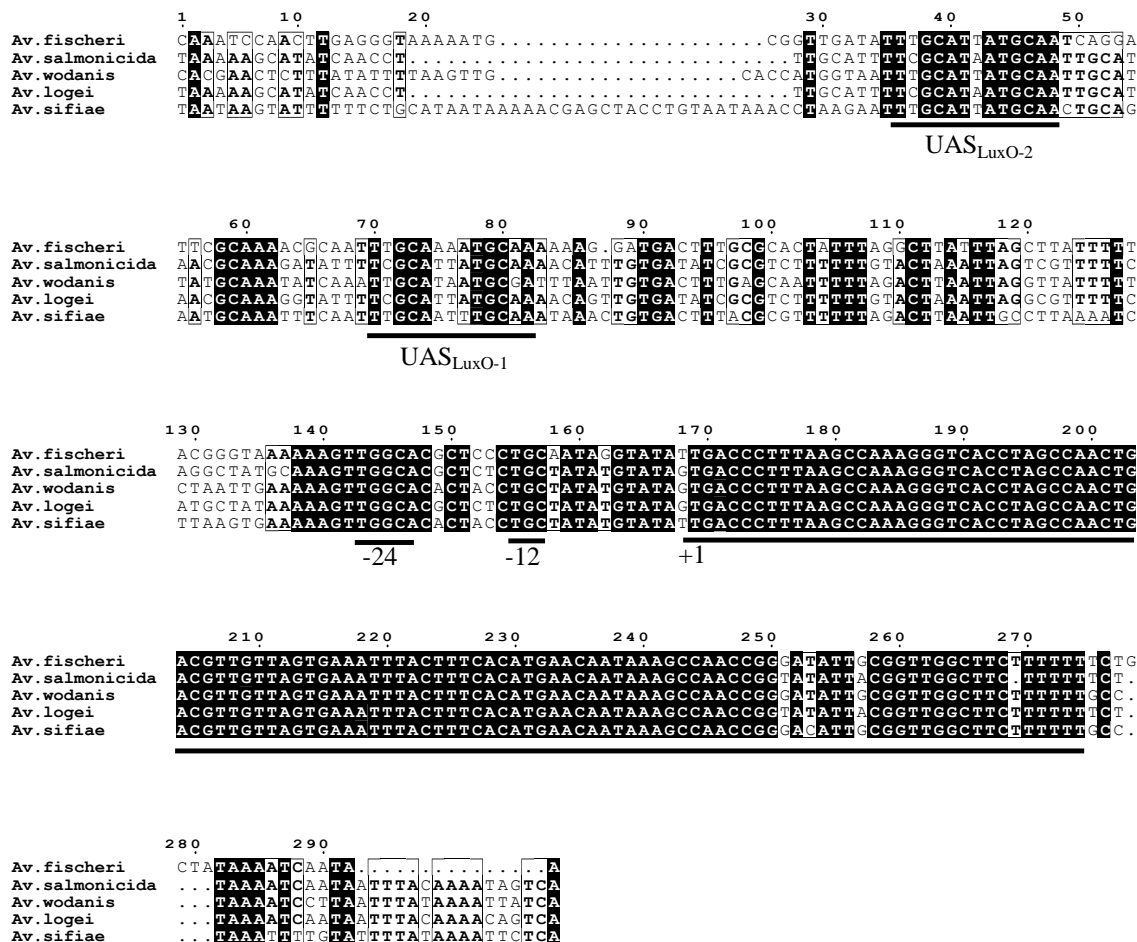


Figure 3.10: *luxO-uvrB* intergenic region in the *Fischeri* clade

The intergenic region of *uvrB* and *luxO* genes of the indicated taxa were aligned using MAFFT. Accessions analyzed: *Vibrio fischeri* = NC_006840.2, *Aliivibrio salmonicida* = NC_011312.1, *Aliivibrio wodanis* = LN554846.1, *Aliivibrio logei* = NZ_MAJU01000008.1, and *Aliivibrio sifiae* = NZ_MSCP01000001.1. The two putative UASs of LuxO are labeled. The -12 and -24 positions of the putative σ_{54} -binding site are also indicated along with the +1 transcriptional start site of *qrr1*. A black line underscores the *qrr1* gene (position 169 – 274). Alignment figure generated using ESPript 3.0 (<https://espript.ibcp.fr/ESPript/cgi-bin/ESPript.cgi>).

To determine whether the potential for SypG activation of *qrr1* in the *Fischeri* clade, each taxon was assessed for the presence of a SypG homolog. A *sypG* gene was located between *sypF* and *sypH* within a *syp* locus was found in all five taxa, suggesting the SypG homolog is conserved within the *Fischeri* Clade (**Fig. 3.11**). An alignment of LuxO and SypG for each taxon revealed the two bEBPs share approximately 48% amino acid sequence identity (**Fig. 3.12A, Appendix A.7**). The regulatory linker is also conserved in all SypG homologs, including the structurally significant glycine residue. These data suggest LuxO and SypG homologs function using similar mechanisms among *Fischeri*. In addition, 14 of the 22 residues within the helix-turn-helix motif were identical between the two homologs within each taxon (**Fig. 3.12B**), indicating the bEBPs may recognize similar DNA sequences. These data highlight the potential for SypG activation of *qrr1* among taxa in the *Fischeri* clade.

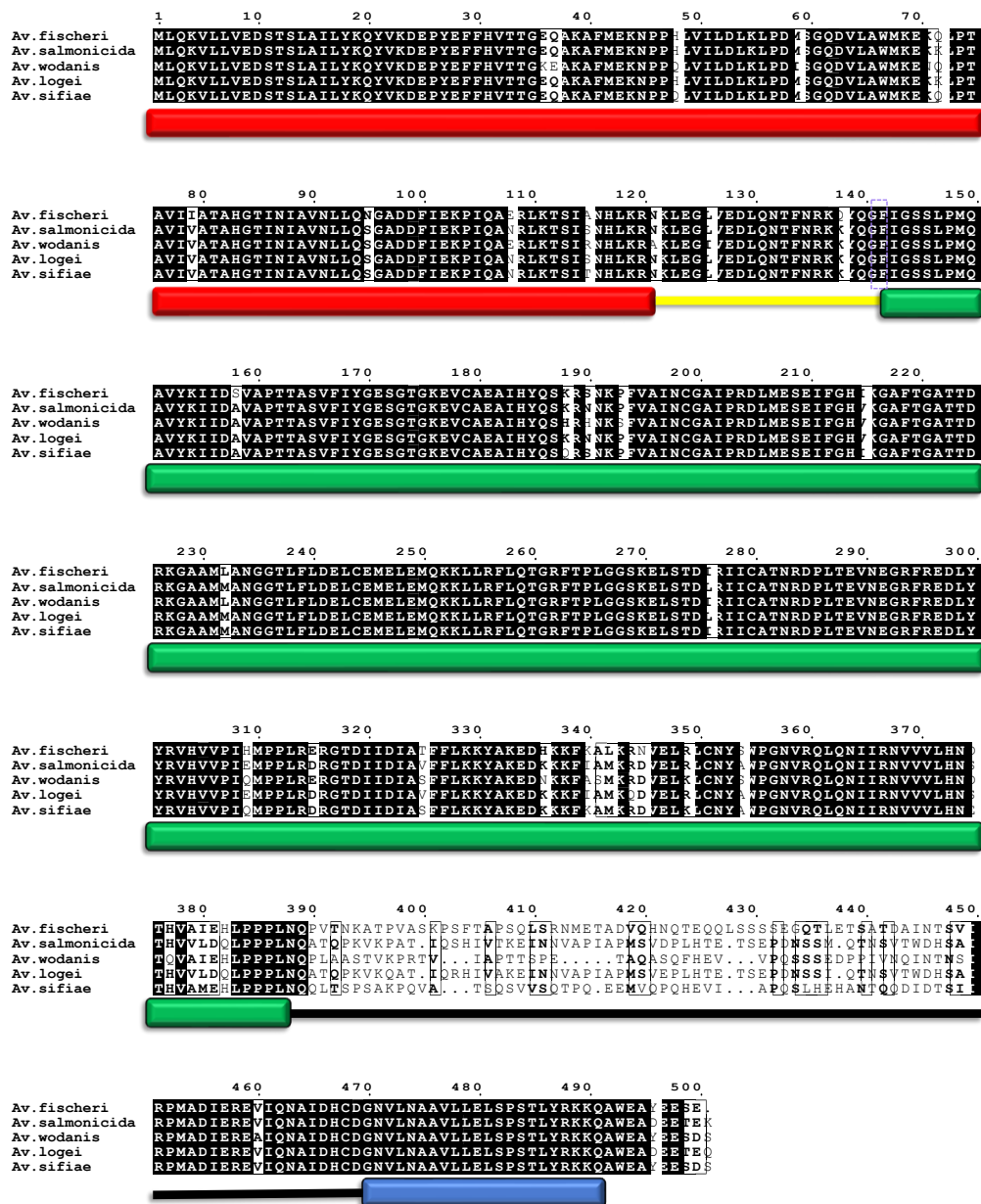


Figure 3.11: SypG in the Fischeri clade

Multiple sequence alignment of SypG homologs. Identical amino acids are highlighted in black; similar amino acids are bolded. The rectangles above indicate the receiver (R) domain (red), the AAA+ (C) domain (green), and the putative helix-turn-helix (HTH) motif (blue) within the DNA-binding (D) domain. The yellow line indicates the residues of the R-C linker (xKLEG...YQGF). The structurally significant glycine is outlined with a purple dashed box. Alignment figure generated using ESPrpt 3.0 (<https://esprpt.ibcp.fr/ESPrpt/cgi-bin/ESPrpt.cgi>).

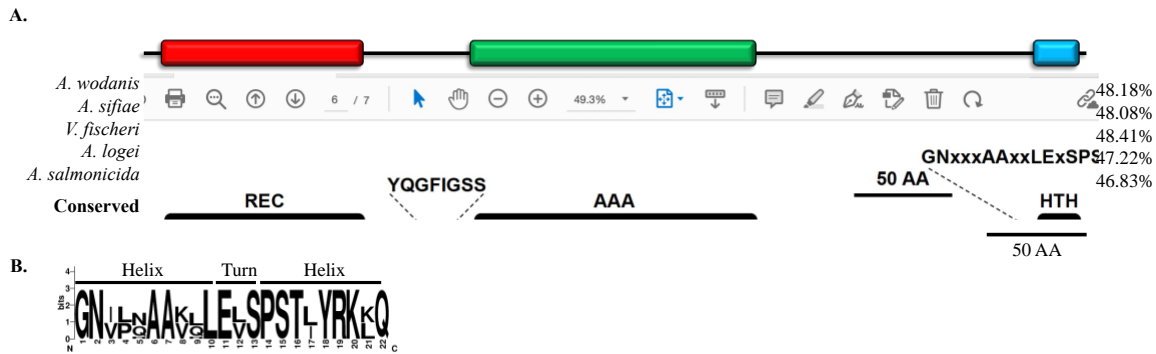


Figure 3.12: The potential for SypG activation of *qrr1* in the *Fischeri* clade

- A.** Each row represents a pairwise sequence alignment of LuxO and SypG homologs encoded in each taxa within the *Fischeri* clade. Each amino acid and gap were assigned a position 1-481 (based on the largest LuxO homolog, which is found in *A. salmonicida*). Black boxes indicate a residue conserved between the two homologs. The percent identity is listed at the end of each row. The *conserved* row highlights amino acids are conserved for all five taxa.
- B.** Consensus sequence of the putative 22 amino acid helix-turn-helix (HTH) domain of all LuxO and SypG homologs (10 total sequences) in the *Fischeri* clade. Sequence logo generated at <https://weblogo.berkeley.edu/logo.cgi>.

SypG activation of P_{qrr1} in *Aliivibrio salmonicida*

To test whether SypG could activate *qrr1* transcription in other taxa within the *Fischeri* clade, *Aliivibrio salmonicida* was selected for further study. *A. salmonicida* is a fish pathogen that causes cold-water vibriosis in Atlantic fishes [137]. LuxO and SypG share 46% identity in *A. salmonicida* (**Fig. 3.12A, Appendix A.7**). In addition, the UASs of LuxO are identical except for a T to C substitution in the 5' half site (**Fig. 3.10**). Therefore, it was worthwhile to assess the extent to which SypG might also activate expression of *qrr1* in this taxon. The *sypG* gene from *A. salmonicida* (AS_{sypG}) harboring an IPTG-inducible promoter was cloned into a *V. fischeri* $\Delta luxO$ $\Delta sypG$ mutant. This strain contained a plasmid containing the *qrr1* promoter from *A. salmonicida* ($AS_{P_{qrr1}}$) upstream of *gfp*. Green fluorescence levels in spots of this strain were elevated relative to the control strain (**Fig. 3.13**), suggesting that SypG can also activate expression of Qrr1 in *A. salmonicida*.

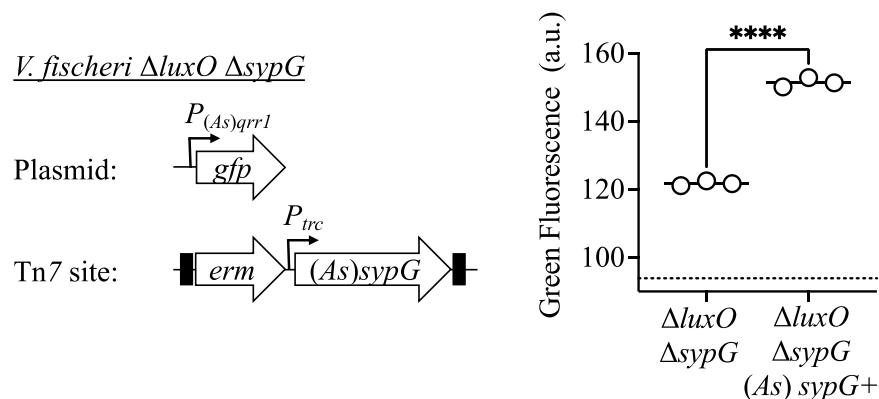


Figure 3.13: The potential for SypG activation of P_{qrr1} in *A. salmonicida*

Left, a diagram of the plasmid and Tn7 integration introduced into the *V. fischeri* $\Delta luxO$ $\Delta sypG$ mutant; *As* = *A. salmonicida*. Right, green fluorescence levels of EDS008 ($\Delta luxO$ $\Delta sypG$ Tn7::*erm*) and EDS021 ($\Delta luxO$ $\Delta sypG$ Tn7:: P_{trc} -(*As*)*sypG*) harboring the *A. salmonicida* P_{qrr1} reporter plasmid pAGC004. An unpaired t-test was used to compare each group ($\alpha = 0.05$; **** = $p < 0.0001$).

Conservation between LuxO and SypG in the *Vibrionaceae*

The *Vibrionaceae* family consists of 23 clades and harbor a diversity of species including pathogens, beneficial microbes, and planktonic bacteria [36, 136]. Many of these taxa encode one or more Qrr homologs [93, 114, 117, 138]. To assess whether the potential for LuxO and SypG activation of *qrr1* was widespread across the *Vibrionaceae*, one representative taxon from each clade was assessed for the presence of all three genetic factors. All taxa that were examined encode a LuxO homolog except *Vibrio rumioensis* (**Fig. 3.14, Appendix A.7**), which suggests LuxO is ancestral to the *Vibrionaceae*. Within the LuxO+ taxa, there was some variability in the length of the putative regulatory R-C linker; however, the glycine residue predicted to make key stabilizing bonds with the R and C domains was conserved across all LuxO+ taxa (**Appendix A.8**). This data suggests the unique regulatory role of the R-C linker may be conserved among LuxO homologs in the *Vibrionaceae*. Furthermore, across the LuxO+ taxa, there was a high degree of identity within the putative helix-turn-helix domain (**Appendix A.8**), which suggests this region is under positive selection and recognizes similar UASs. Of the LuxO+ taxa, 20 also encode a *qrr* homolog located in the intergenic region between *luxO* and *uvrB* (**Fig. 3.14; Appendix A.10**). A putative σ^{54} binding site was located upstream of all the *qrr* homologs, suggesting σ^{54} -dependent regulation of this gene is conserved.

Clade	Taxon	LuxO	SypG	<i>qrr1</i>
Salinivibrio-Grimontia-Enterovibrio	<i>G. hollisae</i>	Gray	Gray	Gray
Rosenbergii	<i>P. lutimaris</i>	Gray	Gray	Gray
Profundum	<i>P. profundum</i>	Gray	Gray	Gray
Damselae	<i>Photobacterium damsela</i> subsp. <i>piscicida</i>	Gray	Gray	Gray
Phosphoreum	<i>P. phosphoreum</i>	Gray	Gray	Gray
Fischeri	<i>V. fischeri</i>	Gray	Gray	Gray
Anguillarum	<i>V. anguillarum</i>	Gray	Gray	Gray
Rumoiensis	<i>V. rumoiensis</i>	Gray	Gray	Gray
Vulnificus	<i>V. vulnificus</i>	Gray	Gray	Gray
Diazotrophicus	<i>V. diazotrophicus</i>	Gray	Gray	Gray
Gazogenes	<i>V. gazogenes</i>	Gray	Gray	Gray
Porteresiae	<i>V. tritonius</i>	Gray	Gray	Gray
Cholerae	<i>V. cholerae</i>	Gray	Gray	Gray
Haliotocoli	<i>V. breoganii</i>	Gray	Gray	Gray
Splendidus	<i>V. splendidus</i>	Gray	Gray	Gray
Pectenocida	<i>V. pectenocida</i>	Gray	Gray	Gray
Scopthalmi	<i>V. ponticus</i>	Gray	Gray	Gray
Nereis	<i>V. nereis</i>	Gray	Gray	Gray
Orientalis	<i>V. tubiashii</i>	Gray	Gray	Gray
Coralliilyticus	<i>V. coralliilyticus</i>	Gray	Gray	Gray
Harveyi	<i>V. harveyi</i>	Gray	Gray	Gray
Nigripulchritudo	<i>V. nigripulchritudo</i>	Gray	Gray	Gray
Mediterranei	<i>V. mediterranei</i>	Gray	Gray	Gray

Figure 3.14: LuxO, SypG, and *qrr* in the *Vibrionaceae*

Gray boxes represent the presence of a LuxO or SypG homolog or a *qrr* gene located in the intergenic region between *uvrB* and *luxO*. The *Salinivibrio-Grimontia-Enterovibrio* group is ancestrally related to the *Vibrionaceae* family and is included as an outgroup in this analysis.

Next, the LuxO+/*qrr1*+ taxa were surveyed for the presence of a *sypG* homolog. Almost half of taxa encoded the bEBP within a *syp* locus (**Fig. 3.15A**). The length of the regulatory R-C linker was conserved, and the structurally significant glycine was conserved in all SypG+ taxa except *V. splendidus*, which had an asparagine (N) substitution (**Appendix A.9**). The majority of residues within the helix-turn-helix domain were identical among the SypG homologs. Comparing LuxO and SypG across the LuxO+/SypG+ positive taxa revealed approximately 48% identity between the two homologs for each taxa assessed. Furthermore, 10 out of the 22 residues within the HTH domain were also identical (**Fig. 3.15B**), suggesting LuxO and SypG may also recognize similar DNA sequences in other taxa. Altogether, these data suggest the conservation between

LuxO and SypG homologs are common across within the *Vibrionaceae* and indicate the possibility of SypG activation of *qrr1* in other taxa besides *V. fischeri*.



Figure 3.15: Conservation of SypG-LuxO structural features in the *Vibrionaceae* family

- A. Each block represents a multiple sequence alignment of LuxO homologs encoded within the indicated *Vibrionaceae* members that has 489 amino acid positions including gaps. Positions marked by a black line indicate that the corresponding amino acid of the LuxO homolog is identical to that of SypG based on pairwise alignments. Shown below each block are the positions of amino acid identity that are conserved among the indicated taxa. The percent identity between each homolog is shown to the right.
- B. Consensus sequence of the putative 22 amino acid helix-turn-helix (HTH) domain of all LuxO and SypG homologs (24 total sequences) in the *Vibrionaceae*. Sequence logo generated at <https://weblogo.berkeley.edu/logo.cgi>.

Discussion

This study identified SypG as a bEBP that promotes transcriptional activation of *qrr1* in *V. fischeri*, which expands the current model of how Qrr1 transcription is regulated in *V. fischeri*. Prior to this work, LuxO was the only known activator of P_{qrr1} activity in *V. fischeri* [83]. This finding is significant in that SypG activation of P_{qrr1} can occur in the presence of C8 HSL and highlights a way *V. fischeri* cells have adapted to overcome quorum-sensing mediated inhibition of gene expression. Stimulation by RscS is sufficient to induce P_{qrr1} activity in the presence of C8 HSL in a SypG-dependent manner, suggesting signaling through the cellular aggregation pathway is sufficient to activate Qrr1 transcription regardless of whether LuxO is active. Furthermore, LuxO and SypG activation of P_{qrr1} activity depends on the same region of promoter DNA, which includes overlapping UASs of each bEBP.

LuxO activates expression of Qrr1 under conditions of low autoinducer, which typically occurs during the free-living stage of *V. fischeri*'s lifecycle. SypG is activated by RscS to promote the aggregation of *V. fischeri* cells at the light organ exterior [97]. Cells within aggregates are encased in a biofilm-like matrix and potentially detecting AI produced within the population. As expression of Qrr1 promotes entry into the light organ crypts presumably by enhancing motility (Chapter 2), SypG activation of Qrr1 likely serves to ensure the small RNA is expressed when it would otherwise be inhibited by AI, allowing *V. fischeri* cells to escape the aggregate and swim to the symbiotic site. Once inside the crypts, Qrr1 expression is low (**Chapter 2**) to permit the expression of genes involved in bioluminescence [83]. Once inside the crypts, the histidine kinase BinK, which inhibits SypG activity, and high AI concentrations ensure Qrr1 transcription remains low.

LuxO and SypG are homologous transcription factors that activate σ^{54} -dependent transcription of the same gene, *qrr1* (**Fig. 3.4**). Because the UASs of each bEBP overlap, it is predicted the two proteins bind the same region of DNA. The ability to recognize similar DNA

sequences is likely due to the similarities in the helix-turn-helix motif of both proteins, particularly the conservation of residues within the second helix, which is predicted to bind DNA [79]. What remains to be uncovered is the extent to which LuxO and SypG might simultaneously occupy the *qrr1* promoter. The data suggest SypG and LuxO are each sufficient to activate P_{qrr1} (**Fig. 3.5**). One hypothesis is that under specific environmental conditions, either SypG or LuxO will bind upstream of *qrr1* to activate its transcription. LuxO is phosphorylated, and thus, activated in the absence of autoinducer. Typically, this occurs when cells are free-living and not associate with a quorum. SypG is phosphorylated by RscS, which is predicted to respond to some unknown host signal when the cells have aggregated at the light organ pores. [112]. Therefore, it is unlikely the two bEBPs are ever active at the same time. Alternatively, the two bEBPs could compete for the UASs upstream of the *qrr1* promoter depending on the cellular concentrations of each activator. For example, if the concentration of LuxO within the cell was higher than that of SypG under a specific condition, this would increase the likelihood that LuxO binds the *qrr1* promoter over SypG. However, how these different environmental conditions impact the cellular levels of each protein is currently unknown.

Lastly, the degree of similarity between LuxO and SypG is common in members of the *Vibrionaceae* that encode both bEBPs, which indicates the potential for SypG activation of *qrr1* in taxa other than *V. fischeri*. Although assessed ectopically, the SypG homolog from *A. salmonicida* was able to increase P_{qrr1} activity in a construct harboring the *qrr1* promoter from this same strain. In *A. salmonicida*, LitR whose homolog is post-transcriptionally repressed by Qrr1 in *V. fischeri*, promotes the expression of virulence factors [139]. Therefore, SypG activation of *qrr1* in *A. salmonicida* could impact the pathogenicity of this species. Interestingly, connections between the quorum-sensing signaling pathway and the cellular aggregation pathway have already been observed in *A. salmonicida* as LitR inhibits biofilm formation by reducing the expression of *syp* genes [140]. Furthermore, the conservation of identity between LuxO and SypG homologs was

observed in other medically relevant microbes, such as the human pathogen *V. vulnificus*. These findings highlight the need to further investigate how the integrations between diverse signaling networks impacts host-microbe associations.

Methods

Media and growth conditions: *V. fischeri* strains were grown at 28°C under aerobic conditions shaking at 200 rpm in LBS (Luria-Broth Salt) media [1% (wt/vol) tryptone, 0.5% (wt/vol) yeast extract, 2% (wt/vol) NaCl, 50mM Tris-HCl (pH 7.5)].

Strains and Plasmids: Strains and plasmids used in this study are listed in **Table 1** and **Table 2**, respectively.

Mutant construction: To generate $\Delta binK \Delta sypG$, $\Delta binK \Delta luxO \Delta sypG$, and $\Delta luxO \Delta sypG$, pEDR007 which contained a $\Delta sypG$ ($\Delta 49-479$) allele was introduced into the $\Delta binK$, $\Delta binK \Delta luxO$, and $\Delta luxO$ mutant, respectively, using the helper plasmid pEVS104. The $\Delta sypG$ allele was introduced into the parent strains via allelic exchange, and double-crossover events were screened by PCR. The plasmid pEDR007 was created as by PCR amplifying 1.2-kb upstream and 1.1-kb downstream of *sypG* from ES114 genomic DNA using PFU Ultra AD Polymerase (Agilent Technologies) and separately cloning each amplicon into intermediate vectors. The fragments were excised, ligated, and cloned into pEVS79. Primers used to amplify regions of homology listed in Table 3.

Construction of truncated *qrr1* promoter constructs: Regions of the putative *qrr1* promoter of varying lengths were amplified from pEDR003 using PFU Ultra AD Polymerase (Agilent Technologies) and the primers listed in **Table 3**. Each fragment was subsequently cloned into pTM267 [83].

Construction of mutated *qrr1* promoter constructs: Single-nucleotide mutations were introduced at specific sites with the *qrr1* promoter region via PCR mutagenesis using PFU Ultra AD Polymerase (Agilent Technologies) and the primers listed in **Table 3**. Each mutated construct was subsequently cloned into pTM267 [83].

Tn7 integrations: The *sypG* gene was amplified from ES114 genomic DNA using PFU Ultra AD Polymerase (Agilent Technologies) and cloned downstream of the IPTG-inducible P_{trc} promoter

within pTM214 [141] to generate plasmid pEDS003. The *sypG* gene was integrated into the Tn7 site of the chromosome via pEDS003 using quadra-parental mating with the helper plasmids pEVS104 and pUX-BF13. The plasmids pEVS107 and pTM239 were used to integrate the *erm* cassette and *P_{qrr1}-gfp* constructs, respectively, into *V. fischeri* strains, also using quadra-parental mating.

Construction of *P_{trc}-AsSypG*: The *sypG* gene was amplified from *Aliivibrio salmonicida* genomic DNA using the primers listed in **Table 3** and cloned into pTM214 downstream of the *P_{trc}* promoter to generate plasmid pAGC003. The IPTG-inducible *sypG* allele was introduced into a *V. fischeri* $\Delta luxO \Delta sypG$ mutant.

Construction of *P_{(AS)qrr1}*: The intergenic region between *uvrB* and *luxO* was amplified from *A. salmonicida* genomic DNA using the primers listed in Table X and cloned into pTM267.

Bioinformatics: Bacterial enhancer binding proteins (bEBPs) in *V. fischeri* were identified by performing a BLAST search against the genome of *V. fischeri* ES114 (tax ID: 312309) using amino acids 145 – 389 of LuxO (WP_011261589.1), which correspond to the putative AAA+ domain [62], as a query. The presence of a GAFTGA motif, which is predicted to interact with σ^{54} , was used as criteria to validate each protein hit as a bEBP. Multiple sequence alignments were performed using ClustalW (<https://www.ebi.ac.uk/>) for proteins or MAFFT for DNA sequences (<https://www.ebi.ac.uk/Tools/msa/mafft/>) [142]. Pairwise alignments were performed using the EMBOSS Needle Pairwise Sequence Alignment Tool [142]. The putative helix-turn-helix motif was generated using NPS@:Network Protein Sequence Analysis [143]. To visualize the positions of residues that are identical between LuxO and SypG homologs across a set of taxa, a multisequence alignment of the LuxO homologs encoded by those taxa was first generated. Each pairwise alignment was used to generate a key that indicates for each residue in LuxO whether the corresponding position within the alignment contains an amino acid that is identical (labeled as 1) or not identical (labeled as 0). The keys from the pairwise alignments were used to replace the

amino acid letters within the LuxO multisequence alignment with the identical/not identical values. Using Excel, cells containing a 1 were formatted with black fill and those cells containing a 0 were formatted with white fill. The resulting table grid was used to generate the corresponding image shown in this report. The consensus array was generated in similar fashion after determining which positions across rows within the alignment contained a value of 1.

Gene-expression spotting assays: *V. fischeri* strains harboring the P_{qrr1} -*gfp* transcriptional reporters pTM268 or pEDR003, as indicated, were grown aerobically overnight in LBS broth and supplemented with 2.5 $\mu\text{g/ml}$ chloramphenicol. Prior to initiating the assay, each culture was adjusted to an $\text{OD}_{600} = 1.0$. To initiate each spot, a 2.5- μl volume of a cell suspension was placed onto the surface of LBS agar supplemented with 2.5 $\mu\text{g/ml}$ chloramphenicol (with 5.0 $\mu\text{g/ml}$ tetracycline for wrinkled colony assays) and 150 μM Isopropyl β -D-1-thiogalactopyranoside (IPTG) where indicated. Plates were incubated at 25°C (for strains with plasmids expressing *rscS**) or 28°C. After 24 h, the spots were examined at 4X magnification using an SZX16 fluorescence dissecting microscope (Olympus) equipped with an SDF PLFL 0.3X objective and both GFP and mCherry filter sets. To quantify gene expression, images of green fluorescence and red fluorescence of the spot were obtained using an EOS Rebel T5 camera (Canon) with the RAW image format setting. Image analysis was performed using ImageJ (NIH) as follows. First, RAW images were converted to RGB TIFF format using the DCRaw macro using the following settings: `use_temporary_directory, white_balance = [Camera white balance], do_not_automatically_brighten, output_colorspace = [sRGB], read_as = [8-bit], interpolation = [High-speed, low-quality bilinear], and half_size`. For each spot, the green channel of the green fluorescence image was used for quantifying GFP fluorescence. The region of interest (ROI) corresponding to the spot was identified in the red channel by thresholding, and this ROI was used to determine the mean red and green fluorescence levels for each spot. A non-fluorescent sample (pVSV105/ES114, pVSV105/EDS008 or pVSV105/TIM313) was used to determine the levels of

cellular auto-fluorescence. Fold changes in fluorescence between groups were calculated by subtracting auto-fluorescence levels from sample fluorescence levels.

Bioluminescence: Starter LBS cultures of the indicated *V. fischeri* strains were grown overnight and then sub-cultured 1:100 into seawater tryptone (SWT) medium. At indicated time points, turbidity (OD_{600}) and luminescence (RLUs) measurements were collected using a Biowave CO8000 Cell Density Meter and a Promega GloMax 20/20 luminometer, respectively. Specific luminescence for each sample was calculated by normalizing each luminescence measurement with the corresponding turbidity measurement.

Chapter 4

Perspectives and Future Direction

The goal of these studies was to increase understanding of how beneficial microbes establish symbiosis with a host organism. The primary finding was that two homologous bacterial enhancer binding proteins, LuxO and SypG, activate σ^{54} -dependent promoter activity of the same gene, *qrr1*, at different stages of the lifecycle of *V. fischeri*. It appears SypG functions as a back-up mechanism to ensure cells express Qrr1 when quorum sensing might inhibit its activation by LuxO, potentially during the initial stages of light organ colonization. In addition, there is evidence that activation of Qrr1 by LuxO and SypG might occur in other members of the *Vibrionaceae*. The outcome of this work centered around three discoveries: i) a mechanism to bypass quorum sensing ii) integration of two distinct signaling networks, and iii) two homologous transcription factors activating expression of the same gene.

Mechanism to bypass quorum sensing

The detection of AI signals can serve as a way to inform cells that they are in the vicinity of kin, and therefore, quorum sensing allows cells to collectively express traits that would be energetically costly to individual cells in isolation. *V. fischeri* only produces light within the squid light organ when the energy expended during the bioluminescence reaction can be restored via the catabolism and utilization of host nutrients. Otherwise, the production of bioluminescence in planktonic *V. fischeri* could reduce the fitness of the cells. However, no system is without the potential for error. AI molecules are diffusible and can travel across biogeographical landscapes that are on a scale relevant to bacteria. Populations of AI-producing *V. fischeri* cells within a crypt can induce the production of light in populations of non-AI producing cells in a neighboring crypt [144]. Thus, cells are subject to detecting AI from others engaged in QS even if those cells are not a part of the population. Such arrangements could lead to the inadvertent expression of energetically-costly traits. Conversely, the detection of AI might inhibit the expression of traits that

are advantageous to isolated cells, such as motility, which enables cells to swim to new nutrient sources. In the case of *V. fischeri*, Qrr1 expression promotes access to the light organ crypts, most likely by enhancing cellular motility, which is required for crypt colonization (**Chapter 2**). During the aggregation stage, which occurs prior to light organ entry, we hypothesize *V. fischeri* cells are engaged in QS due to the number of cells aggregated at the light organ pores. The detection of AI leads to decreased LuxO phosphate, and thus inhibition of Qrr1 transcriptional activity, suggesting Qrr1 is not expressed under these conditions [83, 105]. However, this work highlighted *V. fischeri* suggests a mechanism that overcomes this challenge by depending on SypG to activate transcription of Qrr1 during the cellular aggregation. As SypG activity is unaffected by AI (**Fig. 3.6**) this allows cells to overcome QS-mediated repression of Qrr1 transcription, so the small RNA is expressed when needed.

Typically, studies of QS in bacteria focus on how gene expression changes in response to the presence or absence of AI. However, this mechanism of QS bypass was only discovered by asking whether there were factors that could influence the expression of a QS-regulated gene in an AI-independent manner. The physiology of the BinK mutant permitted increased activation of P_{qrr1} in the presence of AI. The finding that SypG activates P_{qrr1} is consistent with previous work highlighting that BinK inhibits the expression of SypG-regulated genes [99]. SypG activates P_{qrr1} in a LuxO-independent manner, which decouples regulation of Qrr1 transcription from AI concentrations under conditions in which SypG is active. However, green fluorescence in the $\Delta binK \Delta sypG$ mutant was still elevated relative to the $\Delta binK \Delta luxO \Delta sypG$ mutant, which suggest there are also LuxO-dependent mechanisms of activating Qrr1 transcription under conditions of QS when BinK is absent (**Fig. 2.8**). As the majority of the *Vibrionaceae* do not encode a BinK homolog but do harbor homologs of LuxO and SypG (**Table 3.14**), it is worthwhile to investigate how LuxO regulation of Qrr1 transcription functions under QS conditions in BinK- taxa. In *V. fischeri*, overexpression of SypK also results in LuxO activation of P_{qrr1} in the presence of AI,

presumably by contacting the LuxPQ complex in a way that stimulates the phosphatase activity of LuxQ [109]. Altogether, these findings reveal there may exist several QS bypass mechanisms in *V. fischeri* and other members of the *Vibrionaceae*.

The integration of two signaling networks

Signaling networks are typically studied as architectures that operate independently from one another. However, more evidence is emerging that bacterial signaling systems are intricately intertwined. This work revealed a connection between the quorum sensing and biofilm formation pathway in *V. fischeri*. While a link between these two pathways has been previously observed [109], the finding that SypG might directly activate expression of *qrr1* is novel. Prior to this study, Qrr1 expression in *V. fischeri* was only assessed as a function of cell density, *i.e.*, over the growth curve [105]. These culture-based assays are ideal for studying QS-regulated traits as the number of cells in the experiment can be controlled. However, the signaling cascade that stimulates SypG is only naturally induced at the exterior of the squid light organ. While culture-based assays do reveal new regulatory connections, there is an increasing need to study the integration of signaling networks in the context of the host during symbiosis establishment. Bacteria acclimating to the microenvironments associated with a host will experience a myriad of environmental factors, such as changes in pH, temperature, and compounds produced by the host and other microbes. This work revealed that in *V. fischeri*, activation of the cellular aggregation signaling network makes cells blind to AI-mediated repression of Qrr1 expression (**Fig. 3.6**), which highlights that one signaling network can override the activity of another. Generally, studies of how signaling networks influence gene expression are conducted by introducing a signal and assessing the outcome, either on gene expression or the expression of specific traits. This study revealed multiple signals can influence the expression of a small RNA that affects symbiotic traits when expressed. These findings highlight there is a need to understand how different environmental stimuli affect how bacteria express specific traits, like virulence factors, when associated with a host.

Two homologous bEBPs activate transcription of the same gene

Both LuxO and SypG are sufficient to independently activate P_{qrr1} . This is the first reported evidence of a bacteria encoding two homologous transcription factors that can activate the same gene. It is common that bacteria encode homologous transcription factors that arose from a duplication event. Typically, what occurs is the duplicated products will evolve to recognize different targets due to complementary mutations within the DNA-binding domain and the sequence of the cognate binding site. As a result, these homologous transcription factors develop specificity for separate targets such that cross-talk, *i.e.*, transcription factors affecting non-cognate genes, does not occur [145]. The ability for homologous transcription factors to differentiate between cognate and non-cognate targets is essential in maintaining signal fidelity, which ensures the appropriate expression of traits are expressed to promote cellular fitness. However, *V. fischeri* has adapted to having two homologous transcription factors, LuxO and SypG, activate expression of the same gene, *qrr1*, as expressing Qrr1 is advantageous at different stages of the symbiotic lifestyle of the cell.

Broader Impact

Qrrs in other *Vibrios* regulate the expression of virulence factors [91, 93]. Therefore, the finding that SypG can also activate expression of P_{qrr1} could be relevant in pathogenic members of the *Vibrionaceae*. In *V. fischeri*, RscS promotes increased P_{qrr1} through SypG in a LuxO-independent manner (**Fig. 3.6**). RscS activity is presumably regulated by signals the cells encounter when first associated with the squid host [146]. Thus, it is likely the host environment contains compounds that stimulate expression of Qrr1, which allows cells to bypass AI-mediated repression of *qrr1* transcription. One possibility is that the detection of signals within the host environment can alter SypG activity in a way that results in Qrr1 transcription, which would impact the expression of virulence factors. AI analogs are compounds that are structurally similar to bacteria-

produced AI, which is a feature that enables these molecules to bind specific receptors and alter the activity of QS-signaling networks. Because binding of AI analogs could alter the expression of QS-regulated virulence factors, these molecules are potential therapeutics [147-149]. If a cell harbors a mechanism to activate Qrr1 independently of the QS-signaling network, then a therapeutic designed to interfere with this pathway would be ineffective. For this reason, it is important to consider all factors and signaling networks that may influence the expression of specific genes when designing therapeutics.

Future Directions

This work increased understanding of how Qrr1 is regulated in *V. fischeri* during light organ colonization and provided insight into the possibility of SypG activation of Qrr1 transcription in other members of the *Vibrionaceae*. However, there are many questions that remain regarding the mechanism of Qrr1 activation during symbiosis establishment. The following aims seeks to address some of these questions.

Aim I: Determine the extent to which SypG binds to the *qrr1* promoter

SypG binds a consensus sequence that displays a high degree of similarity to the UAS of LuxO (**Fig. 3.8**) [95]. While this study demonstrated that expression of SypG leads to increased Qrr1 transcriptional activity, the ability of SypG to bind to the *qrr1* promoter was not assessed. Therefore, future studies could assess the ability of SypG to bind DNA containing the *qrr1* promoter in **Chapter 3**. Single-nucleotide or paired substitutions could be introduced into the putative UAS to determine which bases are essential for SypG binding and which ones are dispensable. It would also be worthwhile to conduct a binding assay with both bEBPs to determine whether LuxO or SypG has higher binding affinity for the *qrr1* promoter. If SypG does not bind the *qrr1* promoter, this might suggest SypG activates expression of another bEBP that is able to activate *qrr1* transcription.

Aim II: Investigate factors that promote specificity for LuxO and SypG to their cognate UASs

While SypG can activate transcription of the promoters for both *qrr1* and *sypA*, LuxO can only promote P_{qrr1} activity. Therefore, one hypothesis is there are specific protein-DNA interactions that confer specificity for each bEBP. To determine such factors, it would be worthwhile to investigate which residues within the DNA-binding domain are required to bind the UAS of each bEBP. The second helix of the helix-turn-helix motif is predicted to recognize and bind DNA [76]. Therefore, one strategy is to generate amino acid substitutions within this region of LuxO and SypG and evaluate how these mutations impact the ability of each bEBP to bind the *qrr1* promoter. Additionally, single-nucleotide substitutions could be introduced into the UASs located within the P_{qrr1} and P_{sypA} constructs, and the extent to which each bEBP impacts the activity of these promoters could be assessed. If neither strategy yields insight into factors that confer specificity for each bEBP for their cognate UAS, an alternative hypothesis is the specificity determinant lie outside of the DNA-binding domain.

Aim III: Determine the extent to which SypG impacts the expression of Qrr1-regulated traits

This work provided substantial evidence that SypG can activate *qrr1* transcription. What requires further study is the extent to which SypG directly impacts the expression of traits that are regulated by Qrr1, such as motility and bioluminescence. Overexpression of RscS, which promotes SypG activity led to a decrease in bioluminescence (**Fig. 3.7**), and this result is consistent with Qrr1 being expressed [83, 97]. However, to rule out the possibility that RscS leads to a reduction in bioluminescence due to LuxO activation of *qrr1* transcription or an alternative mechanism, it is necessary to directly test whether SypG also inhibits bioluminescence in a Qrr1-dependent manner. Similarly, the impact of SypG on motility should also be evaluated as Qrr1 promotes motility

(**Appendix A.3**). The motility rate of the $\Delta binK$ mutant was comparable to that of WT cells (**Fig. 2.6**). As increased P_{qrr1} in the $binK$ mutant partially depends on SypG, this might suggest SypG does not promote motility through Qrr1. However, SypG activity depends on expression of RscS, which does not occur in cultures of WT cell, but only in host-associated cells [97, 150]. Therefore, it is likely that RscS, and consequently, SypG was not active under the conditions in which the motility assay was performed. If SypG does lead to an increased rate of motility in a Qrr1-dependent manner, this would support the model that SypG promotes Qrr1 transcription within the aggregate to prime cells for motility, and thus, entry into the light organ crypts.

Overexpression of the SypG homolog in *Aliivibrio salmonicida* results in increased $P_{qrr1(AS)}$ activity, which suggests SypG activates *qrr1* transcription in this taxon. In *A. salmonicida*, the LitR homolog regulates the expression of host-associated traits such as motility, adhesion, cellular aggregation, and biofilm formation. In addition, LitR also promotes the expression of virulence factors [139]. As LitR and its homologs are post-transcriptionally regulated by Qrrs in other members of the *Vibrionaceae*, it would be pertinent to determine the extent to which SypG impacts the expression of LitR-regulated traits in *A. salmonicida* through Qrr1. LitR represses expression of the *syp* locus, in *A. salmonicida* [139]. Therefore, studying the SypG-Qrr1-LitR regulatory link in this taxon would also provide insight into how negative feedback loops function in pathogenic microbes.

Aim IV: Assessing SypG activation of *qrr1* in the host

The model developed from this work is that SypG activates expression of the *qrr1* during cellular aggregation. However, efforts to test this *in vivo* are currently challenged by the fact that SypG is absolutely required for symbiosis establishment [94]. Therefore, it is not possible to isolate the impact of SypG on Qrr1 transcription during the initial stages of light organ colonization. However, if the findings from Aim II identify the specificity determinants within either the bEBPS,

their UASs, or both, this could facilitate the generation of a strain in which SypG binding to the *qrr1* promoter is disrupted. One potential target could be the central G within the 5' half site of the LuxO UAS: TTGCA. Mutating this nucleotide to a T led to a greater decrease in SypG activation of *P_{qrr1}* activity than what was observed with LuxO (**Fig. 3.3** & **Fig. 3.8**). If a mutant lacking the ability for SypG to activate *qrr1* transcription fails to colonize the squid, this would suggest SypG, and not LuxO, promotes Qrr1 expression prior to entering the light organ crypts.

The four aims described would expand the current model of SypG activation of Qrr1 in *V. fischeri* and other members of the *Vibrionaceae*. Furthermore, accomplishing these aims would provide greater insight into the molecular mechanisms that allow SypG and LuxO to activate expression of Qrr1. The broader impact of these studies would increase understanding of how the integration of signaling networks function to promote symbiosis establishment by both beneficial and pathogenic microbes, which could facilitate the development designed to enhance or inhibit the expression of host-associated traits.

TABLE 1: Strains

Strain	Genotype	Reference	Construction Acknowledgment
<i>V. fischeri</i>			
ES114	Wild-type <i>V. fischeri</i>	[151]	
TIM305	ES114 $\Delta qrr1$	[83]	
JHK007	ES114 $\Delta ainS \Delta luxIR P_{luxI-lux} CDABEG$	[105]	
CL59	ES114 <i>luxO</i> D55E	[85]	
TIM306	ES114 $\Delta luxO$	[83]	
TIM313	ES114 Tn7:: <i>erm</i>	[83]	
MJM2481	MJM1100 $\Delta binK$ Tn7:: <i>erm</i>		M. Mandel
TIM412	MJM1100 $\Delta binK$ Tn7:: <i>binK</i>	This work	T. Miyashiro
MJM2251	MJM1100 $\Delta binK$	[99]	
KRG003	ES114 $\Delta rpoN$	[50]	
KRG011	ES114 $\Delta rpoN \Delta binK$	This study	K. Guckes
EDR009	ES114 $\Delta binK \Delta luxO$	This study	
EDR013	ES114 $\Delta binK \Delta luxO \Delta sypG$	This study	
EDS008	ES114 $\Delta luxO \Delta sypG$ Tn7:: <i>erm</i>	This study	
EDS010	ES114 $\Delta luxO \Delta sypG$ Tn7:: <i>lacI^q P_{trc}-sypG</i>	This study	
EDS015	ES114 $\Delta sypG$ Tn7:: <i>P_{qrr1}-gfp</i>	This study	S. Cousins
DRO204	ES114 Tn5:: <i>binK</i> [NT]		D. Oehlert
MJM1198	MJM1100 <i>rscS</i> *	[152]	
DRO22	ES114 Tn5:: <i>binK</i>		D. Oehlert
MJM2255	MJM1100 <i>rscS</i> * $\Delta binK$	[99]	
MJM1100	Wild-type <i>V. fischeri</i> (ES114)	[151, 153]	
EDR014	ES114 $\Delta binK \Delta sypG$	This work	
TIM303	ES114 Tn7:: <i>P_{qrr1}-gfp</i>	[109]	
MJM2839	MJM1100 <i>rscS</i> * $\Delta qrr1$		D. Ludvik
MJM2012	MJM1100 <i>rscS</i> * Tn5:: <i>binK</i>		D. Ludvik
MJM2834	MJM1100 <i>rscS</i> * $\Delta qrr1$ Tn5:: <i>binK</i>		D. Ludvik
EDR010	ES114 $\Delta binK \Delta qrr1$	This work	
EDS021	ES114 $\Delta luxO \Delta sypG$ Tn7:: <i>lacI^q P_{trc}-sypG_(As)</i>	This work	
<i>E. coli</i>			
DH5 α	<i>E. coli endA1 hsdR17 (r_K⁻ m_K⁺) glnV44 thi-1 recA1 gyrA (Nal^r) relA $\Delta(lacIZYA-argF)U169 deoR$ [ϕ80dlac$\Delta(lacZ)M15$]</i>	[154]	
BW23474	<i>E. coli $\Delta lac-169 robA1 creC510 hsdR514 uidA(\Delta MluI)::pir116 endA(BT33) recA1$</i>	[155]	
CC118 λ pir	<i>E. coli $\Delta(ara-leu) araD \Delta lacX74 galE galK phoA20 thi-1 rpsE rpoB argE(Am) recA1 \lambda pir$</i>	[156]	
S17-1 λ pir	<i>E. coli thi pro hsdR hsdM⁺ recA λpir</i>	[157]	
π 3813	B462 $\Delta thyA::(erm-pir-116)$ (Erm ^r)	[158]	

TABLE 2: Plasmids

Plasmid	Genotype	Reference	Construction Acknowledgment
pYS112	pVSV105 $P_{proD-cfp}$ $P_{tetA-mCherry}$	[107]	
pSCV38	pVSV105 $P_{tetA-yfp}$ $P_{tetA-mCherry}$	[44]	
pVSV105	R6Kori <i>ori</i> (pES213) RP4 <i>oriT cat</i>	[159]	
pTM312	pVSV105 $P_{tetA-qrr1}$	[83]	
pEDR003	pTM267 $P_{qrr1-gfp}$ $P_{tetA-mCherry}$	This work	
pEDR011	pEDR003 $P_{qrr1-gfp}$ (truncated to -357) $P_{tetA-mCherry}$	This work	
pEDR012	pEDR003 $P_{qrr1-gfp}$ (truncated to -209) $P_{tetA-mCherry}$	This work	
pEDR006	pEDR003 $P_{qrr1-gfp}$ (truncated to -175) $P_{tetA-mCherry}$	This work	
pEDR008	pEDR003 $P_{qrr1-gfp}$ (truncated to -60) $P_{tetA-mCherry}$	This work	
pEDR009	pEDR003 $P_{qrr1-gfp}$ (truncated to -106) $P_{tetA-mCherry}$	This work	
pEDR010	pEDR003 $P_{qrr1-gfp}$ (truncated to -262) $P_{tetA-mCherry}$	This work	
pEDS007	pEDR003 $P_{qrr1(G-97 T)-gfp}$ $P_{tetA-mCherry}$	This work	
pEDS008	pEDR003 $P_{qrr1(C-96 A)-gfp}$ $P_{tetA-mCherry}$	This work	
pEDS009	pEDR003 $P_{qrr1(A-95 C)-gfp}$ $P_{tetA-mCherry}$	This work	
pEDS004	pEDR003 $P_{qrr1(G-131 T)-gfp}$ $P_{tetA-mCherry}$	This work	
pEDS005	pEDR003 $P_{qrr1(C-130 A)-gfp}$ $P_{tetA-mCherry}$	This work	
pEDS006	pEDR003 $P_{qrr1(A-129 C)-gfp}$ $P_{tetA-mCherry}$	This work	
pTM268	pVSV105 $P_{qrr1-gfp}$ $P_{tetA-mCherry}$	[83]	
pEDR007	pEVS79 $\Delta sypG$	This work	
pEDS003	pTM318 lac^{lq} $P_{trc-sypG}$	This work	
pEVS79	pBC SK(+) <i>oriT cat</i>	[160]	
pTM318	pEVS107 lac^{lq} $P_{trc-mCherry}$		T. Miyashiro
pEVS104	Conjugal helper plasmid (<i>tra trb</i>); Kn^r	[160]	
pUX-BF13	Encodes Tn7 transposase (<i>tnsABCDE</i>); Ap^r	[161]	
pEVS107	pEVS94S derivative, mini-Tn7; <i>mob</i> ; Em^r Kn^r	[162]	
plostfox	$tfoX^+$, Cm^r	[163]	
pKV494	pJET + FRT- Em^r	[25]	
pKV496	pEVS79- Kn^r + flp^+	[25]	
pTM214	pVSV105 lac^{lq} $P_{trc-mCherry}$		T. Miyashiro
pKG11	pKV69 <i>rscSI</i> ; Cm^R Tet^R	[112]	
pKV69	Mobilizable vector; Cm^R Tet^R	[150]	
pEDS001	pEDR003 $P_{qrr1(UAS2: TG-CT)-gfp}$ $P_{tetA-mCherry}$	This study	
pVF_A1020P	pTM267 $P_{sypA-gfp}$ $P_{tetA-mCherry}$	This study	S. Verma
pAGC004	pVSV105 $P_{qrr1(AS)-gfp}$ $P_{tetA-mCherry}$	This study	A. Cecere
pTM239	pEVS107 Tn7:: $P_{qrr1-gfp}$	[109]	
pACG003	pTM318 $lacI^q$ $P_{trc-sypG(AS)}$	This study	A. Cecere

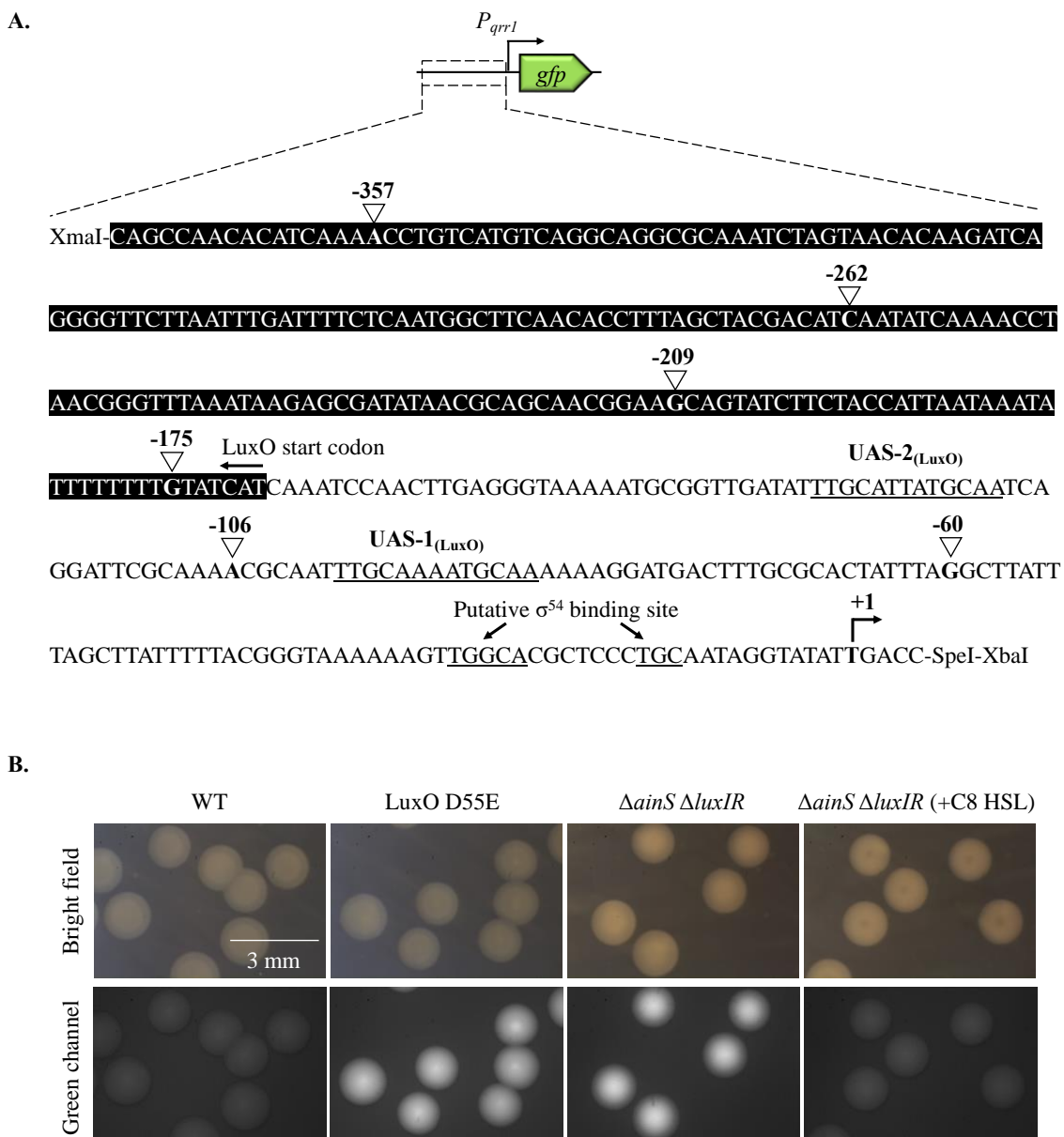
TABLE 3: Primers

Primer name	5' → 3'
TIM412	
VF_A0360-XmaI-u1	GGCCCGGGAAAGTGCTAGGTTTTTTTATGAATA
VF_A0360-SalI-l1	GGGTCGACTTATGTATACGCTTCCAATTTTTTC
KRG011	
ES_rpoN Del Up F	CCTCAAGAAGCTTCTATTTTTAGAA
	TAGGCGGCCGCACTAAGTATGGTATTTAGCGATACCTTTTGTAC
ES_rpoN Del Up R	ATT
	GGATAGGCCTAGAAGGCCATGGTTAATGAAAAGGAAGTGTTAT
ES_rpoN Del Down F	GCAA
ES_rpoN Del Down R	GATAGCTATCCCATTACCTATACCA
cL1	CCATACTTAGTGC GGCCGCCTA
cL2	CCATGGCCTTCTAGGCCTATCC
pEDR007	
sypG-del-XbaI-l1	CGGTCTAGATGTGGTGGATTCTTTTCCATAAATGCC
sypG-del-XbaI-u1	GGCTCTAGAGTTAAGCCCGTCAACACTCT
sypF-KpnI-u1	GGTACCGTTCTGGTTT AGGGTTAGCTATTTGTCA
sypH-SacI-l1	GAGCTCCAGACAATAAAGAGGGGATGATAGC
pEDS003	
sypG-pTrc-KpnI-u1	GGTACCTTCGCTAGGTAAAACAGGATGTTA
sypG-pTrc-BsrGI-l1	GGTGTACAGTAACCATATTTTCATCATTCCGAT
pEDR003	
qrr1-prom-XmaI-u2	GGCCCGGGCAGCCAACACATCAAACCTGTCA
qrr1-prom-XbaI-l2	GGTCTAGA ACTAGTGGTCAATATACCTATTGCAGGGAG
pEDR006	
qrr1-prom-XmaI-u3	GGCCCGGGGTATCATCAAATCCAACCTTGAGGG
qrr1-prom-XbaI-l2	GGTCTAGA ACTAGTGGTCAATATACCTATTGCAGGGAG
pEDR008	
qrr1-XmaI-reg1-u1	GCGCCCGGGGGCTTATTTAGCTTATTTTTACG
gfp-XhoI-l1	TACTCGAGTTTGTGTCCGAGAATGTTTCCATC
pEDR009	
qrr1-XmaI-reg2-u1	CCGCCCGGGACGCAATTTGCAAAATGC
gfp-XhoI-l1	TACTCGAGTTTGTGTCCGAGAATGTTTCCATC
pEDR0010	
qrr1-XmaI-reg5-u1	GGCCCGGGCAATATCAAACCTAACGGG
gfp-XhoI-l1	TACTCGAGTTTGTGTCCGAGAATGTTTCCATC
pEDR011	
qrr1-XmaI-reg7-u1	GGCCCGGGACCTGTCATGTCAGGC
gfp-XhoI-l1	TACTCGAGTTTGTGTCCGAGAATGTTTCCATC
pEDR012	
qrr1-XmaI-reg4-u1	CCGCCCGGGGCAGTATCTTCTACCATTAATAAA
gfp-XhoI-l1	TACTCGAGTTTGTGTCCGAGAATGTTTCCATC
pEDS004	
qrr1-prom-SDM-G243T-u1	TAAAAATGCGGTTGATATTTTCATTATGCAATCAGGATTCCG
qrr1-prom-SDM-G243T-l1	CGAATCCTGATTGCATAATGAAAATATCAACCGCATTTTTA

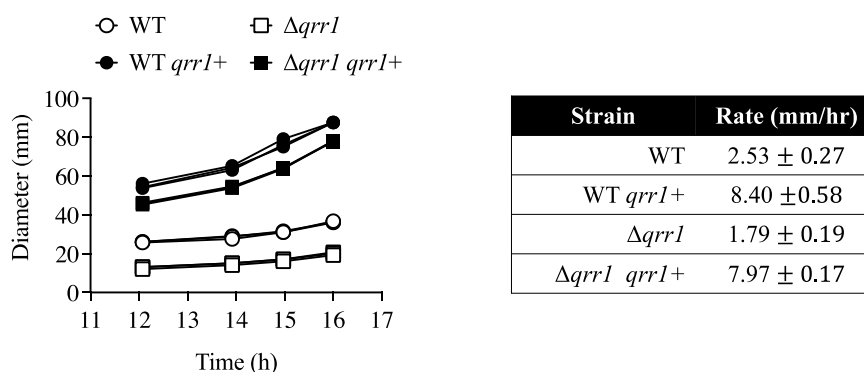
TABLE 3: Primers (continued)

pEDS005	
qrr1-prom-SDM-C244A-u1	AAAAATGCGGTTGATATTTGAATTATGCAATCAGGATTTCGC
qrr1-prom-SDM-C244A-l1	GCGAATCCTGATTGCATAATTCAAATATCAACCGCATTTTT
pEDS006	
qrr1-prom-SDM-A245C-u1	AAAATGCGGTTGATATTTGCCTTATGCAATCAGGATTTCGCA
qrr1-prom-SDM-A245C-l1	TGCGAATCCTGATTGCATAAGGCAAATATCAACCGCATTTTT
pEDS007	
qrr1prom-mut_G277T_u1	GGATTTCGCAAAAACGCAATTTTTCAAATGCAAAAAAGGATG
qrr1prom-mut_G277T_l1	CATCCTTTTTTGCATTTTTGAAAATTGCGTTTTGCGAATCC
pEDS008	
qrr1prom-mut_G278A_u1	GATTTCGCAAAAACGCAATTTGAAAAATGCAAAAAAGGATGAC
qrr1prom-mut_G278A_l1	GTCATCCTTTTTTGCATTTTTCAAATTGCGTTTTGCGAATC
pEDS009	
qrr1prom-mut_G279C_u1	CGCAAAAACGCAATTTGCCAAATGCAAAAAAGGATG
qrr1prom-mut_G279C_l1	CATCCTTTTTTGCATTTGGCAAATTGCGTTTTGCG
pAGC004	
AS-Qrr1-XmaI-U1	CCCGGGGTCCAGTCATATCCGGCAAGC
AS-Qrr1-XbaI-L1	TCTAGAGGTCACTATACATATAGCAGAG
pAGC003	
AS-KpnI-SypG-U1	GGTACCTGCACAAGGCTTCACTA
AS-BsrGI-SypG-L1	TGTACACAAAAGCCATACCTCAAAAG

APPENDIX

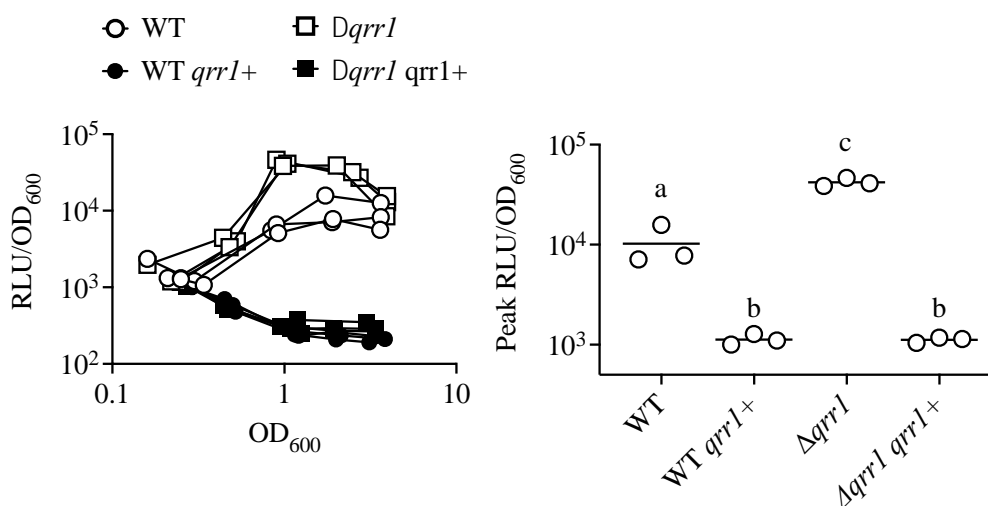
**Appendix A.1: The *qrr1* transcriptional reporter pEDR003**

- A. Shown are the 378 nucleotides from the *luxO-qrr1* intergenic region cloned upstream of *gfp* in pEDR003. The transcriptional start site of *qrr1* is indicated with a +1. The upstream activating sequences (UASs) of LuxO and putative σ^{54} -binding site are underlined and labeled. Triangles above the bases indicate the site of plasmid truncations relative to the +1 transcriptional start site of *qrr1*.
- B. Colonies of *V. fischeri* cells ES114 (WT), CL59 (LuxO D55E; constitutively active allele of LuxO), JHK007 ($\Delta ainS \Delta luxIR P_{luxI-luxICDABEG}$) harboring the *P_{qrr1}-gfp* reporter pTM268. Images of *top*, bright field and *bottom*, green channel images of the colonies.



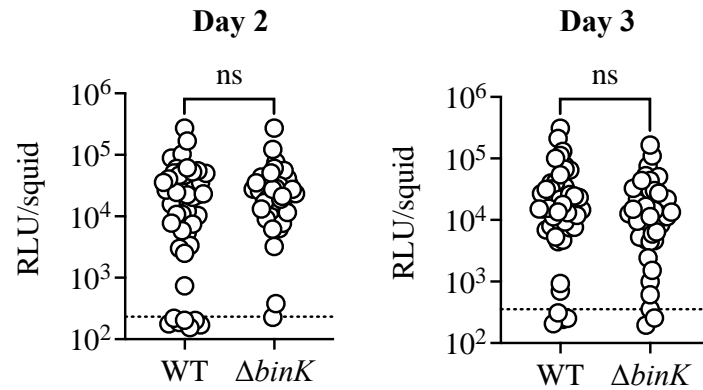
Appendix A.2: Qrr1 expression enhances motility

Left, The *V. fischeri* strains ES114 (WT), TIM305 ($\Delta qrr1$), MJM2251 ($\Delta binK$), and EDR010 ($\Delta binK \Delta qrr1$) were injected into minimal media soft agar motility plates and incubated at 28°C. The diameter of the motility ring was measured over time starting at 14 hours post incubation. *Right*, The slope of each line was calculated. Experiment performed by Shyan Cousins.



Appendix A.3: Expression of *qrr1* decreases luminescence *in vitro*

Left, Luminescence values of *V. fischeri* strains ES114 (WT) and TIM305 ($\Delta qrr1$) grown in SWTO were obtained every hour. Plotted is the specific luminescence, or relative light units (RLU) divided by the optical density (OD_{600}), for each culture as a function of growth. *Right*, Peak specific luminescence values for each culture. Each point represents an independent sample with bars indicating the average. Peak specific luminescence (Peak RLU/OD_{600}) values were log-transformed. Statistical significance among group means was determined by one-way ANOVA ($F_{3,8} = 173$, $d.f. = 11$). A Tukey's *post-hoc* test was used to determine statistical significances among groups, with *p*-values adjusted for multiple comparisons. Comparisons between groups marked by different letters indicate significant differences ($p < 0.0001$), whereas comparisons between groups with same letter indicating no significant difference ($\alpha = 0.05$). Experiment performed by Roxy Evande.



Appendix A.4: The impact of BinK on luminescence

Juvenile squid were exposed to an inoculum of ES114 (WT) or MJM2251 ($\Delta binK$) cells harboring the P_{qrr1} -*gfp* transcriptional reporter pTM268. Shown are the relative light units, or RLU, of the animals within each group for 24- and 48- hours. A Mann-Whitney test was conducted to compare the mean ranks between the two groups (**** = $p < 0.0001$; n.s. = not significant).

```

LuxO .....MIQKKYL
SypG .....MLQKV
GlnC .....MSKFI
FlrC .....MAQSKV
AtoC .....MVKSDWNAFSV
FlrA .....MQGLAKT
TyrR MRLEVQCKDRGLGLTRELLDI.....LASQHIDL.....RDIEDKSGLIYLNFP.E.IDEDEF SQ...LM
NorR1 .....MKNIKDEWVQIALDLTSGLSSKDRFERLLSTIRNALKCDASALLLEKN...QYFSPLATNGLDGD
NorR2 .....MKPSMEKVLQIALDLNLSNLSDDLHYQRLINSIHQVFPQDASALFI LDND...HC LKPVAVKGLSQA
PspF .....
Hyp.Pro. ....MPPELLMNI.....TSEQQSD.F.....NKFTQCWLSGILKHSGAQKVICLSQP.SGAQLF
VpsR .....MG.....TQFRMDSV.PGSLV

```

```

10 20 30 40 50 60
LuxO L M V E D T A S V A A L Y R S . Y . . . . . L N P L G F D I D V V A K G V E A I E . K I K L R T P D L V L L . . . . . D L R L L P D M T G F . . . . .
SypG L L V E D S T S L A I L Y K Q . Y . . . . . V K D E P Y E F F H V T T G E Q A K A . F M E K N P P H L V L L . . . . . D L K L L P D M S G Q . . . . .
GlnC W V V D D S S I R W V L E K . T . . . . . L T S T N M M C E S F G D A E S V I Q . A L E R N V P D V I I S . . . . . D I F M P G M D G L . . . . .
FlrC L I V E D D E G L R E A L I D . T . . . . . L E L A G Y E W V E A D S A E T A L L . I L K K E P V D I V V S . . . . . D V I M A G M G G L . . . . .
AtoC L V V D D E I G M Q T I L K K . A . . . . . L S K Q F G Q V H T A G T I E E A E E . I R Q S H H L D L I I L . . . . . D I N L P G Q T G L . . . . .
FlrA L I I E D D A Q S R H N L K V . I . . . . . L E F I G E H C H A I S A S . E L S T . F E W S E P W S A C F L G Q V . S D Q A L K D I K S . . . . .
TyrR A K I R R L D G V M D V R K I Q F L P S E R R N T E L L . . . . . A V L S T L P D P V F . . . . . S I N L K G K I D T I N D A V V S L F
NorR1 V I G R R F A I S Q H P . . . . . R . . . . . L E A I A R A G D I V R . . . . . F P S D . S D L P D P Y D G L I A N . E E R L Q V H S C I G L . . . . .
NorR2 V L G R C F P P Q V H P . . . . . R . . . . . L E A I L Q S K H P V R . . . . . F E S N . S D L P D P F D G L L L V D E N I N I E V H C W G L C G . . . . .
PspF .....
Hyp.Pro. R M A E G Y S D S K H Q P Q I T S L P F E N K N D K N N I I N T . . . . . D . Y R E F N T L T L C M S E G R N F N L H E S Q C T D D I K H . . . . .
VpsR V V G G S Y E P W L A . . . . . V . . . . . L E Q V G W R C H R C Y D L R A A Q A L F D E I G P C I G I V D . L S Q D D E S I N G I A T L . . . . .

```

```

70 80 90 100
LuxO . . . . . D V L . . . . . A E I . . . . . R K . . . . . D N Q S I P V L I T A H G S I D A A V F A M Q L G A O D . . . . . F L I K P
SypG . . . . . D V L . . . . . A W M . . . . . K E . . . . . K O L P T A V I I T A H G T I N I A V N L L Q N G A O D . . . . . F I E K P
GlnC . . . . . S L L . . . . . H H I . . . . . Q E . . . . . N Y P E L P V I I T A H S D L D A A V S A Y Q K G A F E . . . . . Y L P K P
FlrC . . . . . A L L . . . . . R S I . . . . . K L . . . . . N W P N L P V L L T A Y A N I E D A V S A M K D G A I D . . . . . Y M A K P
AtoC . . . . . E W Q . . . . . E S I . . . . . A C . . . . . D A R N Y D V I F M T G Y A E L D T A I C A L R L G A S D . . . . . F I L K P
FlrA . . . . . S L V . . . . . . . . . . . V H N H I P V I M L A G A M H D V E E L T N Y V G E L N Q P V . . . . . N Y P Q
TyrR K L D K T S L I G Q S A T V L L S D F N V Q . L W L E E S R I R Q R E P M L I D G M N Y I M E I M P V Y I T D S N T S I L T S A . . . . . V V I I K P
NorR1 . . . . . F L L . . . . . . . . . . . V N E R L I G A V T I . . . . . D A F D P T O F D S F T N K E L R I I S A
NorR2 . . . . . S L Y . . . . . . . . . . . V D D T L V G V L T L . . . . . D A L E V G A F K I D D I T I E T F A A
PspF . . . . .
Hyp.Pro. . . . . I L F E Q S E Y Y T L T D G E V E F M P L . . . . . R N . . . . . S Q Q R I S G V L M F . . . . . Y F S N E S T Y Q R S D R O T I Y T L N S
VpsR . . . . . . . . . . . V N N N K Q V R W M A F I R E . . . . . S Q L S S . . . . . D T I C G F I V N F C I D . . . . . F E T A P

```

```

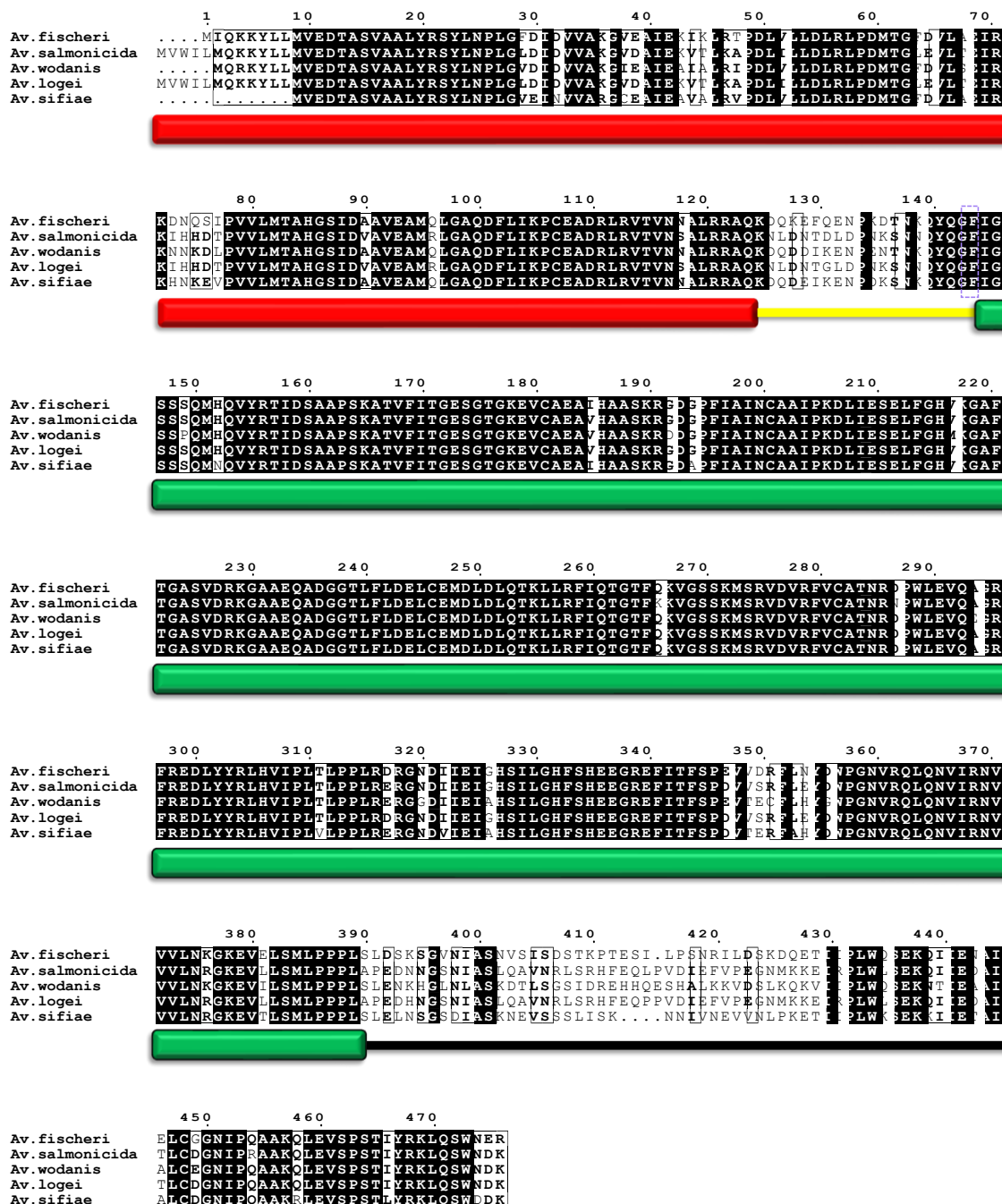
110 120 130 140 150 160 170
LuxO C E A D R L R V T V N N . . . . . A L R R A Q K D Q E F Q E N P K D T N K Q Y Q G F I C S S S O M H Q V Y R T P S A A S K A T V F I T C E S
SypG I Q A E R L K T S I A N . . . . . H L K R N K L E G L V E D L O N T E N R K Q Y Q G F I C S S L P M Q A V Y K I I D S V A E T T A S V F I N C E S
GlnC E D I D E T L T L V E R . . . . . A L A H S Q E Q K . Q O S I N T P K K E H H V P E I I C E A P A M Q E V E R A I G R L S E S S I S V L I N C E S
FlrC F A P E V L L N M V S R . . . . . Y A P V . . . . . . . . . . . K T E Q T G D A I V A D E K S L K L K L A G K V A R T D A N V M V I C P S
AtoC E N L E N M L Q A V K R . . . . . C M D R R L V E R T N F A L K R E V E K K N P I E I I C N A E K T L Q L K K M V A Q L A E S N A A V L I E C E S
FlrA L T D . . . . . A L R H C Q E F M G . . . . . R R G L E V P H L G R K N T L F R S M V C Q S T A I S T V R H L I E Q V S G T E A S V L V I C E S
TyrR . . . . . . . . . . . A I E A Q N A R P F I P E S N L G E E H F V C S S T Y K Q L I S O A K K L S I D O S L L I C E T
NorR1 L A A . . . . . T S L H T A L L M E R L E N Q S G E . N S N N S S F E R S P D N H V E M I C E S L A M Q E L Q A N I N A V A N T E L S V L I C E T
NorR2 L A A . . . . . A T L H N K A L I K T L Q D S N Q O Q K S I N Q T L I Q Q A R I Q K G E L I C I S P O I T R L K S N I S T V A H S D Y A V L I C E T
PspF . . . . . . . . . . . M R K D S . . . . . L V C E S D A F L S A L D H A S Q L A T I D R E I L I C E R
Hyp.Pro. L A I D R I A L A I K N S Y A L L D . . . . . Q K . I A P H S S T T H I P S D E N I V C D S S A I K E V R L N I S K A L H I N R N V L V I C E T
VpsR I P D A Q L L S T I G H Q L G M L K . . . . . L E R K V W E N M G N K S D L G I L C E A P A V K R L R D O I R R V A P T D V S I L I C E S

```

```

180 190 200 210 220 230 240
LuxO C T C K E V C A E A I H A S K R C D G P F T A I N C A A I P K D L E S E L F C H V K C A F T C A S V D R K C A A E C A D C T F L F L D E L C E M D
SypG C T C K E V C A E A I H Y O S K R S N K P F V A I N C A A I P R D L M E S E I F C H I K C A F T C A T T D R K C A A M I A N C T F L F L D E L C E M E
GlnC C T C K E L V A H A L H R H S E R A N N E F I A L N M A A I P K D L E S E L F C H E K C A F T C A N S V R K G R E F C A N C T F L F L D E I S D M P
FlrC G S C K E V M S R Y I H N N S Q R E G P F V A I N C A A I P D N M L E A T L F C Y E K C A F T C A V Q A C R K F E C A Q C G T I L L D E I S E M D
AtoC C T C K E L V A R G L H Q S E R R K G P F V E L N C A A I P D L L E S E L F C H T S C A F T C A K K G R C L E R V A N G C T F L F L D E I S E M P
FlrA C T C K E V V A R N L H Y H S E R R K G P F V E V N C A A I P F D L L E S E L F C H E K C A F T C A I T A R K G R E F A Q C G T F L F L D E I S D M P
TyrR C T C R E M L A R A C H N A S I R S G K A F M V V N C A A M P D D V A E T L F G H A P C A F E N M P E G K K G I E O A D G C T V F E D E I S E M S
NorR1 C V C R E L V A S A L H Q R S T R A Q O N L V Y L N C A A L P E S V A E S E L F C H V K C A F T C A I S N R K G K E S A D N C T F L F L D E I S E L S
NorR2 C T C R E L V A S V H A Q S R N E L P M I Y V N C A A L P E S L A E S E L F C H V K C A F T C A N N H R A G K E E A D R C T F L F L D E I S E L P
PspF G S C R E L I A Q R L H F L S R R W N E P L I S L N C A A L N S G T L D S E L F C H D A C S F T C A K Q R H Q C R F E R A D G C S L F L D E I T A P
Hyp.Pro. G S C R E L I A K A I H Q F G N R R N E P Y V V O N C A S I P E H L L E S E L F G Y Q K C A F T C A D R D Y I G L I R S A D R C I L F L D E I S D M P
VpsR C V C K D A V A K A V H E S S I R N K G P F V S L N C G S L S E N K I E Q E L F G S H S . . . . . S P E S K L F Q A N G C T F L F L N D I N D L P

```

Appendix A.6: LuxO in the *Fischeri* clade

Multiple sequence alignment of LuxO homologs. Identical amino acids are highlighted in black; similar amino acids are bolded. The rectangles above indicate the receiver (R) domain (red), the AAA+ (C) domain (green), and the putative helix-turn-helix (HTH) motif (blue) within the DNA-binding (D) domain. The yellow line indicates the residues of the R-C linker (KQx....QYQGF). The structurally significant glycine is outlined with a purple dashed box. Alignment figure generated using ESPript 3.0 (<https://espript.ibcp.fr/ESPrIPT/cgi-bin/ESPrIPT.cgi>).

V. fischeri

WP_011261589.1: M[Q]K[Q]Y[L]M[V]E[D]T[A]S[V]A[A]L[Y]R[S]Y[L]N[P]L[G]V[E]I[D]V[V]A[K]C[V]E[A]I[E]K[I]K[L]R[T]E[D]L[V]L[D]L[R]L[P]D[M]T[G]F[D]V[L]A[E]I[E]K[D]N[Q]S[I]P[V]V 80
 WP_011263835.1: M[L]Q[K]--V[L]L[V]E[D]S[T]S[L]A[L]Y[K]Q[Y]V[K]D[E]P[Y]E[F]F[H]V[T]T[G]E[Q]A[K]A[F]M[E]K[N]P[E]H[V]L[V]L[D]L[K]L[P]D[M]S[G]Q[D]V[L]A[M]M[E]K[L]P[T]A[V]I 78

WP_011261589.1: L[M]T[A]H[G]S[I]D[A]A[V]E[A]M[L]G[A]O[D]F[L]I[K]P[C]E[A]D[R]L[V]T[V]N[N]A[L]R[R]A[Q]K[D]Q[E]K[E]E[N]P[K]D[T]N[K]Q[Y]G[F]I[G]S[S]Q[M]H[V]Y[E]T[I]D[S] 160
 WP_011263835.1: T[A]T[A]H[G]T[I]N[A]V[N]L[L]Q[S]G[A]D[D]F[E]K[F]I[Q]A[N]R[L]K[T]S[I]N[H]L[K]R[N]K[L]E[G]L[V]E[D]L[Q]N[T]F[N]R[K]K[Y]Q[G]F[I]G[S]S[L]P[M]Q[A]V[Y]K[I]I[D]S 158

WP_011261589.1: A[A]P[S]K[A]T[V]F[I]G[E]S[G]T[G]K[E]V[C]A[E]A[I]H[A]A[S]K[R]G[C]G[F]T[A]I[N]C[A]A[I]P[K]D[L]E[S]E[L]F[G]H[V]K[G]A[F]T[G]A[S]V[D]R[K]G[A]E[A]Q[A]D[G]G[T]L 240
 WP_011263835.1: V[A]P[T]P[A]S[V]F[I]G[E]S[G]T[G]K[E]V[C]A[E]A[I]H[Y]Q[S]K[R]S[N]K[P]F[V]A[I]N[C]G[A]I[P]R[D]L[M]E[S]E[L]F[G]H[V]K[G]A[F]T[G]A[T]D[R]K[G]A[M]L[A]N[G]G[T]L 238

WP_011261589.1: F[L]D[E]L[C]E[M]D[L]L[Q]K[L]L[R]F[I]Q[T]G[T]E[F]K[V]G[S]S[K]M[S]R[V]D[V]R[F]V[C]A[T]N[R]D[P]W[L]E[V]Q[A]G[R]F[R]E[D]L[Y]R[L]H[V]I[P]T[L]P[L]R[D]R[G]N 320
 WP_011263835.1: F[L]D[E]L[C]E[M]E[L]M[Q]K[L]L[R]F[I]Q[T]G[R]E[T]P[L]G[S]K[E]L[S]T[D]I[R]I[C]A[T]N[R]D[E]L[T]E[V]N[E]G[R]F[R]E[D]L[Y]R[V]H[V]V[P]H[M]P[L]R[E]R[G]T 318

WP_011261589.1: D[I]E[I]C[H]S[I]L[C]H[S]E[E]G[R]E[F]I[T]F[S]P[V]D[E]F[L]N[Y]D[W]P[G]N[V]R[Q]L[Q]N[V]I[R]N[V]V[L]N[R]G[K]E[V]L[S]M[L]P[P]P[L]S[L]D[S]K[S]C[V]N-- 399
 WP_011263835.1: D[I]I[D]I[A]T[F]F[L]K[Y]A[K]E[D]H[K]K[F]A[M]K[R]D[V]E[L]N[C]Y[A]W[P]G[N]V[R]Q[L]Q[N]I[R]N[V]V[L]H[N]D[T]H[V]A[E]H[L]P[P]L[N]Q[F]V[T]N[K]A[T]P 398

WP_011261589.1: A[S]N[V]S[S]D[S]T[K]P-----T[E]S[I]L[S]N[R]-----L[L]S[K]Q[E]T[I]E[L]M[Q]S[E]K[Q]I[E]N[A]I[E]L[Q]C[G]N[P]Q[A]A[K]Q 458
 WP_011263835.1: A[S]X[P]E[T]A[P]S[Q]L[S]R[N]M[E]T[A]D[V]Q[H]N[C]T[E]Q[L]S[S]E[G]Q[T]L[E]S[T]E[A]I[N]T[S]V[I]R[E]M[A]I[E]R[E]V[I]Q[N]A[I]D[H]C[D]G[N]V[L]N[A]A[V]L 478

WP_011261589.1: L[E]V[S]P[S]T[Y]R[K]L[S]W[N]E[R]---- 476
 WP_011263835.1: L[E]L[S]P[S]T[Y]R[K]Q[A]W[E]A[Y]E[E]S 500

A. salmonicida

WP_173362130.1: M[V]W[I]L[M]Q[K]Y[L]M[V]E[D]T[A]S[V]A[A]L[Y]R[S]Y[L]N[P]L[G]V[E]I[D]V[V]A[K]C[V]E[A]I[E]K[V]T[L]K[A]P[D]L[I]L[D]L[R]L[P]D[M]T[G]E[V]I[T]E[R]K[I]H[D] 80
 WP_044583634.1: ---M[L]Q[K]--V[L]L[V]E[D]S[T]S[L]A[L]Y[K]Q[Y]V[K]D[E]P[Y]E[F]F[H]V[T]T[G]E[Q]A[K]A[F]M[E]K[N]P[E]H[V]L[V]L[D]L[K]L[P]D[M]S[G]Q[D]V[L]A[M]M[E]K[L]P 74

WP_173362130.1: T[P]V[V]L[M]T[A]H[G]S[I]D[A]A[V]E[A]M[R]I[G]A[D]D[F]L[I]K[P]C[E]A[D]R[L]E[V]T[V]N[S]A[L]R[R]A[Q]K[N]I[D]N[T]D[L]D[P]N[K]S[N]N[Q]Y[Q]G[F]I[G]S[S]Q[M]H[V]Y[R] 160
 WP_044583634.1: T[A]V[V]L[M]T[A]H[G]T[I]N[A]V[N]L[L]Q[S]G[A]D[D]F[E]K[F]I[Q]A[N]R[L]K[T]S[I]N[H]L[K]R[N]K[L]E[G]L[V]E[D]L[Q]N[T]F[N]R[K]K[Y]Q[G]F[I]G[S]S[L]P[M]Q[A]V[Y]K 154

WP_173362130.1: T[I]D[S]A[A]P[S]K[A]T[V]F[I]G[E]S[G]T[G]K[E]V[C]A[E]A[V]H[A]A[S]K[R]G[C]G[F]T[A]I[N]C[A]A[I]P[K]D[L]E[S]E[L]F[G]H[V]K[G]A[F]T[G]A[S]V[D]R[K]G[A]E[A]Q[A]D 240
 WP_044583634.1: I[I]D[A]V[A]P[T]A[S]V[F]I[G]E[S]G[T]G[K]E[V]C[A]E[A]I[H]Y[Q]S[K]R[N]K[P]E[V]A[I]N[C]G[A]I[P]R[D]L[M]E[S]E[L]F[G]H[V]K[G]A[F]T[G]A[T]D[R]K[G]A[M]M[A]N 234

WP_173362130.1: G[G]T[L]F[L]D[E]L[C]E[M]D[L]L[Q]K[L]L[R]F[I]Q[T]G[T]E[F]K[V]G[S]S[K]M[S]R[V]D[V]R[F]V[C]A[T]N[R]D[P]W[L]E[V]Q[A]G[R]F[R]E[D]L[Y]R[L]H[V]I[P]T[L]P[L]R 320
 WP_044583634.1: G[G]T[L]F[L]D[E]L[C]E[M]E[L]M[Q]K[L]L[R]F[I]Q[T]G[R]E[T]P[L]G[S]K[E]L[S]T[D]I[R]I[C]A[T]N[R]D[E]L[T]E[V]N[E]G[R]F[R]E[D]L[Y]R[V]H[V]V[P]H[M]P[L]R 314

WP_173362130.1: E[R]G[N]D[I]E[I]C[H]S[I]L[C]H[S]E[E]G[R]E[F]I[T]F[S]P[V]D[E]F[L]N[Y]D[W]P[G]N[V]R[Q]L[Q]N[V]I[R]N[V]V[L]N[R]G[K]E[V]L[S]M[L]P[P]P[L]A[P]E[D]N[G] 400
 WP_044583634.1: D[R]G[D]I[D]I[A]V[F]F[L]K[Y]A[K]E[D]H[K]K[F]A[M]K[R]D[V]E[L]N[C]Y[A]W[P]G[N]V[R]Q[L]Q[N]I[R]N[V]V[L]H[N]S[T]H[V]L[D]Q[L]P[P]L[N]Q[A]T[Q]P 394

WP_173362130.1: S[N]I[A]S[I]Q-----A[V]N[R]L[S]----R[H]F[E]O[L]P[V]D[E]F[V]P[E]G[M]K[K]-----E[T]R[L]W[L]S[E]K[Q]I[E]D[A]I[T]L[C]D[G]N[I]P[R]A[A]K 462
 WP_044583634.1: V[K]P[A]T[I]Q[S]H[V]T[K]E[I]N[N]V[A]P[A]P[M]S[V]D[P]L[H]T[E]T[S]E[P]D[N]S[S]M[Q]T[N]S[V]T[W]D[H]S[A]I[R]E[M]A[D]I[E]R[E]V[I]Q[N]A[I]D[H]C[D]G[N]V[L]N[A]A[V] 474

WP_173362130.1: Q[L]E[V]S[P]S[T]Y[R]K[L]S[W]N[D]K----- 481
 WP_044583634.1: L[L]E[L]S[P]S[T]Y[R]K[Q]A[W]E[A]D[E]T[E]K 498

A. sifiae

WP_172794763.1: -----M[V]E[D]T[A]S[V]A[A]L[Y]R[S]Y[L]N[P]L[G]V[E]I[N]V[V]A[R]G[C]E[A]I[E]A[V]A[L]R[V]P[D]L[V]L[D]L[R]L[P]D[M]T[G]F[D]V[L]A[E]I[R]K[N]K[E]V[E]V[M] 74
 WP_105064188.1: M[L]Q[K]V[L]L[V]E[D]S[T]S[L]A[L]Y[K]Q[Y]V[K]D[E]P[Y]E[F]F[H]V[T]T[G]E[Q]A[K]A[F]M[E]K[N]P[E]H[V]L[V]L[D]L[K]L[P]D[M]S[G]Q[D]V[L]A[M]M[E]K[L]P[T]A[V]I 80

WP_172794763.1: T[A]H[G]S[I]D[A]A[V]E[A]M[L]G[A]O[D]F[L]I[K]P[C]E[A]D[R]L[V]T[V]N[N]A[L]R[R]A[Q]K[D]Q[E]I[K]E[N]P[D]K[S]N[K]Q[Y]G[F]I[G]S[S]Q[M]H[V]Y[E]T[I]D[S]A 154
 WP_105064188.1: T[A]H[G]T[I]N[A]V[N]L[L]Q[S]G[A]D[D]F[E]K[F]I[Q]A[N]R[L]K[T]S[I]N[H]L[K]R[N]K[L]E[G]L[V]E[D]L[Q]N[T]F[N]R[K]K[Y]Q[G]F[I]G[S]S[L]P[M]Q[A]V[Y]K[I]I[D]A 160

WP_172794763.1: P[S]K[A]T[V]F[I]G[E]S[G]T[G]K[E]V[C]A[E]A[I]H[A]A[S]K[R]G[C]G[F]T[A]I[N]C[A]A[I]P[K]D[L]E[S]E[L]F[G]H[V]K[G]A[F]T[G]A[S]V[D]R[K]G[A]E[A]Q[A]D[G]G[T]L 234
 WP_105064188.1: P[T]P[A]S[V]F[I]G[E]S[G]T[G]K[E]V[C]A[E]A[I]H[Y]Q[S]K[R]S[N]K[P]F[V]A[I]N[C]G[A]I[P]R[D]L[M]E[S]E[L]F[G]H[V]K[G]A[F]T[G]A[T]D[R]K[G]A[M]M[A]N[G]G[T]L 240

WP_172794763.1: D[E]L[C]E[M]D[L]L[Q]K[L]L[R]F[I]Q[T]G[T]E[F]K[V]G[S]S[K]M[S]R[V]D[V]R[F]V[C]A[T]N[R]D[P]W[L]E[V]Q[A]G[R]F[R]E[D]L[Y]R[L]H[V]I[P]T[L]P[L]R[E]R[G]N 314
 WP_105064188.1: D[E]L[C]E[M]E[L]M[Q]K[L]L[R]F[I]Q[T]G[R]E[T]P[L]G[S]K[E]L[S]T[D]I[R]I[C]A[T]N[R]D[E]L[T]E[V]N[E]G[R]F[R]E[D]L[Y]R[V]H[V]V[P]H[M]P[L]R[D]R[G]T 320

WP_172794763.1: I[E]I[A]H[S]I[L]C[H]S[E]E[G]R[E]F[I]T]F[S]P[V]D[E]F[A]H[V]D[W]P[G]N[V]R[Q]L[Q]N[V]I[R]N[V]V[L]N[R]G[K]E[V]L[S]M[L]P[P]P[L]S[L]E[I]N[S]S[D]A[S]K 394
 WP_105064188.1: I[D]I[A]S[F]F[L]K[Y]A[K]E[D]H[K]K[F]A[M]K[R]D[V]E[L]N[C]Y[A]W[P]G[N]V[R]Q[L]Q[N]I[R]N[V]V[L]H[N]E[T]H[V]A[E]H[L]P[P]L[N]Q[F]V[T]S[P]S--A[K]P 399

WP_172794763.1: N[E]V[S]S[L]I[S]K[N]---N[I]V[N]---E[V]V[N]-----P[K]E[T]I[E]L[W]K[S]E[K]I[E]T[A]T[A]L[C]D[G]N[I]P[Q]A[K]R[L]E[V]S[P]S[T] 455
 WP_105064188.1: V[A]T[S]Q[S]V[S]Q[T]P[Q]E[V]M[V]Q[P]Q[E]V[A]P[Q]S[L]H[E]H[A]N[T]Q[D]D[T]S[I]I[R]E[M]A[D]I[E]R[E]V[I]Q[N]A[I]D[H]C[D]G[N]V[L]N[A]A[V]L[E]L[S]P[S]T 479

WP_172794763.1: Y[R]K[L]S[W]D[D]K----- 465
 WP_105064188.1: Y[R]K[Q]A[W]E[A]Y[E]E[S]D[S] 494

A. loei

WP_175365415.1: MVWILMQRKYLLMVEDTASVAALYRSYINPLGLIDVVAKCVDAIEKVTLKAPDLTLLDLRLPDMTGLEVITTEIRKIHHD 80
 WP_065611272.1: ----MLQR--VLLVEDSTSLAALLYKCYVKDEPYEFFHVTTCEAKAFMEKNPPLVLLDLKLPDMSGDVLAWMKEKLP 74

WP_175365415.1: TPVVLMTAHGSIDVAEAMRLGAODFLIKPCADRLRVTVNSALRRAQKNIDNTGLDPNKSNNQYQGFIGSSSQMHQVYR 160
 WP_065611272.1: TAVLMTAARGTINTAVNLLQSGADDFTEKPTQANRLKTSISNHLKRNKLEGLVEDLQNTFNRRKYQGFIGSSLFVQAVYK 154

WP_175365415.1: TIDSAAPSKATVFTGESGTGKEVCAEAVHAASKRGGCPFTAINCAAIKDLIESEIFGHVKGAFTGASVDRKGAAEQAD 240
 WP_065611272.1: IIDAVAPTASVFIYGESGTGKEVCAEAEHYQSKRNKPEVAINCGAIPRDLMESEIFGHVKGAFTGATDRKGAAEMMAN 234

WP_175365415.1: GGTFLDELCEMDLIDLQTKLLRFIQGTTFQKVGSSKMSRVDVRFVCATNRDPWLEVOAGRFREDLYYRLHVIPITLPPLR 320
 WP_065611272.1: GGTFLDELCEMELEMCKKLLRFIQGTTFPLGGSKELSTDIRIICATNRDPLETEVNEGRFREDLYYRVHVVPTEMPPLR 314

WP_175365415.1: DRGNDIIEIHSIICHFSHEEGREFTTFSPDVVSFLIYWPGNVRQLQNVIRNVVVLNRGKEVILSMLEPPPLAPEDHNG 400
 WP_065611272.1: DRGNDIIDLAVFFLKKYAKEDKMKFTAMKQDVELRLCNYWPGNVRQLQNVIRNVVVLHNSTHVLLDQLPPPLNQATQPK 394

WP_175365415.1: SNIASIQ-----AVNRDS--RHFEQPPVDIEFVPEGN-----MKKETRPLWLSKQIIEEATITLCDGNIPQAAK 462
 WP_065611272.1: VKQATIQRHIVAKETINNVAPIAEMSVEPIHTEITSEPNSSIQNTSVTWDESAITRPMADIEREVIQNAIDHCDGNVLAAV 474

WP_175365415.1: QLEVPSTIYRKLQSNWDK----- 481
 WP_065611272.1: LLELSPSTIYRKKQAWDADETEQ 498

A. wodanis

CED71013.1: MQRKYLLMVEDTASVAALYRSYINPLGVLDVVAKCVDAIEAIALRIPDLVLLDLRLPDMTGLEVITSEIRKNNKDLPVVI 80
 CED57805.1: MLQR--VLLVEDSTSLAALLYKCYVKDEPYEFFHVTTCEAKAFMEKNPPLVLLDLKLPDMTSGDVLAWMKENQLPTAVIV 79

CED71013.1: MTAHGSIDAAVEAMRLGAODFLIKPCADRLRVTVNSALRRAQKQDDIKENPENTN--KQYQGFIGSSSQMHQVYRITD 158
 CED57805.1: ATARGTINTAVNLLQSGADDFTEKPTQANRLKTSISNHLKRNKLEGLVEDLQNTFNRRKYQGFIGSSLFVQAVYRITD 157

CED71013.1: SAAPSKATVFTGESGTGKEVCAEAVHAASKRGGCPFTAINCAAIKDLIESEIFGHVKGAFTGASVDRKGAAEQADGGT 238
 CED57805.1: AVAPTASVFIYGESGTGKEVCAEAEHYQSHREKSEVAINCGAIPRDLMESEIFGHVKGAFTGATDRKGAAMLANGGT 237

CED71013.1: LFLDELCEMDLIDLQTKLLRFIQGTTFQKVGSSKMSRVDVRFVCATNRDPWLEVOEGRFREDLYYRLHVIPITLPPLRER 318
 CED57805.1: LFLDELCEMELEMCKKLLRFIQGTTFPLGGSKELSTDIRIICATNRDPLETEVNEGRFREDLYYRVHVVPTEMPPLRER 317

CED71013.1: GDITETIASIICHFSHEEGREFTTFSPDVVTECFLEHYWPGNVRQLQNVIRNVVVLNKGKEVILSMLEPPPLSLENKHCLNI 398
 CED57805.1: TDIIDIASFFLKKYAKEDKMKFTAMKQDVELRLCNYWPGNVRQLQNVIRNVVVLHNDTQVAIEHLPPPLNQF-LAESTV 396

CED71013.1: ASKDTLQSGSIDREHHCESHALKKWDSE-----KQKVIIFLWQSEKNTIEAATAICEGNIPQAAKOLEVSPSTIY 467
 CED57805.1: KPRVTIAPTSPETACASQFHEVWPQSSSEDDPIVNOENTNSIREMADIEREVIQNAIDHCDGNVLAAVLLELSPSTIY 476

CED71013.1: RKLQSNWDK----- 476
 CED57805.1: RKKQAWDAEYESDS 490

Appendix A.7: Pairwise alignments of LuxO (top sequence) and SypG (bottom sequence) homologs encoded by indicated *Fischeri* clade members.

Amino acids highlighted in black (gray) indicate identity (similarity). (Figure generated by T. Miyashiro)

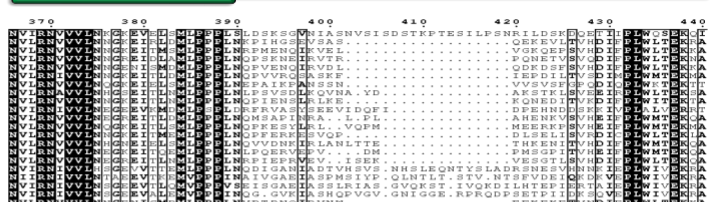
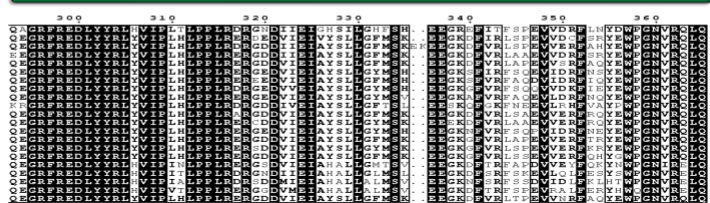
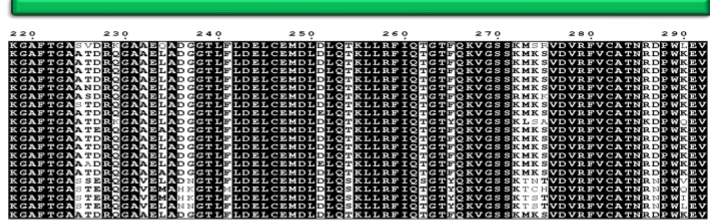
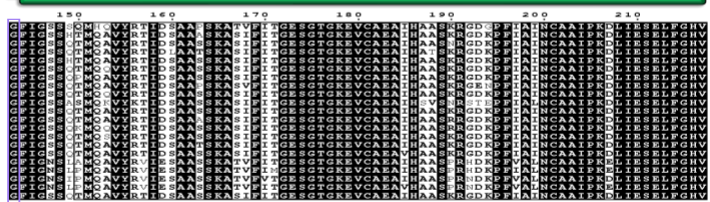
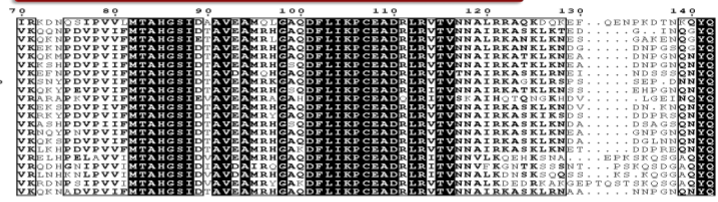
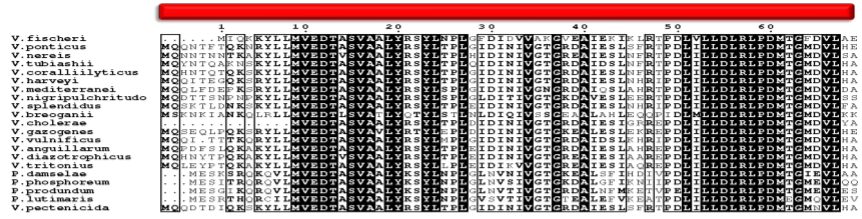
Clade	Taxon	LuxO homolog ¹	Accession	SypG homolog ²	Accession	Identity	Similarity
Salinivibrio-Grimontia-Enterovibrio ³	<i>G. hollisae</i>	WP_005503370.1	NZ_CP014056	N.D.	-	N.A.	N.A.
Rosenbergii	<i>P. lutimaris</i>	WP_107348500.1	NZ_SNZO01000002	N.D.	-	N.A.	N.A.
Profundum	<i>P. profundum</i>	WP_065814467.1	NC_006370	N.D.	-	N.A.	N.A.
Damselae	<i>Photobacterium damsela</i> subsp. <i>piscicida</i>	WP_086957069.1	NZ_AP018045	N.D.	-	N.A.	N.A.
Phosphoreum	<i>P. phosphoreum</i>	WP_045027808.1	NZ_MSCQ01000001	WP_105026695.1	NZ_MSCQ01000001	237/499 (47.49%)	310/499 (62.93%)
Fischeri	<i>V. fischeri</i>	WP_011261589.1	NC_006840	WP_011263835.1	NC_006841	243/502 (48.41%)	326/502 (64.94%)
Anguillarum	<i>V. anguillarum</i>	WP_026028983.1	NC_022223	N.D.	-	N.A.	N.A.
Rumoiensis	<i>V. rumoiensis</i>	N.D.	-	N.D.	-	N.A.	N.A.
Vulnificus	<i>V. vulnificus</i>	WP_011149911.1	NC_014965	WP_013571858.1	NC_014965	247/508 (48.62%)	320/508 (62.99%)
Diazotrophicus	<i>V. diazotrophicus</i>	WP_042486207.1	NZ_POSL01000002	N.D.	-	N.A.	N.A.
Gazogenes	<i>V. gazogenes</i>	WP_021019492.1	NZ_CP018835	N.D.	-	N.A.	N.A.
Porteresiae	<i>V. tritonius</i>	WP_068714228.1	NZ_AP014635	N.D.	-	N.A.	N.A.
Cholerae	<i>V. cholerae</i>	WP_001888250.1	NC_002505	N.D.	-	N.A.	N.A.
Haliotocoli	<i>V. breoganii</i>	WP_065209630.1	NZ_CP016177	WP_065210697.1	NZ_CP016178	228/513 (44.44%)	298/513 (57.70%)
Splendidus	<i>V. splendidus</i>	WP_004734031.1	NZ_CP031055	WP_065205220.1	NZ_CP031055	237/511 (46.38%)	314/511 (61.45%)
Pectenocida	<i>V. pectenocida</i>	WP_125320437.1	NZ_RSFA01000020	WP_125322971.1	NZ_RSFA01000107	237/501 (47.31%)	321/501 (64.07%)
Scopthalmi	<i>V. ponticus</i>	WP_075650093.1	NZ_AP019657	WP_075649540.1	NZ_AP019657	229/506 (45.26%)	319/506 (63.04%)
Nereis	<i>V. nereis</i>	WP_061781622.1	NZ_BCUD01000001	N.D.	-	N.A.	N.A.
Orientalis	<i>V. tubiashii</i>	WP_038550519.1	NZ_CP009354	WP_004748949.1	NZ_CP009354	242/497 (48.69%)	319/497 (64.19%)
Coralliilyticus	<i>V. coralliilyticus</i>	WP_019275536.1	NZ_CP048693	WP_021455926.1	NZ_CP048693	242/503 (48.11%)	322/503 (64.02%)
Harveyi	<i>V. harveyi</i>	WP_005444697.1	NZ_CP009467	WP_050907635.1	NZ_CP009467	244/522 (46.74%)	320/522 (61.30%)
Nigripulchritudo	<i>V. nigripulchritudo</i>	WP_022603175.1	NC_022528	WP_022550524.1	NC_022528	247/508 (48.62%)	331/508 (65.16%)
Mediterranei	<i>V. mediterranei</i>	WP_062462808.1	NZ_CP018308	WP_088875891.1	NZ_CP018308	236/503 (46.92%)	318/503 (63.22%)

Appendix A.8: LuxO and SypG in the *Vibrionaceae*

¹ N.D. (not detected) indicates that the top hit from BLAST was a bEBP other than LuxO.

² N.D. (not detected) indicates that the top hit from BLAST was a bEBP other than SypG.

³ The *Salinivibrio-Grimontia-Enterovibrio* group is ancestrally related to the *Vibrionaceae* family and is included as an outgroup in this analysis. (Figure generated by T. Miyashiro)



Appendix A.9: LuxO in the *Vibrionaceae*

Multiple sequence alignment of LuxO homologs. Identical amino acids are highlighted in black; similar amino acids are bolded. The rectangles above indicate the receiver (R) domain (red), the AAA+ (C) domain (green, and the putative helix-turn-helix (HTH) motif (blue) within the DNA-binding (D) domain. The yellow line indicates the residues of the R-C linker. The structurally significant glycine is shaded in a purple box. Alignment figure generated using ESPript 3.0 (<https://espript.ibcp.fr/ESPript/cgi-bin/ESPript.cgi>).

1 10 20 30 40 50 60 70
V. fischeri M L Q K V L L V E D S S L A L L Y K Q Y V K D P Y E F H V T G C A A F F E R N N P L V L I D L K L P D M C E D I L D W I N E M O V P
V. pectenicida M E A R K V L L I E D S S L A L L Y K Q Y V K D P Y D L F H V T G C E A A F F E R N N P L V L I D L K L P D M C E E I D W I N E M O V P
V. tubiashii M K R F R V L L I E D S S L A L L Y K Q Y V K D P Y D L F H V T G C E A A F F E R N N P L V L I D L K L P D M C E E I D W I N E M O V P
V. ponticus M E A R K V L L I E D S S L A L L Y K Q Y V K D P Y D L F H V T G C E A A F F E R N N P L V L I D L K L P D M C E D I D W I N E M O V P
V. corallilyticus M E A R K V L L I E D S S L A L L Y K Q Y V K D P Y D L F H V T G C E A A F F E R N N P L V L I D L K L P D M C E D I D W I N E M O V P
V. harveyi M R F R V L L I E D S S L A L L Y K Q Y V K D P Y D L F H V T G C E A A F F E R N N P L V L I D L K L P D M C E D I D W I N E M O V P
V. mediterranei M T O P R V L L I E D S S L A L L Y K Q Y V K D P Y D F H V T G C E A K I F E R H S P L V L I D L K L P D M C E V I D W I N E M O I S
V. nigripulchritudo M T O P R V L L I E D S S L A L L Y K Q Y V K D P Y D F H V T G C E A K I F E R H S P L V L I D L K L P D M C E V I D W I N E M O I S
V. splendidus M E R F R V L L I E D S S L A L L Y K Q Y V K D P Y D L F H V T G C D A K F F E R H A P L V L I D L K L P D M C E E I D W I N E M O I P
V. breoganii M E R F R V L L I E D S S L A L L Y K Q Y V K D P Y D L F H V T G C D A K F F E R H A P L V L I D L K L P D M C E E I D W I N E M O I P
V. vulnificus M E A R K V L L I E D S S L A L L Y K Q Y V K D P Y D I F H V T G C D A I Q F E R N N P L V L I D L K L P D M C E D I D W I N E M O I P
P. phosphoreum M L Q K V L L V E D S S L A L L Y K Q Y V K D P Y E F H V T G C A A F F E R N N P L V L I D L K L P D M C E D I L D W I N E M O V P

80 90 100 110 120 130 140
V. fischeri T V I V I A T A H C T I D H A V L L I Q G A D F L E K P Q A D R L K T S I A L H L Q O V R K L E N L V E I E A R F P D R R R F G F G S L P M
V. pectenicida T S V V V A T A H C S V D I A V L L L Q K C A D F L E K P Q A D R L K T S I A L H L Q O V R K L E N L V E I E A R F P D R R R F G F G S L P M
V. tubiashii T S V V I A T A H C S V D I A V L L V Q K C A D F L E K P N A D R L K T S I A L H L Q O V R K L E N L V E I E A R F P D R R R F G F G S L P M
V. ponticus T S V I V A T A H C S V N I A V L L L Q K G A D F L E K P I S D R L K T S I Q L H L Q R T K L E N L V E I E A R F P D R R R F G F G S I V M
V. corallilyticus T S V V V A T A H C S V D I A V L L L Q K C A D F L E K P Q A D R L K T S I A L H L Q O V R K L E N L V E I E A R F P D R R R F G F G S L P M
V. harveyi T S V I V A T A H C S V N I A V L L I Q K G A D F L E K P I A D R L K T S I A L H L Q O V R K L E N L V E I E A R F P D R R R F G F G S L P M
V. mediterranei T S V I V A T A H C S V D I A V L L I Q K C A D F L E K P I A D R L K T S I A L H L Q O V R K L E N L V E I E A R F P D R R R F G F G S L P M
V. nigripulchritudo T S V I V A T A H C S V N I A V L L M R I C A D F L E K P I N A D R L K T S I K N H L Q R N K L E N L V E I E A R F P D R R R F G F G S L P M
V. splendidus T S V I V A T A H C S V N I A V L L I Q G A D F L E K P Q A D R L K T S I A L H L Q O V R K L E N L V D M O S R F P D R R R F N F G S L P M
V. breoganii T S V I V A T A H C S V N I A V L L I Q G A D F L E K P Q A D R L K T S I A L H L Q O V R K L E N L V D M O S R F P D R R R F N F G S L P M
V. vulnificus T S V I V A T A H C S V D I A V L L Q K C A D F L E K P I A D R L K T S I A L H L Q O V R K L E N L V E I E A R F P D R R R F G F G S L P M
P. phosphoreum T S V I V A T A H C T I D H A V L L I Q G A D F L E K P I Q A D R L K T S I R N H L A H N K L E L V E I E M D F R R R K Y G F G S L P M

150 160 170 180 190 200 210 220
V. fischeri Q V Y Y K I D S V A P T N A S V F I C E S C T G K E V C A A H H S S R R N R P F V A N C C A I P R D L M E S E I F G H K C A F T G A T
V. pectenicida Q V Y Y K I D S V A P T N A S V F I C E S C T G K E V C A A H H S S R R N R P F V A N C C A I P R D L M E S E I F G H K C A F T G A T
V. tubiashii Q V Y Y K I D S V A P T N A S V F I C E S C T G K E V C A A H H S S R R N R P F V A N C C A I P R D L M E S E I F G H K C A F T G A T
V. ponticus Q V L Y K I D A V A P T N A S V F I C E S C T G K E V C A A H H S S R R N R P F V A N C C A I P R D L M E S E I F G H K C A F T G A T
V. corallilyticus Q V Y Y K I D S V A P T N A S V F I C E S C T G K E V C A A H H S S R R N R P F V A N C C A I P R D L M E S E I F G H K C A F T G A T
V. harveyi Q V Y Y K I D A V A P T N A S V F I C E S C T G K E V C A A H H S S R R N R P F V A N C C A I P R D L M E S E I F G H K C A F T G A T
V. mediterranei Q V Y Y K I D A V A P T N A S V F I C E S C T G K E V C A A H H S S R R N R P F V A N C C A I P R D L M E S E I F G H K C A F T G A T
V. nigripulchritudo Q V Y Y K I D S V A P T N A S V F I C E S C T G K E V C A A H H S S R R N R P F V A N C C A I P R D L M E S E I F G H K C A F T G A T
V. splendidus Q V Y Y K I D S V A P T N A S V F I C E S C T G K E V C A A H H S S R R N R P F V A N C C A I P R D L M E S E I F G H K C A F T G A T
V. breoganii Q V Y Y K I D S V A P T N A S V F I C E S C T G K E V C A A H H S S R R N R P F V A N C C A I P R D L M E S E I F G H K C A F T G A T
V. vulnificus Q V Y Y K I D S V A P T N A S V F I C E S C T G K E V C A A H H S S R R N R P F V A N C C A I P R D L M E S E I F G H K C A F T G A T
P. phosphoreum Q V Y Y K I D A V A P T N A S V F I C E S C T G K E V C A A H H S S R R N R P F V A N C C A I P R D L M E S E I F G H K C A F T G A T

230 240 250 260 270 280 290
V. fischeri D R K G A A M I A N G G T L F L D E L C E M L E M O K K L L R F L O T C R F T P L C S S R E L S T D R I C A N R D P L E V E E G R F R E D L
V. pectenicida D R K G A A S I A N G G T L F L D E L C E M L E M O K K L L R F L O T C R F T P L C S S R E L K V D V R I C A N R D P L E V E E G R F R E D L
V. tubiashii D R K G A A S I A N G G T L F L D E L C E M L E M O K K L L R F L O T C R F T P L C A N K E M K V D V R I C A N R D P L E V E E G R F R E D L
V. ponticus D R K G A A S I A N G G T L F L D E L C E M L E M O K K L L R F L O T C R F T P L C A S K E J K V D V R I C A N R D P L E V E E G R F R E D L
V. corallilyticus D R K G A A S I A N G G T L F L D E L C E M L E M O K K L L R F L O T C R F T P L C A S K E J K V D V R I C A N R D P L E V E E G R F R E D L
V. harveyi D R K C A A T I A N G G T L F L D E L C E M L E M O K K L L R F L O T C R F T P L C A T R E M K V D V R I C A N R D P L E V E E G R F R E D L
V. mediterranei D R K G A A S I A N G G T L F L D E L C E M L E M O K K L L R F L O T C R F T P L C A T R E K V D V R I C A N R D P L E V E E G R F R E D L
V. nigripulchritudo D R K G A A S I A N G G T L F L D E L C E M L E M O K K L L R F L O T C R F T P L C T R E I Q V D V R I C A N R D P L E V E E G R F R E D L
V. splendidus D R K G A A M I A N G G T L F L D E L C E M L E M O K K L L R F L O T C R F T P L C S S R E L K A D V R I C A N R D P L E V E E G R F R E D L
V. breoganii D R K G A A M I A N G G T L F L D E L C E M L E M O K K L L R F L O T C R F T P L C S S R E L K A D V R I C A N R D P L E V E E G R F R E D L
V. vulnificus D R K G A A M I A N G G T L F L D E L C E M L E M O K K L L R F L O T C R F T P L C S S R E L K V D V R I C A N R D P L E V E E G R F R E D L
P. phosphoreum D R K G A A M I A N G G T L F L D E L C E M L E M O K K L L R F L O T C R F T P L C S S R E I A T D R I C A N R D P L E V E E G R F R E D L

300 310 320 330 340 350 360 370
V. fischeri Y Y R V H V P I H M P P R R G C T D I I L A H F L K Y A R E D K K R N A L K R N V E L R L C N Y W P G N V R Q L Q N I R N V V L N H
V. pectenicida Y Y R V H V P I H M P P R R G C N D I I L A H F L K V F A K E D K K K N G I N R D A E S L L K R Y W P G N V R Q L Q N I R N I V V L N H
V. tubiashii Y Y R V H V P I H M P P R R G C T D I I L A H F L K Y A R E D K K R N A L K R N V E L R L C N Y W P G N V R Q L Q N I R N I V V L N H
V. ponticus Y Y R V H V P I H M P P R R G C N D I I L A H F L K Y A R E D K K K N A T H R D A E S L L K R Y W P G N V R Q L Q N I R N I V V L N H
V. corallilyticus Y Y R V H V P I H M P P R R G C N D I I L A H F L K Y A R E D K K K N G I N R D A E S L L K R Y W P G N V R Q L Q N I R N I V V L N H
V. harveyi Y Y R V H V P I H M P P R R G S D I V L A H F L T Y A K D K K K N N I D S E A Q H V I K H Y W P G N V R Q L Q N I R N I V V L N H
V. mediterranei Y Y R V H V P I H M P P R R R D R I V L A H F L K Y A R E D K R R P E S I S K E A Q R Y L K R Y W P G N V R Q L Q N I R N I V V L N H
V. nigripulchritudo Y Y R V H V P I H M P P R R G C T D I I L A H F L R Y A R E D K K K T G F R D A E L V L C N Y W P G N V R Q L Q N I R N I V V L N H
V. splendidus A N E T V A S P E K V I R P M W H E R E L Q A I E C D G N V I N A V L E L S P S T V Y R K K Q A W E A E D E S S V E
V. breoganii Y Y R V H V P I H M P P R R G C N D I V L A H F L K Y A R E D K K K S I D K T Q L K R Y W P G N V R Q L Q N I R N I V V L N H
V. vulnificus Y Y R V H V P I H M P P R R G C N D I V L A H F L K Y A R E D K K K S I S K E A Q S I L K K Y W P G N V R Q L Q N I R N I V V L N H
P. phosphoreum Y Y R V H V P I H M P P R R R C T D I I L A H F L K Y A R E D K K R B A L K R N V E L R L C H Y W P G N V R Q L Q N I R N I V V L N H

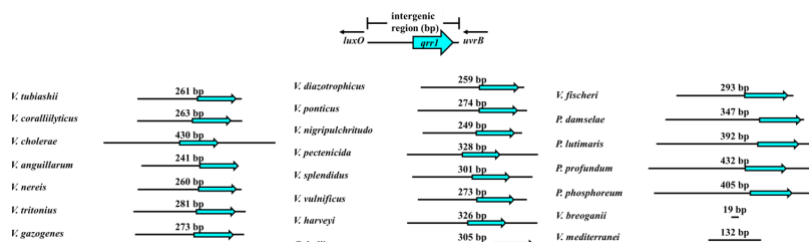
380 390 400 410 420 430
V. fischeri D T H V A E H L P P E L N Q P V T N K A T V A S K P S F T A . . . P S Q L S R N M E . . . T A D V O H N Q T E Q O L . . . S S S S E . . . O T L .
V. pectenicida D A K L S I E H L P E C I S R G P K A P K S P L O S I P S Q H S H V M O D I . A A A Q S E P T P L A S .
V. tubiashii D S H L R L E H L P D Q V T T S R K L K S S I S P K P A P . A V T P P P P P A S E E L E G N T I Q P .
V. ponticus D T L R A E H P A C E T T T R K T P H R S V P T A T . . . P S P P K S E H V N H V A L D E Q H I S A E H Q V V A D A .
V. corallilyticus E S L S N A H L P D Q V T T S R K S A K P A A Q A A I . . R Y E A P A Q A S P V E A V D T . A I Q A S . N F . V V .
V. harveyi E D K V S L A H L P A Q L T R K P A K E R S A T I E H D A . . R Y N D S S F S P L E N P P A G T V N L S A R E S E M P V A T E S S L V S A V T .
V. mediterranei D K S L G V N H L P A E M V Q T R P A T V V R P S T P O S M L S V V Q H P T Q E S T V D H N M V E T V Q M A A V Q P .
V. nigripulchritudo E P Q V S M E H L P P E L N S M S A G V G S A S R V . I R A P V . P K P E P V V S . . . I E P P V H A E A V A V S A A T A F E A P .
V. splendidus A N E T V A S P E K V I R P M W H E R E L Q A I E C D G N V I N A V L E L S P S T V Y R K K Q A W E A E D E S S V E S A A T A F E A P .
V. breoganii E T V T A T T H E L P P E L N S V N P A K P A V V A I P A V A T L T P A P V A . V Q A P P A T N V E E V V N Q I T S P T E S Q A P .
V. vulnificus E T V T A T T H E L P P E L N S V N P A K P A V V A I P A V A T L T P A P V A . V Q A P P A T N V E E V V N Q I T S P T E S Q A P .
P. phosphoreum N T H S M E H L P P E L N S F K T T A K T P D K O H I R L N N I T P K P I T N I E P P L H . T M T L K S .

440 450 460 470 480 490 500
V. fischeri E T S A T D A I N T S V I R P M W I E R E V T I Q A I D F C D G N V I N A A V L E L S P S T V Y R K K Q A W E A E D E S S V E
V. pectenicida E D I S K S Q A T N I T I R P M W I E R E V T I Q A I D F C D G N V I N A A V L E L S P S T V Y R K K Q A W E A E D E S S V E
V. tubiashii I S A N S Q A D R P V T I R P M W I E R E V T I Q A I D F C D G N V I N A A V L E L S P S T V Y R K K Q A W E A E D E S S V E
V. ponticus E S V N T O S S T F V I R P M W I E R E V T I Q A I D F C D G N V I N A A V L E L S P S T V Y R K K Q A W E A E D E S S V E
V. corallilyticus P V A S P Y F N S D G T I R P M W I E R E V T I Q A I D F C D G N V I N A A V L E L S P S T V Y R K K Q A W E A E D E S S V E
V. harveyi P Q P S D T E P R T F I R P M W I E R E V T I Q A I D F C D G N V I N A A V L E L S P S T V Y R K K Q A W E A E D E S S V E
V. mediterranei P A P E P V E V G M F I R P M W I E R E V T I Q A I D F C D G N V I N A A V L E L S P S T V Y R K K Q A W E A E D E S S V E
V. nigripulchritudo P M T F A T T H E L P P E L N S V N P A K P A V V A I P A V A T L T P A P V A . V Q A P P A T N V E E V V N Q I T S P T E S Q A P .
V. splendidus P M T F A T T H E L P P E L N S V N P A K P A V V A I P A V A T L T P A P V A . V Q A P P A T N V E E V V N Q I T S P T E S Q A P .
V. breoganii T T V S S E S S T F A V R P M W I E R E V T I Q A I D F C D G N V I N A A V L E L S P S T V Y R K K Q A W E A E D L Q V S E
V. vulnificus L T H N A F H H S D G S I R P M W I E R E V T I Q A I D F C D G N V I S A A V L E L S P S T V Y R K K Q A W E A E D L Q V S E
P. phosphoreum E P D D K K A I N T H I R P M W I E R E V T I Q A I D F C D G N V I N A A V L E L S P S T V Y R K K Q A W E A E D L Q V S E

Appendix A.10: SypG in the *Vibrionaceae*

Multiple sequence alignment of SypG homologs. Identical amino acids are highlighted in black; similar amino acids are bolded. The rectangles above indicate the receiver (R) domain (red), the AAA+ (C) domain (green, and the putative helix-turn-helix (HTH) motif (blue) within the DNA-binding (D) domain. The yellow line indicates the residues of the R-C linker. The position corresponding to the structurally significant glycine is shaded in purple.

A.



B.

```

Vtubiashii      TGGCAGCCTATAGCGTAAATCTGTTA-TGACCCCTCA-----TGGGTCACTAGCCAACTGACGTGTTTCTGCAACTT 71
Vcoralliilyticus TGGCAGCTTAAGCGT--GTTATAACATTGACCCCTTA-----TGGGTCACTAGCCAACTGACGTGTTTCTGCAACTT 71
Vcholerae      TGGCAGATATGCGCTTGATTACTAC--TGACCCGCA-----AGGGTCACCTAGCCAACTGACGTGTTTCTGCAATAA 71
Vanguillarum  TGGCAGATATGCGCTCTATTCAATA--TGACCCCTTA-----GGGGTCACCTAGCCAACTGACGTGTTTCTGCAATAA 71
Vnereis       TGGCAGATATGCGCTTATATTAGGA--GACCCCTTA-----TGGGTCACTAGCCAACTGACGTGTTTCTGCAACTA 71
Vtritonius    TGGCAGAGTTTACCGATTAAATAAT--TGACCTGCA-----AGAGTCACCTAGCCAACTGACGTGTTTCTGCAATTT 71
Vgazogenes   TGGCAGATATAGCGCTT-ATAGTAATCTTGACCCCTCA-----CGGGTCACCTAGCCAACTGACGTGTTTCTGCAATA 72
Vdiazotrophicus TGGCAGCTTAAGCGCTTGACTTAA--TGACCCCTAA-----CGGGTCACCTAGCCAACTGACGTGTTTCTGCAATAC 71
Vponticus     TGGCAGGATATGCGA--GTATTAACAATGACCCCTAA-----CGGGTCACCTAGCCAACTGACGTGTTTCTGCAACTT 71
Vnigrispulchritudo TGGCAGCAATGCGCACTGCATGTA--TGACCCCTAA-----CGGGTCACCTAGCCAACTGACGTGTTTCTGCAACAA 71
Vpectenicida  TGGCAGCTTAAAGCGT--GATATAAATTGACCTGTA-----TGGGTCACTAGCCAACTGACGTGTTTCTGCAACAA 71
Vsplendidus  TGGCAGCAACGCGCAACCTAAG--TGACCCCTT-----CGGGTCACCTAGCCAACTGACGTGTTTCTGCAACG 69
Vvulnificus  TGGCAGAAACGCGCTTAAACTAAAG--TGACCCCT-----CGGGTCACCTAGCCAACTGACGTGTTTCTGCAACT 70
Vharveyi     TGGCAGAAACGCGCTTAAACTAA--TGACCCCT-----CGGGTCACCTAGCCAACTGACGTGTTTCTGCAACGA 70
Ghollisae    TGGCAGCTTACCGCTTCAATACAA--TGACCCCTT-----CTA--GGGTCACTAGCCAACTGACGTGTTTCTGCAAGGAC 72
Vfischeri    TGGCAGGTCCCGCATAGGTATAT--TGACCCCTTAAAGCCAAAGGGTCACCTAGCCAACTGACGTGTTTCTGCAAAATT 78
Pdamelsae   TGGCAGGTCTCTCGTTTATATAAG--TAGCTCTT-A-CCTAAGAGTTACCTAGCCAACTGACGTGTTTCTGCAAAATC 76
Plutimaris  TGGCAGATATGCGCTTATAGACATA--TGACCTCT-----CGTAGAGTCACTAGCCAACTGACGTGTTTCTGCAAGATT 75
Pprofundum  TGGCAGAAACGCGCTTAAATAGAA--TGACCTCT- AATGTA-GAGTCACTAGCCAACTGACGTGTTTCTGCAAAATG 76
Pphosphoreum TGGCAGACGTATCGCTTATAACAC--TGACCTCT-ATCTTAGGAGTCACTAGCCAACTGACGTGTTTCTGCAATTC 77

Vtubiashii      ---AG--ATTACA-AATTACAGCCATTAACCAAGTT-TACTGGCGATTTTTT-- 122
Vcoralliilyticus --AG--ATTACA-AATTACAGCCATTAACCAAGTT-TACTGGCGATTTTTT-- 122
Vcholerae      TC--AG--ATTACA-AATTACAGCCATTAACCAAGTT-TACTGGCGATTTTTT-- 122
Vanguillarum  ---AG--ATTACA-AATAACAGCCATTAACCAAGTT-TACTGGCGATTTTTT-- 121
Vnereis       ---AG--ATTACAATAATGA-AGCCATTAATC-ATT-TACTGGCGATTTTTT-- 120
Vtritonius    ---AG--ATTACAGAAATTAAGCCATTAAGGCTTA-TT-TACTGGCGATTTTTT-- 123
Vgazogenes   ---AG--ATTACACATCTGACAGCCATTAATGACTC-TT-TACTGGCGATTTTTT-- 124
Vdiazotrophicus ---GAT--ATTACAGAAATTAACAGCCATTAAGGCTTA-TT-TACTGGCGATTTTTT-- 123
Vponticus     ---AG--ATTACA-AATTACAGCCATTAACCAAGTT-TACTGGCGATTTTTT-- 121
Vnigrispulchritudo ---AG--ATTACAGAAATTAAGCCATTAAGGCTTA-TT-TACTGGCGATTTTTT-- 121
Vpectenicida  ---AG--ATTACA-AGA-ATAGCCATTAACATT--T-ACTGGCGATTTTTT-- 119
Vsplendidus  ---AG--ATTACA-AACTGAGCCATTAAGGCTTA-ATT-TACTGGCGATTTTTT-- 119
Vvulnificus  ---AG--ATTACA-ATTGATAGCCATTAAGGCTTA-TT-TACTGGCGATTTTTT-- 119
Vharveyi     ---TAT--ATTACA-AAACG-AGCCATTAATCCGACTG-CGATGGCGATTTTTT-- 121
Ghollisae    TTGTTCACTGAAACAGAT-AGCCATTAAGGCTTTTGT--GGTGGCGATTTTTT-- 126
Vfischeri    TACTTTCACATGAAACATA-AGCCATTAAGGCTTTTGT--GGTGGCGATTTTTT-- 133
Pdamelsae   TA--TTACTATAA-CAATGA-AGCCATTAAGGCTTTTGT--GGTGGCGATTTTTT-- 129
Plutimaris  TA--TTACTATAA-CAATGA-AGCCATTAAGGCTTTTGT--GGTGGCGATTTTTT-- 128
Pprofundum  AA--TTACTATAA-CAATGA-AGCCATTAAGGCTTTTGT--GGTGGCGATTTTTT-- 128
Pphosphoreum T--TTACTATAA-CAATGA-AGCCATTAAGGCTTTTGT--GGTGGCGATTTTTT-- 130

```

Appendix A.11: Conservation of *qrr* gene within *uvrB-luxO* intergenic region among *Vibrionaceae*

(A) Cartoon indicating length in bp of *uvrB-luxO* intergenic region for indicated taxa. Location of putative gene encoding a Qrr is denoted by the cyan arrow.

(B) Sequences of homologs of Qrr1 (denoted by the black lines) encoded within the *uvrB-luxO* intergenic region of each indicated taxon. Each homolog was identified by first using the locations of the -24 (GGC) and -12 (GC) sites corresponding to σ^{54} binding sites to determine the putative transcriptional start site and then locating the thymidine repeat corresponding to the likely terminator sequence. (Figure generated by T. Miyashiro)

APPENDIX METHODS

Media and growth conditions: *V. fischeri* strains were grown at 28°C under aerobic conditions shaking at 200 rpm in LBS (Luria-Broth Salt) media [1% (wt/vol) tryptone, 0.5% (wt/vol) yeast extract, 2% (wt/vol) NaCl, 50mM Tris-HCl (pH 7.5)].

Strains and Plasmids: Strains and plasmids used in this study are listed in **Table 1** and **Table 2**, respectively.

Motility Assay: Overnight cultures of *V. fischeri* were diluted 1:100 into LBS. Once cultures reached mid-log, cells were injected into minimal media soft agar motility plates (50 mM MgSO₄, 10 mM CaCl₂, 300 mM NaCl, 10 mM KCl, 0.0058% (wt/vol) K₂HPO₄, 0.1 mM FeSO₄, 84 mM Tris-HCl (pH 7.5) containing 1 mM GlcNAc and 0.25% agar). Plates were incubated at 28°C. After a 14-hour incubation, the diameter of the rings that formed was measured over time.

Bioluminescence assay: *V. fischeri* cells were grown overnight in LBS, then sub-cultured 1:100 into seawater tryptone (SWT) media. Hourly measurements were collected for OD₆₀₀ (16 mm-width tube or 10 mm cuvette measured in a Biowave CO8000 Cell Density Meter) and luminescence (100 µl measured in a 1.5 ml microfuge tube in the Promega Glomax 20/20 luminometer). Specific luminescence for each sample was calculated as RLU (relative light units)/OD₆₀₀.

Squid luminescence: *V. fischeri* cells harboring the *P_{qrr1}-gfp* promoter reporter pTM268 inoculated into 3 ml LBS media supplemented with chloramphenicol at 2.5 µg/ml (Cm 2.5 µg/ml) and incubated at 28°C shaking at 200 rpm. 30 µl of cultures grown overnight were diluted into 3 ml LBS with Cm 2.5 µg/ml and grown until cultures reached an OD₆₀₀ close to 1.0. Intermediate cultures were diluted 1:100 into FSSW (20 µl culture into 980 µl FSSW). 200 µl of the diluted cells were added to 50 ml FSSW, and the bacterial suspension was added to animals in 50 ml FSSW. 25 µl of the inoculum was plated in duplicate onto LBS solid agar plates. Plates were

incubated at 28°C and the resultant CFU were enumerated to determine the inoculum ratio and total inoculum size. 3.5 hours after animals were exposed to the single-strain inoculums, the animals were washed by transferring to 4 ml FSSW. Luminescence values were measured on Days 2 and 3 post-inoculation using a Glomax Luminometer.

Bioinformatics: Bacterial enhancer binding proteins (bEBPs) in *V. fischeri* were identified by performing a BLAST search against the genome of *V. fischeri* ES114 (tax ID: 312309) using amino acids 145 – 389 of LuxO (WP_011261589.1), which correspond to the putative AAA+ domain [62], as a query. The presence of a GAFTGA motif, which is predicted to interact with σ^{54} , was used as criteria to validate each protein hit as a bEBP. Multiple sequence alignments were performed using ClustalW (<https://www.ebi.ac.uk/>) for proteins or MAFFT for DNA sequences <https://www.ebi.ac.uk/Tools/msa/mafft/> [142]. Pairwise alignments were performed using the EMBOSS Needle Pairwise Sequence Alignment Tool [142]. The putative helix-turn-helix motif was generated using NPS@:Network Protein Sequence Analysis [143].

References

1. Agarwal, J., S. Srivastava, and M. Singh, *Pathogenomics of uropathogenic Escherichia coli*. Indian J Med Microbiol, 2012. **30**(2): p. 141-9.
2. Jones, M.K. and J.D. Oliver, *Vibrio vulnificus: disease and pathogenesis*. Infect Immun, 2009. **77**(5): p. 1723-33.
3. Pal, R.R., et al., *Pathogenic E. coli Extracts Nutrients from Infected Host Cells Utilizing Injectisome Components*. Cell, 2019. **177**(3): p. 683-696 e18.
4. Silva, A.J. and J.A. Benitez, *Vibrio cholerae Biofilms and Cholera Pathogenesis*. PLoS Negl Trop Dis, 2016. **10**(2): p. e0004330.
5. Kastl, A.J., Jr., et al., *The Structure and Function of the Human Small Intestinal Microbiota: Current Understanding and Future Directions*. Cell Mol Gastroenterol Hepatol, 2020. **9**(1): p. 33-45.
6. Rowland, I., et al., *Gut microbiota functions: metabolism of nutrients and other food components*. Eur J Nutr, 2018. **57**(1): p. 1-24.
7. Rago, J.V., et al., *Detection and analysis of Staphylococcus aureus isolates found in ambulances in the Chicago metropolitan area*. Am J Infect Control, 2012. **40**(3): p. 201-5.
8. Swaney, M.H. and L.R. Kalan, *Living in Your Skin: Microbes, Molecules, and Mechanisms*. Infect Immun, 2021. **89**(4).
9. Taylor, R.K., et al., *Use of phoA gene fusions to identify a pilus colonization factor coordinately regulated with cholera toxin*. Proc Natl Acad Sci U S A, 1987. **84**(9): p. 2833-7.
10. Kim, S.M., et al., *LuxR homologue SmcR is essential for Vibrio vulnificus pathogenesis and biofilm detachment, and its expression is induced by host cells*. Infect Immun, 2013. **81**(10): p. 3721-30.
11. Ribet, D. and P. Cossart, *How bacterial pathogens colonize their hosts and invade deeper tissues*. Microbes Infect, 2015. **17**(3): p. 173-83.
12. Oldroyd, G.E., *Speak, friend, and enter: signalling systems that promote beneficial symbiotic associations in plants*. Nat Rev Microbiol, 2013. **11**(4): p. 252-63.
13. Jones, K.M., et al., *How rhizobial symbionts invade plants: the Sinorhizobium-Medicago model*. Nat Rev Microbiol, 2007. **5**(8): p. 619-33.
14. Ruby, E.G., *Symbiotic conversations are revealed under genetic interrogation*. Nat Rev Microbiol, 2008. **6**(10): p. 752-62.
15. Tebo, B.M., D.S. Linthicum, and K.H. Nealson, *Luminous bacteria and light emitting fish: ultrastructure of the symbiosis*. Biosystems, 1979. **11**(4): p. 269-80.
16. Ruby, E.G., *Lessons from a cooperative, bacterial-animal association: the Vibrio fischeri-Euprymna scolopes light organ symbiosis*. Annu Rev Microbiol, 1996. **50**: p. 591-624.
17. Visick, K.L., E.V. Stabb, and E.G. Ruby, *A lasting symbiosis: how Vibrio fischeri finds a squid partner and persists within its natural host*. Nat Rev Microbiol, 2021. **19**(10): p. 654-665.

18. Nyholm, S.V. and M.J. McFall-Ngai, *A lasting symbiosis: how the Hawaiian bobtail squid finds and keeps its bioluminescent bacterial partner*. Nat Rev Microbiol, 2021. **19**(10): p. 666-679.
19. Jones, B.W. and M.K. Nishiguchi, *Counterillumination in the Hawaiian bobtail squid, Euprymna scolopes Berry (Mollusca: Cephalopoda)*. Marine Biology, 2004. **144**(6): p. 1151-1155.
20. Nyholm, S.V. and M.J. McFall-Ngai, *Sampling the light-organ microenvironment of Euprymna scolopes: description of a population of host cells in association with the bacterial symbiont Vibrio fischeri*. Biol Bull, 1998. **195**(2): p. 89-97.
21. Wier, A.M., et al., *Transcriptional patterns in both host and bacterium underlie a daily rhythm of anatomical and metabolic change in a beneficial symbiosis*. Proc Natl Acad Sci U S A, 2010. **107**(5): p. 2259-64.
22. Sycuro, L.K., E.G. Ruby, and M. McFall-Ngai, *Confocal microscopy of the light organ crypts in juvenile Euprymna scolopes reveals their morphological complexity and dynamic function in symbiosis*. J Morphol, 2006. **267**(5): p. 555-68.
23. Naughton, L.M. and M.J. Mandel, *Colonization of Euprymna scolopes squid by Vibrio fischeri*. J Vis Exp, 2012(61): p. e3758.
24. Ruby, E.G., et al., *Complete genome sequence of Vibrio fischeri: a symbiotic bacterium with pathogenic congeners*. Proc Natl Acad Sci U S A, 2005. **102**(8): p. 3004-9.
25. Visick, K.L., et al., *Tools for Rapid Genetic Engineering of Vibrio fischeri*. Appl Environ Microbiol, 2018. **84**(14).
26. Nyholm, S.V., et al., *Establishment of an animal-bacterial association: recruiting symbiotic vibrios from the environment*. Proc Natl Acad Sci U S A, 2000. **97**(18): p. 10231-5.
27. Wei, S.L. and R.E. Young, *Development of symbiotic bacterial bioluminescence in a nearshore cephalopod, Euprymna scolopes*. Marine Biology, 1989. **103**(4): p. 541-546.
28. Nawroth, J.C., et al., *Motile cilia create fluid-mechanical microhabitats for the active recruitment of the host microbiome*. Proc Natl Acad Sci U S A, 2017. **114**(36): p. 9510-9516.
29. Yip, E.S., et al., *A novel, conserved cluster of genes promotes symbiotic colonization and sigma-dependent biofilm formation by Vibrio fischeri*. Mol Microbiol, 2005. **57**(5): p. 1485-98.
30. Nyholm, S.V. and M.J. McFall-Ngai, *Dominance of Vibrio fischeri in secreted mucus outside the light organ of Euprymna scolopes: the first site of symbiont specificity*. Appl Environ Microbiol, 2003. **69**(7): p. 3932-7.
31. Millikan, D.S. and E.G. Ruby, *Alterations in Vibrio fischeri motility correlate with a delay in symbiosis initiation and are associated with additional symbiotic colonization defects*. Appl Environ Microbiol, 2002. **68**(5): p. 2519-28.
32. Mandel, M.J., et al., *Squid-derived chitin oligosaccharides are a chemotactic signal during colonization by Vibrio fischeri*. Appl Environ Microbiol, 2012. **78**(13): p. 4620-6.

33. Wollenberg, M.S. and E.G. Ruby, *Population structure of Vibrio fischeri within the light organs of Euprymna scolopes squid from Two Oahu (Hawaii) populations*. Appl Environ Microbiol, 2009. **75**(1): p. 193-202.
34. Koropatnick, T.A., et al., *Microbial Factor-Mediated Development in a Host-Bacterial Mutualism*. Science, 2004. **306**(5699): p. 1186-1188.
35. Taga, M.E. and B.L. Bassler, *Chemical communication among bacteria*. Proc Natl Acad Sci U S A, 2003. **100 Suppl 2**: p. 14549-54.
36. Girard, L., *Quorum sensing in Vibrio spp.: the complexity of multiple signalling molecules in marine and aquatic environments*. Crit Rev Microbiol, 2019. **45**(4): p. 451-471.
37. Kovacicova, G. and K. Skorupski, *Regulation of virulence gene expression in Vibrio cholerae by quorum sensing: HapR functions at the aphA promoter*. Mol Microbiol, 2002. **46**(4): p. 1135-47.
38. Yang, Q. and T. Defoirdt, *Quorum sensing positively regulates flagellar motility in pathogenic Vibrio harveyi*. Environ Microbiol, 2015. **17**(4): p. 960-8.
39. Zhu, J. and J.J. Mekalanos, *Quorum sensing-dependent biofilms enhance colonization in Vibrio cholerae*. Dev Cell, 2003. **5**(4): p. 647-56.
40. Boylan, M., et al., *Lux C, D and E genes of the Vibrio fischeri luminescence operon code for the reductase, transferase, and synthetase enzymes involved in aldehyde biosynthesis*. Photochem Photobiol, 1989. **49**(5): p. 681-8.
41. Nijvipakul, S., et al., *LuxG is a functioning flavin reductase for bacterial luminescence*. J Bacteriol, 2008. **190**(5): p. 1531-8.
42. Engebrecht, J., K. Nealson, and M. Silverman, *Bacterial bioluminescence: isolation and genetic analysis of functions from Vibrio fischeri*. Cell, 1983. **32**(3): p. 773-81.
43. Miyashiro, T. and E.G. Ruby, *Shedding light on bioluminescence regulation in Vibrio fischeri*. Mol Microbiol, 2012. **84**(5): p. 795-806.
44. Verma, S.C. and T. Miyashiro, *Niche-Specific Impact of a Symbiotic Function on the Persistence of Microbial Symbionts within a Natural Host*. Appl Environ Microbiol, 2016. **82**(19): p. 5990-6.
45. Koch, E.J., et al., *Features governing symbiont persistence in the squid-vibrio association*. Mol Ecol, 2014. **23**(6): p. 1624-34.
46. Mazumder, A. and A.N. Kapanidis, *Recent Advances in Understanding sigma70-Dependent Transcription Initiation Mechanisms*. J Mol Biol, 2019. **431**(20): p. 3947-3959.
47. Schaller, H., C. Gray, and K. Herrmann, *Nucleotide sequence of an RNA polymerase binding site from the DNA of bacteriophage fd*. Proc Natl Acad Sci U S A, 1975. **72**(2): p. 737-41.
48. Danson, A.E., et al., *Mechanisms of sigma(54)-Dependent Transcription Initiation and Regulation*. J Mol Biol, 2019. **431**(20): p. 3960-3974.
49. Paget, M.S. and J.D. Helmann, *The sigma70 family of sigma factors*. Genome Biol, 2003. **4**(1): p. 203.
50. Guckes, K.R., et al., *The Bacterial Enhancer Binding Protein VasH Promotes Expression of a Type VI Secretion System in Vibrio fischeri during Symbiosis*. J Bacteriol, 2020.

51. Wolfe, A.J., et al., *Vibrio fischeri sigma54 controls motility, biofilm formation, luminescence, and colonization*. Appl Environ Microbiol, 2004. **70**(4): p. 2520-4.
52. Morett, E. and M. Buck, *In vivo studies on the interaction of RNA polymerase-sigma 54 with the Klebsiella pneumoniae and Rhizobium meliloti nifH promoters. The role of NifA in the formation of an open promoter complex*. J Mol Biol, 1989. **210**(1): p. 65-77.
53. Gao, F., et al., *Bacterial Enhancer Binding Proteins-AAA(+) Proteins in Transcription Activation*. Biomolecules, 2020. **10**(3).
54. Snider, J. and W.A. Houry, *AAA+ proteins: diversity in function, similarity in structure*. Biochem Soc Trans, 2008. **36**(Pt 1): p. 72-7.
55. Bush, M. and R. Dixon, *The role of bacterial enhancer binding proteins as specialized activators of sigma54-dependent transcription*. Microbiol Mol Biol Rev, 2012. **76**(3): p. 497-529.
56. Zimmer, D.P., et al., *Nitrogen regulatory protein C-controlled genes of Escherichia coli: scavenging as a defense against nitrogen limitation*. Proc Natl Acad Sci U S A, 2000. **97**(26): p. 14674-9.
57. Jiang, P. and A.J. Ninfa, *Regulation of autophosphorylation of Escherichia coli nitrogen regulator II by the PII signal transduction protein*. J Bacteriol, 1999. **181**(6): p. 1906-11.
58. Paget, M.S., *Bacterial Sigma Factors and Anti-Sigma Factors: Structure, Function and Distribution*. Biomolecules, 2015. **5**(3): p. 1245-65.
59. Bose, D., et al., *Dissecting the ATP hydrolysis pathway of bacterial enhancer-binding proteins*. Biochem Soc Trans, 2008. **36**(Pt 1): p. 83-8.
60. Joly, N., P.C. Burrows, and M. Buck, *An intramolecular route for coupling ATPase activity in AAA+ proteins for transcription activation*. J Biol Chem, 2008. **283**(20): p. 13725-35.
61. Joly, N., N. Zhang, and M. Buck, *ATPase site architecture is required for self-assembly and remodeling activity of a hexameric AAA+ transcriptional activator*. Mol Cell, 2012. **47**(3): p. 484-90.
62. Boyaci, H., et al., *Structure, Regulation, and Inhibition of the Quorum-Sensing Signal Integrator LuxO*. PLoS Biol, 2016. **14**(5): p. e1002464.
63. Chen, B., et al., *Regulation and action of the bacterial enhancer-binding protein AAA+ domains*. Biochem Soc Trans, 2008. **36**(Pt 1): p. 89-93.
64. Bordes, P., et al., *Communication between Esigma(54) , promoter DNA and the conserved threonine residue in the GAFTGA motif of the PspF sigma-dependent activator during transcription activation*. Mol Microbiol, 2004. **54**(2): p. 489-506.
65. Dago, A.E., et al., *A role for the conserved GAFTGA motif of AAA+ transcription activators in sensing promoter DNA conformation*. J Biol Chem, 2007. **282**(2): p. 1087-97.
66. Zhang, N., et al., *The role of the conserved phenylalanine in the sigma54-interacting GAFTGA motif of bacterial enhancer binding proteins*. Nucleic Acids Res, 2009. **37**(18): p. 5981-92.
67. Doucleff, M., et al., *Negative regulation of AAA + ATPase assembly by two component receiver domains: a transcription activation mechanism that is*

- conserved in mesophilic and extremely hyperthermophilic bacteria.* J Mol Biol, 2005. **353**(2): p. 242-55.
68. Lee, S.Y., et al., *Regulation of the transcriptional activator NtrC1: structural studies of the regulatory and AAA+ ATPase domains.* Genes Dev, 2003. **17**(20): p. 2552-63.
 69. Meyer, M.G., et al., *A dimeric two-component receiver domain inhibits the sigma54-dependent ATPase in DctD.* FASEB J, 2001. **15**(7): p. 1326-8.
 70. Park, S., et al., *Biochemical evidence for multiple dimeric states of the Sinorhizobium meliloti DctD receiver domain.* Biochemistry, 2002. **41**(36): p. 10934-41.
 71. Shingler, V., *Signal sensing by sigma 54-dependent regulators: derepression as a control mechanism.* Mol Microbiol, 1996. **19**(3): p. 409-16.
 72. Porter, S.C., et al., *Oligomerization of NTRC at the glnA enhancer is required for transcriptional activation.* Genes Dev, 1993. **7**(11): p. 2258-73.
 73. Bush, M., et al., *Transcriptional regulation by the dedicated nitric oxide sensor, NorR: a route towards NO detoxification.* Biochem Soc Trans, 2011. **39**(1): p. 289-93.
 74. Bush, M., et al., *Nitric oxide-responsive interdomain regulation targets the sigma54-interaction surface in the enhancer binding protein NorR.* Mol Microbiol, 2010. **77**(5): p. 1278-88.
 75. Vidangos, N., et al., *Structure, function, and tethering of DNA-binding domains in sigma(5)(4) transcriptional activators.* Biopolymers, 2013. **99**(12): p. 1082-96.
 76. Contreras, A. and M. Drummond, *The effect on the function of the transcriptional activator NtrC from Klebsiella pneumoniae of mutations in the DNA-recognition helix.* Nucleic Acids Res, 1988. **16**(9): p. 4025-39.
 77. Dworkin, J., G. Jovanovic, and P. Model, *Role of upstream activation sequences and integration host factor in transcriptional activation by the constitutively active prokaryotic enhancer-binding protein PspF.* J Mol Biol, 1997. **273**(2): p. 377-88.
 78. Martin Buck, S.M., Martin Drummond, Ray Dixon *Upstream activator sequences are present in the promoters of nitrogen fixation genes.* Nature, 1986. **320**: p. 374-378.
 79. Vidangos, N.K., et al., *DNA recognition by a sigma(54) transcriptional activator from Aquifex aeolicus.* J Mol Biol, 2014. **426**(21): p. 3553-68.
 80. Morris, A.R. and K.L. Visick, *Inhibition of SypG-induced biofilms and host colonization by the negative regulator SypE in Vibrio fischeri.* PLoS One, 2013. **8**(3): p. e60076.
 81. Popham, D.L., et al., *Function of a bacterial activator protein that binds to transcriptional enhancers.* Science, 1989. **243**(4891): p. 629-35.
 82. Weiner, L., J.L. Brissette, and P. Model, *Stress-induced expression of the Escherichia coli phage shock protein operon is dependent on sigma 54 and modulated by positive and negative feedback mechanisms.* Genes Dev, 1991. **5**(10): p. 1912-23.
 83. Miyashiro, T., et al., *A single qrr gene is necessary and sufficient for LuxO-mediated regulation in Vibrio fischeri.* Mol Microbiol, 2010. **77**(6): p. 1556-67.

84. Freeman, J.A. and B.L. Bassler, *A genetic analysis of the function of LuxO, a two-component response regulator involved in quorum sensing in Vibrio harveyi*. Mol Microbiol, 1999. **31**(2): p. 665-77.
85. Lupp, C. and E.G. Ruby, *Vibrio fischeri uses two quorum-sensing systems for the regulation of early and late colonization factors*. J Bacteriol, 2005. **187**(11): p. 3620-9.
86. Lupp, C. and E.G. Ruby, *Vibrio fischeri LuxS and AinS: comparative study of two signal synthases*. J Bacteriol, 2004. **186**(12): p. 3873-81.
87. Bassler, B.L., M. Wright, and M.R. Silverman, *Multiple signalling systems controlling expression of luminescence in Vibrio harveyi: sequence and function of genes encoding a second sensory pathway*. Mol Microbiol, 1994. **13**(2): p. 273-86.
88. Neiditch, M.B., et al., *Regulation of LuxPQ receptor activity by the quorum-sensing signal autoinducer-2*. Mol Cell, 2005. **18**(5): p. 507-18.
89. Gilson, L., A. Kuo, and P.V. Dunlap, *AinS and a new family of autoinducer synthesis proteins*. J Bacteriol, 1995. **177**(23): p. 6946-51.
90. Freeman, J.A. and B.L. Bassler, *Sequence and function of LuxU: a two-component phosphorelay protein that regulates quorum sensing in Vibrio harveyi*. J Bacteriol, 1999. **181**(3): p. 899-906.
91. Lenz, D.H., et al., *The small RNA chaperone Hfq and multiple small RNAs control quorum sensing in Vibrio harveyi and Vibrio cholerae*. Cell, 2004. **118**(1): p. 69-82.
92. Fidopiastis, P.M., et al., *LitR, a new transcriptional activator in Vibrio fischeri, regulates luminescence and symbiotic light organ colonization*. Mol Microbiol, 2002. **45**(1): p. 131-43.
93. Tu, K.C. and B.L. Bassler, *Multiple small RNAs act additively to integrate sensory information and control quorum sensing in Vibrio harveyi*. Genes Dev, 2007. **21**(2): p. 221-33.
94. Husa, E.A., et al., *Two-component response regulators of Vibrio fischeri: identification, mutagenesis, and characterization*. J Bacteriol, 2007. **189**(16): p. 5825-38.
95. Ray, V.A., et al., *The syp enhancer sequence plays a key role in transcriptional activation by the sigma54-dependent response regulator SypG and in biofilm formation and host colonization by Vibrio fischeri*. J Bacteriol, 2013. **195**(23): p. 5402-12.
96. Norsworthy, A.N. and K.L. Visick, *Signaling between two interacting sensor kinases promotes biofilms and colonization by a bacterial symbiont*. Mol Microbiol, 2015. **96**(2): p. 233-48.
97. Husa, E.A., C.L. Darnell, and K.L. Visick, *RscS functions upstream of SypG to control the syp locus and biofilm formation in Vibrio fischeri*. J Bacteriol, 2008. **190**(13): p. 4576-83.
98. Darnell, C.L., E.A. Husa, and K.L. Visick, *The putative hybrid sensor kinase SypF coordinates biofilm formation in Vibrio fischeri by acting upstream of two response regulators, SypG and VpsR*. J Bacteriol, 2008. **190**(14): p. 4941-50.

99. Brooks, J.F., 2nd and M.J. Mandel, *The Histidine Kinase BinK Is a Negative Regulator of Biofilm Formation and Squid Colonization*. J Bacteriol, 2016. **198**(19): p. 2596-607.
100. Tischler, A.H., et al., *Discovery of Calcium as a Biofilm-Promoting Signal for Vibrio fischeri Reveals New Phenotypes and Underlying Regulatory Complexity*. J Bacteriol, 2018. **200**(15).
101. La Reau, A.J. and G. Suen, *The Ruminococci: key symbionts of the gut ecosystem*. J Microbiol, 2018. **56**(3): p. 199-208.
102. Nyholm, S.V., et al., *Roles of Vibrio fischeri and nonsymbiotic bacteria in the dynamics of mucus secretion during symbiont colonization of the Euprymna scolopes light organ*. Appl Environ Microbiol, 2002. **68**(10): p. 5113-22.
103. Visick, K.L., et al., *Vibrio fischeri lux genes play an important role in colonization and development of the host light organ*. J Bacteriol, 2000. **182**(16): p. 4578-86.
104. Eberhard, A., et al., *Structural identification of autoinducer of Photobacterium fischeri luciferase*. Biochemistry, 1981. **20**(9): p. 2444-9.
105. Kimbrough, J.H. and E.V. Stabb, *Substrate specificity and function of the pheromone receptor AinR in Vibrio fischeri ES114*. J Bacteriol, 2013. **195**(22): p. 5223-32.
106. Wasilko, N.P., et al., *Sulfur availability for Vibrio fischeri growth during symbiosis establishment depends on biogeography within the squid light organ*. Mol Microbiol, 2019. **111**(3): p. 621-636.
107. Sun, Y., et al., *Intraspecific Competition Impacts Vibrio fischeri Strain Diversity during Initial Colonization of the Squid Light Organ*. Appl Environ Microbiol, 2016. **82**(10): p. 3082-91.
108. Guckes, K.R., et al., *Incompatibility of Vibrio fischeri Strains during Symbiosis Establishment Depends on Two Functionally Redundant hcp Genes*. J Bacteriol, 2019. **201**(19).
109. Miyashiro, T., et al., *The putative oligosaccharide translocase SypK connects biofilm formation with quorum signaling in Vibrio fischeri*. Microbiologyopen, 2014. **3**(6): p. 836-48.
110. Moller, T.S., et al., *Relation between tetR and tetA expression in tetracycline resistant Escherichia coli*. BMC Microbiol, 2016. **16**: p. 39.
111. Ray, V.A., A.R. Morris, and K.L. Visick, *A semi-quantitative approach to assess biofilm formation using wrinkled colony development*. J Vis Exp, 2012(64): p. e4035.
112. Yip, E.S., et al., *The symbiosis regulator rscS controls the syp gene locus, biofilm formation and symbiotic aggregation by Vibrio fischeri*. Mol Microbiol, 2006. **62**(6): p. 1586-600.
113. Ludvik, D.A., K.M. Bultman, and M.J. Mandel, *Hybrid Histidine Kinase BinK Represses Vibrio fischeri Biofilm Signaling at Multiple Developmental Stages*. J Bacteriol, 2021. **203**(15): p. e0015521.
114. Svenningsen, S.L., C.M. Waters, and B.L. Bassler, *A negative feedback loop involving small RNAs accelerates Vibrio cholerae's transition out of quorum-sensing mode*. Genes Dev, 2008. **22**(2): p. 226-38.

115. Tu, K.C., et al., *Negative feedback loops involving small regulatory RNAs precisely control the Vibrio harveyi quorum-sensing response*. Mol Cell, 2010. **37**(4): p. 567-79.
116. Tague, J.G., et al., *Regulatory small RNA, Qrr2 is expressed independently of sigma factor-54 and can function as the sole Qrr sRNA to control quorum sensing in Vibrio parahaemolyticus*. J Bacteriol, 2021: p. JB0035021.
117. Wen, Y., I.H. Kim, and K.S. Kim, *Iron- and Quorum-sensing Signals Converge on Small Quorum-regulatory RNAs for Coordinated Regulation of Virulence Factors in Vibrio vulnificus*. J Biol Chem, 2016. **291**(27): p. 14213-30.
118. Bhattacharyya, N., et al., *An Aspartate-Specific Solute-Binding Protein Regulates Protein Kinase G Activity To Control Glutamate Metabolism in Mycobacteria*. mBio, 2018. **9**(4).
119. Chantranupong, L., R.L. Wolfson, and D.M. Sabatini, *Nutrient-sensing mechanisms across evolution*. Cell, 2015. **161**(1): p. 67-83.
120. Buck, M., et al., *The bacterial enhancer-dependent sigma(54) (sigma(N)) transcription factor*. J Bacteriol, 2000. **182**(15): p. 4129-36.
121. Hayrapetyan, H., et al., *Bacillus cereus ATCC 14579 RpoN (Sigma 54) Is a Pleiotropic Regulator of Growth, Carbohydrate Metabolism, Motility, Biofilm Formation and Toxin Production*. PLoS One, 2015. **10**(8): p. e0134872.
122. Dong, T.G. and J.J. Mekalanos, *Characterization of the RpoN regulon reveals differential regulation of T6SS and new flagellar operons in Vibrio cholerae O37 strain V52*. Nucleic Acids Res, 2012. **40**(16): p. 7766-75.
123. Tsang, J. and T.R. Hoover, *Themes and Variations: Regulation of RpoN-Dependent Flagellar Genes across Diverse Bacterial Species*. Scientifica (Cairo), 2014. **2014**: p. 681754.
124. Riordan, J.T. and A. Mitra, *Regulation of Escherichia coli Pathogenesis by Alternative Sigma Factor N*. EcoSal Plus, 2017. **7**(2).
125. Kimbrough, J.H. and E.V. Stabb, *Antisocial luxO Mutants Provide a Stationary-Phase Survival Advantage in Vibrio fischeri ES114*. J Bacteriol, 2015. **198**(4): p. 673-87.
126. Vance, R.E., J. Zhu, and J.J. Mekalanos, *A constitutively active variant of the quorum-sensing regulator LuxO affects protease production and biofilm formation in Vibrio cholerae*. Infect Immun, 2003. **71**(5): p. 2571-6.
127. Wigneshweraraj, S.R., et al., *The second paradigm for activation of transcription*. Prog Nucleic Acid Res Mol Biol, 2005. **79**: p. 339-69.
128. Bassler, B.L., M. Wright, and M.R. Silverman, *Sequence and function of LuxO, a negative regulator of luminescence in Vibrio harveyi*. Mol Microbiol, 1994. **12**(3): p. 403-12.
129. Neuwald, A.F., et al., *AAA+: A class of chaperone-like ATPases associated with the assembly, operation, and disassembly of protein complexes*. Genome Res, 1999. **9**(1): p. 27-43.
130. Mogk, A., et al., *Roles of individual domains and conserved motifs of the AAA+ chaperone ClpB in oligomerization, ATP hydrolysis, and chaperone activity*. J Biol Chem, 2003. **278**(20): p. 17615-24.

131. Monroe, N., et al., *The oligomeric state of the active Vps4 AAA ATPase*. J Mol Biol, 2014. **426**(3): p. 510-25.
132. Nyholm, S.V. and M.J. McFall-Ngai, *The winnowing: establishing the squid-vibrio symbiosis*. Nat Rev Microbiol, 2004. **2**(8): p. 632-42.
133. Verma, S.C. and T. Miyashiro, *Quorum sensing in the squid-Vibrio symbiosis*. Int J Mol Sci, 2013. **14**(8): p. 16386-401.
134. Lilley, B.N. and B.L. Bassler, *Regulation of quorum sensing in Vibrio harveyi by LuxO and sigma-54*. Mol Microbiol, 2000. **36**(4): p. 940-54.
135. Thompson, C.M., et al., *Vibrio fischeri Biofilm Formation Prevented by a Trio of Regulators*. Appl Environ Microbiol, 2018. **84**(19).
136. Sawabe, T., et al., *Updating the Vibrio clades defined by multilocus sequence phylogeny: proposal of eight new clades, and the description of Vibrio tritonius sp. nov.* Front Microbiol, 2013. **4**: p. 414.
137. Egidius, E., et al., *Vibrio salmonicida sp. nov., a New Fish Pathogen*. International Journal of Systematic and Evolutionary Microbiology, 1986. **36**(4): p. 518-520.
138. Michaela J. Eickhoff, C.F., Xiuliang Huang, Bonnie L. Bassler, *LuxT controls specific quorum-sensing-regulated behaviors in Vibrionaceae spp. via repression of qrr1, encoding a small regulatory RNA*. bioRxiv, 2021.
139. Bjelland, A.M., et al., *LitR of Vibrio salmonicida is a salinity-sensitive quorum-sensing regulator of phenotypes involved in host interactions and virulence*. Infect Immun, 2012. **80**(5): p. 1681-9.
140. Hansen, H., et al., *LitR is a repressor of syp genes and has a temperature-sensitive regulatory effect on biofilm formation and colony morphology in Vibrio (Aliivibrio) salmonicida*. Appl Environ Microbiol, 2014. **80**(17): p. 5530-41.
141. Miyashiro, T., et al., *The N-acetyl-D-glucosamine repressor NagC of Vibrio fischeri facilitates colonization of Euprymna scolopes*. Mol Microbiol, 2011. **82**(4): p. 894-903.
142. Madeira, F., et al., *The EMBL-EBI search and sequence analysis tools APIs in 2019*. Nucleic Acids Res, 2019. **47**(W1): p. W636-W641.
143. Combet, C., et al., *NPS@: network protein sequence analysis*. Trends Biochem Sci, 2000. **25**(3): p. 147-50.
144. Septer, A.N. and E.V. Stabb, *Coordination of the arc regulatory system and pheromone-mediated positive feedback in controlling the Vibrio fischeri lux operon*. PLoS One, 2012. **7**(11): p. e49590.
145. Shen, N., et al., *Divergence in DNA Specificity among Paralogous Transcription Factors Contributes to Their Differential In Vivo Binding*. Cell Syst, 2018. **6**(4): p. 470-483 e8.
146. Geszvain, K. and K.L. Visick, *The hybrid sensor kinase RscS integrates positive and negative signals to modulate biofilm formation in Vibrio fischeri*. J Bacteriol, 2008. **190**(13): p. 4437-46.
147. Ng, W.L., et al., *Broad spectrum pro-quorum-sensing molecules as inhibitors of virulence in vibrios*. PLoS Pathog, 2012. **8**(6): p. e1002767.
148. Han, B., et al., *Sodium Ascorbate as a Quorum-Sensing Inhibitor Leads to Decreased Virulence in Vibrio campbellii*. Front Microbiol, 2020. **11**: p. 1054.

149. Ni, N., et al., *Inhibition of quorum sensing in Vibrio harveyi by boronic acids*. Chem Biol Drug Des, 2009. **74**(1): p. 51-6.
150. Visick, K.L. and L.M. Skoufos, *Two-component sensor required for normal symbiotic colonization of euprymna scolopes by Vibrio fischeri*. J Bacteriol, 2001. **183**(3): p. 835-42.
151. Boettcher, K.J. and E.G. Ruby, *Depressed light emission by symbiotic Vibrio fischeri of the sepiolid squid Euprymna scolopes*. J Bacteriol, 1990. **172**(7): p. 3701-6.
152. Singh, P., et al., *CysK Plays a Role in Biofilm Formation and Colonization by Vibrio fischeri*. Appl Environ Microbiol, 2015. **81**(15): p. 5223-34.
153. Mandel, M.J., E.V. Stabb, and E.G. Ruby, *Comparative genomics-based investigation of resequencing targets in Vibrio fischeri: focus on point miscalls and artefactual expansions*. BMC Genomics, 2008. **9**: p. 138.
154. Woodcock, D.M., et al., *Quantitative evaluation of Escherichia coli host strains for tolerance to cytosine methylation in plasmid and phage recombinants*. Nucleic Acids Res, 1989. **17**(9): p. 3469-78.
155. Metcalf, W.W., W. Jiang, and B.L. Wanner, *Use of the rep technique for allele replacement to construct new Escherichia coli hosts for maintenance of R6K gamma origin plasmids at different copy numbers*. Gene, 1994. **138**(1-2): p. 1-7.
156. Herrero, M., V. de Lorenzo, and K.N. Timmis, *Transposon vectors containing non-antibiotic resistance selection markers for cloning and stable chromosomal insertion of foreign genes in gram-negative bacteria*. J Bacteriol, 1990. **172**(11): p. 6557-67.
157. Simon, R., U. Priefer, and A. Pühler, *A Broad Host Range Mobilization System for In Vivo Genetic Engineering: Transposon Mutagenesis in Gram Negative Bacteria*. Nat Biotechnol, 1983. **1**: p. 784-791.
158. Le Roux, F., et al., *Construction of a Vibrio splendidus mutant lacking the metalloprotease gene vsm by use of a novel counterselectable suicide vector*. Appl Environ Microbiol, 2007. **73**(3): p. 777-84.
159. Dunn, A.K., et al., *New rfp- and pES213-derived tools for analyzing symbiotic Vibrio fischeri reveal patterns of infection and lux expression in situ*. Appl Environ Microbiol, 2006. **72**(1): p. 802-10.
160. Stabb, E.V. and E.G. Ruby, *RP4-based plasmids for conjugation between Escherichia coli and members of the Vibrionaceae*. Methods Enzymol, 2002. **358**: p. 413-26.
161. Bao, Y., et al., *An improved Tn7-based system for the single-copy insertion of cloned genes into chromosomes of gram-negative bacteria*. Gene, 1991. **109**(1): p. 167-8.
162. McCann, J., et al., *Population dynamics of Vibrio fischeri during infection of Euprymna scolopes*. Appl Environ Microbiol, 2003. **69**(10): p. 5928-34.
163. Pollack-Berti, A., M.S. Wollenberg, and E.G. Ruby, *Natural transformation of Vibrio fischeri requires tfoX and tfoY*. Environ Microbiol, 2010. **12**(8): p. 2302-11.

VITA

Ericka D. Surrett

Education

Ph.D. in Biochemistry, Microbiology, and Molecular Biology
The Pennsylvania State University; University Park, PA

Aug 2022

B.S. in Chemistry (May 2013)

The University of West Alabama; Livingston, AL

May 2013

Research Experience

Research Assistant

The Pennsylvania State University; University Park, PA
Department of Biochemistry and Molecular Biology

Researched factors that promote the ability of the marine microbe *Vibrio fischeri* to establish symbiosis with its host, the Hawaiian bobtail squid. This work specifically focused on how two bacterial enhancer binding proteins activated expression of a small RNA that regulates symbiotic traits in *V. fischeri*.

Undergraduate Summer Research Opportunities Program Scholar

The Pennsylvania State University; University Park, PA

Department of Chemical Engineering

Researched the impact of Rho-dependent transcription termination on biofilm formation in *E. coli*

Fellowships & Scholarships

Howard Hughes Medical Institute (HHMI) Gilliam Fellowship for Advanced Study

Aug 2017

Alfred P. Sloan Scholarship

Jul 2016

Bunton-Waller Fellowship

Aug 2020

Publication

Ericka D. Surrett, Kirsten R. Guckes, Shyan Cousins, Terry R. Ruskoski, Andrew G. Cecere, Denise A. Ludvik, C. Denise Okafor, Mark J. Mandel, and Tim I. Miyashiro. "Two bacterial enhancer binding proteins activate σ^{54} -dependent transcription of a small regulatory RNA in a bacterial symbiont." (*in revision following peer review*)